Journal of Medicinal Chemistry

pubs.acs.org/jmc Article

# From Pyrazolones to Azaindoles: Evolution of Active-Site SHP2 Inhibitors Based on Scaffold Hopping and Bioisosteric Replacement

Yelena Mostinski, Guus J. J. E. Heynen, Maria Pascual López-Alberca, Jerome Paul, Sandra Miksche, Silke Radetzki, David Schaller, Elena Shanina, Carola Seyffarth, Yuliya Kolomeets, Nandor Ziebart, Judith de Schryver, Sylvia Oestreich, Martin Neuenschwander, Yvette Roske, Udo Heinemann, Christoph Rademacher, Andrea Volkamer, Jens Peter von Kries, Walter Birchmeier, and Marc Nazaré*

Cite This: https://dx.doi.org/10.1021/acs.jmedchem.0c01265 Read Online

ACCESS | Metrics & More | Article Recommendations | Supporting Information

**ABSTRACT:** The tyrosine phosphatase SHP2 controls the activity of pivotal signaling pathways, including MAPK, JAK-STAT, and PI3K-Akt. Aberrant SHP2 activity leads to uncontrolled cell proliferation, tumorigenesis, and metastasis. SHP2 signaling was recently linked to drug resistance against cancer medications such as MEK and BRAF inhibitors. In this work, we present the development of a novel class of azaindole SHP2 inhibitors. We applied scaffold hopping and bioisosteric replacement concepts to eliminate unwanted structural motifs and to improve the inhibitor characteristics of the previously reported pyrazolone SHP2 inhibitors. The most potent azaindole **45** inhibits SHP2 with an $IC_{50}$ = 0.031 $\mu$M in an enzymatic assay and with an $IC_{50}$ = 2.6 $\mu$M in human pancreas cells (HPAF-II). Evaluation in a series of cellular assays for metastasis and drug resistance demonstrated efficient SHP2 blockade. Finally, **45** inhibited proliferation of two cancer cell lines that are resistant to cancer drugs and diminished ERK signaling.

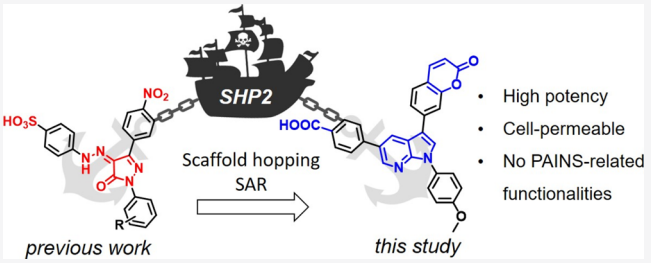


## INTRODUCTION

The protein tyrosine phosphatase SHP2 is a member of a human protein phosphatases family (PTPs) and encoded by the *PTPN11* proto-oncogene.[1,2] This ubiquitously expressed enzyme controls the activation of several intracellular signaling pathways, including receptor tyrosine kinase (e.g., met-receptor), MAPK, JAK-STAT, and PI3K-Akt.[3,4] It has been reported that mutations in *PTPN11* lead to the development of various diseases, such as Noonan syndrome, LEOPARD syndrome, juvenile myelomonocytic leukemia, and several types of solid tumors.[2,5,6] The clear connection between activating mutations of *PTPN11* and these disorders qualify SHP2 as a highly relevant biological target for the development of anticancer therapeutics. Moreover, the regulatory function of SHP2 in intracellular signaling pathways provides an opportunity for controlling the activity of known oncogenes, such as *BRAF* and *RAS*. Identifying alternative ways to block these targets is of utmost importance, especially in view of the emerging clinical threat of drug resistance and relapsing tumors.[7−9] Furthermore, recent reports on previously unrevealed key functions of SHP2 in various intracellular pathways are successively illustrating its key pathophysiological significance in several cancers and in development of drug resistance.[10−14] Therefore, several studies were devoted to the discovery of small-molecule inhibitors of SHP2 as a prime phosphatase target for anticancer therapy.[3,15−25]

Structurally, SHP2 consists of three domains—N-terminal and C-terminal SH2 recognition elements and a PTP catalytic domain. When the enzyme is in a basal auto-inhibited state, the SH2 domains are covering the catalytic cavity of the PTP site. After activation by binding of the phosphorylated tyrosine-bearing proteins and peptides to SH2 domains, SHP2 undergoes conformational changes disrupting the autoinhibitory interaction between the SH2 domain and the PTP site, thereby transforming into an open conformation and exposing the substrate-binding catalytic site.[2,26] The development of a small molecule that will compete with the endogenous substrates and block the catalytic site is one of the main strategies of inhibition of SHP2 (Figure 1, compounds **1**−**4**).[2,19−22] Despite several promising reports, none of the described inhibitors proceeded to advanced clinical studies so far. One of the major reasons for the low success rate in the development of SHP2 inhibitors is the shallow, highly polar, lysine and arginine-rich active site, which is highly conserved

Received: July 28, 2020

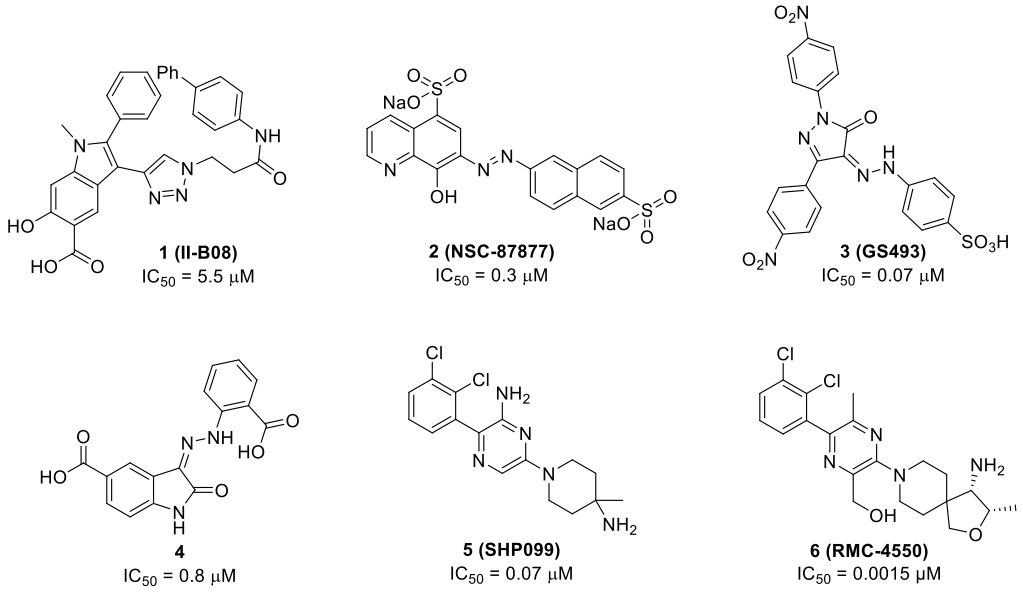


**Figure 1.** Previously reported SHP2 inhibitors and their $IC_{50}$ values. Compounds **1**−**4** represent active-site inhibitors and **5**−**6** are allosteric binders.

among the PTPs.[27,28] Therefore, the design and synthesis of potent but selective and cell-permeable small-molecule inhibitors is a complex and challenging endeavor. Recently, in an attempt to overcome these obstacles of active-site inhibition, allosteric modulation of SHP2 activity was investigated. The allosteric mechanism is based on stabilization of the auto-inhibited conformation of SHP2 by simultaneous binding to all three domains and shifting the equilibrium from the active state to the inactive state (the "inverse agonist principle"). Several small-molecule inhibitors, acting as a so-called "molecular glue", that bind and inhibit SHP2 through an allosteric mechanism were reported (Figure 1, compounds **5**−**6**).[17,29−31] These small molecules demonstrated remarkable phosphatase selectivity and potency, and several candidates entered clinical trials.[3] However, some studies indicated that the allosteric modulators may exhibit limited hERG selectivity[15,29] and exert a surprisingly low efficacy against distinct oncogenic SHP2 variants in advanced biological studies.[32−36] This limitation is associated with the high vulnerability of the allosteric three-domain-binding mode to mutations and to the existing high degree of aberrant activation of SHP2 in several cancers.[32−36] Therefore, although allosteric inhibition of SHP2 seems to be an excellent mode of suppression for some oncogenic SHP2 variants, these specific compounds might not be clinically useful to inhibit frequently encountered mutated SHP2 variants.[29] Consequently, the development of chemically different SHP2 inhibitors, which are less sensitive to oncogenic mutations and underlie a robust mode of action, which address the activated state of SHP2 is highly desirable.

In our previous work, we described the development of pyrazolone-based inhibitors of SHP2. The hit candidate PHPS1 was identified through virtual high-throughput screening and optimized to GS493.[37,38] These molecules are selective, active-site-directed competitive inhibitors with prominent activity in enzymatic and cellular assays. We demonstrated that these active-site inhibitors have a remarkable synergistic efficacy with the *MEK* and *BRAF* inhibitors and achieved sustained inhibition of tumor cell proliferation *in vitro* and *in vivo*.[7,9]

Despite its potency, the identified compound class possesses several unfavorable functionalities and liabilities, which prevents it from being a suitable platform for further lead optimization. A major concern is related to a chemically unstable hydrazone fragment attached to the pyrazolone scaffold that potentially releases toxic metabolites *in vivo* and shares structural features belonging to promiscuous pan-assay interference compounds (PAINS).[39,40] The presence of a nitro group in PHPS1, and in GS493, which incorporates two nitro groups, may account for potential cytotoxicity *in vivo*,[41,42] and the sulfonic acid hampers the cell permeability of the inhibitors. However, both the nitro and sulfonic groups are thought to be engaged in key binding interactions with the SHP2 catalytic site, and therefore, their replacement is a challenging task.[37,38] In the current work, we designed and synthesized highly potent, selective, and drug-like inhibitors of SHP2,[43−45] based on the substitution of these detrimental structural features according to structure-activity relationship (SAR) studies, which included scaffold hopping and bioisosteric replacement approaches.

## RESULTS AND DISCUSSION

**Scaffold Hopping of the Pyrazolone Core.** Our optimization study started with the investigation of a rescaffolding of the pyrazolone core and elimination of the hydrazone moiety.[46,47] Unfortunately, the cocrystal structure of SHP2 and the respective pyrazolone inhibitor is not available. Moreover, the determination of the endogenous substrates of SHP2 is still limited to date; thus, it is a daunting endeavor to successfully mimic their putative interactions. We therefore resorted to a ligand-based alignment approach preserving the vectorial information and structural features commonly known to be essential to address the phosphatase catalytic mechanism. For the initial attempts of scaffold hopping, we preserved the monocyclic framework by incorporation of the stable carboxamide-imidazole backbone. Unfortunately, the corresponding imidazole analogue **8** of PHPS1 was inactive (Table


https://dx.doi.org/10.1021/acs.jmedchem.0c01265
J. Med. Chem. XXXX, XXX, XXX−XXX

1). Supported by comparative alignment studies with PHPS1, we concluded that a more rigid bicyclic core might be crucial for inhibitor binding, as the carboxamide-imidazole backbone is too flexible to provide optimal orientation of the substituents for favorable interactions with the catalytic site. Hence, we proceeded to a conformational lock/ring-closure strategy and synthesized a bicyclic pyrazolo-triazole PHPS1 analogue **9**, which gratifyingly exhibited inhibitory activity with an $IC_{50}$ = 12 $\mu$M (see Supporting Information, Figure S1). This supported our hypothesis that a ring-closure to a bicyclic aromatic system would be a viable strategy for further variations and would not impose significant detrimental effects on the molecular recognition of the peripheral substituents of the small-molecule ligand with the active site of SHP2.

**Table 1. Heterocyclic Candidates for Pyrazolone Scaffold Replacement**

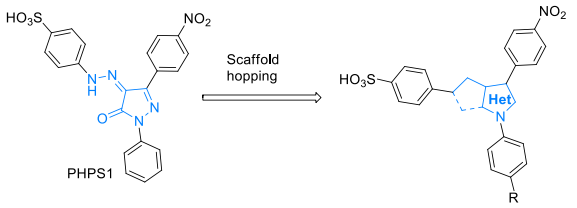


| Compound | Het | R | SHP2 $IC_{50}$ ($\mu$M)[a] |
|---|---|---|---|
| 7 (PHPS1) | 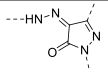 | -H | 3.0[b] |
| 8 | 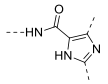 | -H | >100 |
| 9 |  | -H | 12 |
| 10 |  | -OMe | 5.9 |
| 11 |  | -OMe | 4.6 |

[a]To evaluate the $IC_{50}$ of compounds **7**–**11**, a DiFMUP concentration of 20 $\mu$M was used. For full assay details see the Experimental Section. [b]Lit. value for $IC_{50}$ of PHPS1 = 2.1 $\mu$M. See ref 34. Other reference compounds values: $IC_{50}$ PTP II-B08 = 30 $\mu$M; $IC_{50}$ NSC-87877 = 4.5 $\mu$M.

This finding led us to examine additional heterocycles, with lower apparent similarity to the pyrazolone hit, but with higher abundance among existing drugs or drug candidates. In addition, we hypothesized that a 5,6-fused system would provide optimal geometrical preorientation, preserving the original trajectory for the sulfonic group.[48] We focused our efforts on the replacement of the pyrazolone core by azaindole and indazole analogues. These privileged heterocyclic cores attracted our attention because of their high stability, straightforward synthetic derivatization possibilities, and good drug-like properties.[49−53] Satisfyingly, indazole **10** and azaindole **11** showed higher inhibitory activity than the parent triazolo-pyrazole analogue. Because of the highly privileged nature of the azaindole candidate, we considered this framework as the most promising starting point and focused therefore our further optimization efforts on this scaffold.

**Chemistry.** 1,3,5-Trisubstituted 7-azaindoles were synthesized as outlined in Scheme 1. The synthetic route commenced with the iodination of the 3-position of commercially available 5-bromo-7-azaindole **12** following a previously reported procedure.[54] The second step involved a Chan-Lam N-arylation to generate intermediate compound **14**. Unfortunately, the yield of the products was low, despite considerable

**Scheme 1. General Synthesis of Azaindoles**[a]

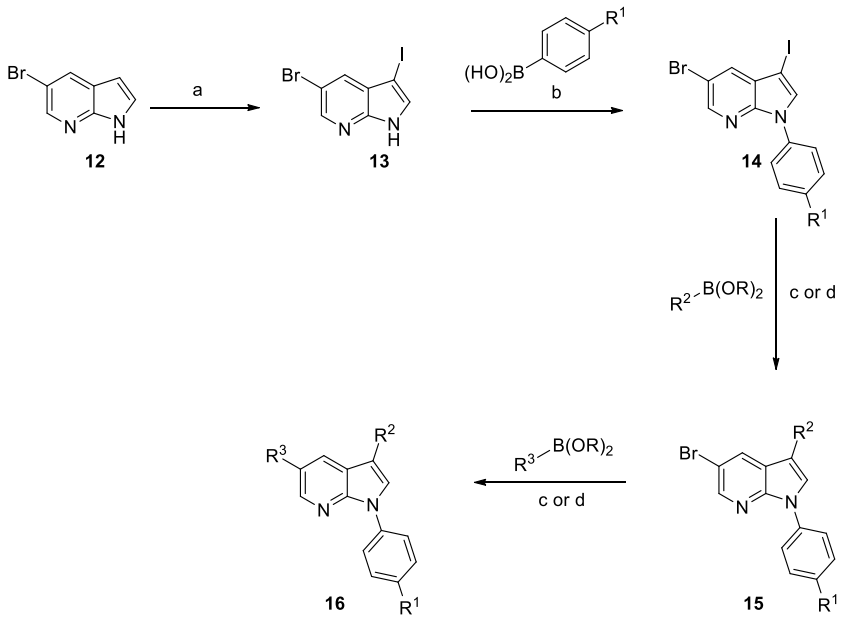


[a]Reagents and conditions (a) NIS, acetone, rt; 2−4 h, 92% (b) $Cu(OAc)_2$, DIPEA, rt, 48 h; 18−21% (c) $NaHCO_3$, $Pd(PPh_3)_4$, 3:1 ACN/water, 100 °C, 12 h, 42−69% for the first coupling, 2−98% for the second coupling (d) $K_2CO_3$, $Pd(dppf)Cl_2$, dioxane/water, 80 °C, 3−6 h, 22−71% for the first coupling, 2.5−38% for the second coupling.


https://dx.doi.org/10.1021/acs.jmedchem.0c01265
J. Med. Chem. XXXX, XXX, XXX−XXX

excess of reagents used. To overcome these limitations, we varied the solvent, base, temperature, and copper source. Nonetheless, no significant improvements in yield were observed. This poor outcome is in line with other literature precedents, where only a scarce number of examples for N-arylation of substituted azaindoles with typically low yields are reported.[55,56] The poor outcome of the reaction can be explained by the deactivating nature of the substituents and "trapping" effect of the neighboring nitrogen of the pyridine unit. Subsequent Suzuki couplings required $K_2CO_3$/Pd(dppf)-$Cl_2$ or $NaHCO_3$/Pd$(PPh_3)_4$ catalytic systems depending on the nature of the employed boron species. In order to overcome the limitations of the Chan-Lam coupling step, we attempted first to carry out Suzuki coupling; however, this transformation failed—no conversion to the desired product was observed and the starting material slowly decomposed over time. Seeking an alternative route, we protected the *N1* of the azaindole with a Boc moiety, and sequentially substituted the 3- and 5-positions with corresponding aryl groups utilizing Suzuki coupling, followed by removal of the Boc group. The final N-substitution was performed using Ullman conditions (for the detailed scheme see Supporting Information, Scheme S1). Overall, the synthesis of azaindoles **16** was successfully accomplished by both Ullman and Chan-Lam protocols. However, the Ullman protocol requires a protection−deprotection strategy, thus this synthetic path is longer and despite higher yields obtained in each step of this route, it has a similar overall yield. Therefore, we resorted to the Chan-Lam reaction-based approach as the main strategy for the synthesis of the azaindole products. In summary, all compounds could be obtained by the developed synthetic route, which is robust, efficient, and short, providing the final molecules in only four steps. For the preparation of the product with nonaromatic substituents on the pyrrole ring, we replaced the Chan-Lam arylation step by a classic NaH-assisted reaction (for details see the Experimental Section for the compounds **28** and **30**−**32**).

**Bioisosteric Replacement of Nitro and Sulfonic Acid Functionalities and SAR Evaluation of Azaindoles.** After rescaffolding of the pyrazolone core, the next step was to investigate the potential for a bioisosteric replacement of the highly charged permeability-hampering sulfonic acid group.[46,47,57] In stark contrast to previous replacement attempts at the pyrazolone core,[38,58] this structural fragment could be successfully exchanged by a simple carboxylic acid (Table 2).[59] Compounds **17** and **18** bearing such a carboxylic acid in para- or meta-position showed superior inhibitory activity with $IC_{50}$ of 0.13 and 0.41 $\mu$M, respectively. We therefore concluded that the azaindoles incorporating a benzoic acid functionality would provide a promising basis for further SAR exploration. Moreover, besides the fact that the carboxylic group represents a physiologically much more benign functionality compared to the sulfonic acid, in particular for intracellular targets, it is a convenient synthetic platform for a potential pro-drug approach. Because meta- and para-substituted benzoic acids were similarly active, we continued the SAR exploration aiming for a replacement of the nitro group by testing both benzoic acid isomers and varying the $R^2$ substitution at the 3-position of the azaindole.

Finding an appropriate replacement of the nitro moiety has proven to be challenging[60] because systematic studies of a general bioisosteric relationship of the nitro functionality with other chemical groups are lacking. Intuitively, strong electron-withdrawing groups, such as trifluoromethyl and −CN, are

**Table 2. SAR of $R^2$ and $R^3$**[a]

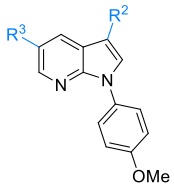


| Compound | $R^3$ | $R^2$ | SHP2 $IC_{50}$ (μM)[b] |
|---|---|---|---|
| **17** | 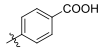 |  | 0.13 |
| **18** | 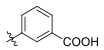 |  | 0.41 |
| **19** | 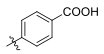 |  | 0.24 |
| **20** | 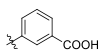 |  | 0.41 |
| **21** | 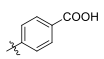 |  | 0.12 |
| **22** | 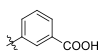 |  | 1.5 |
| **23** | 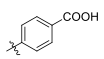 |  | 7.5 |
| **24** | 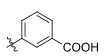 |  | 2 |
| **25** | 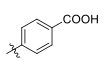 |  | > 10 |
| **26** | 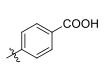 |  | 2 |
| **27** | 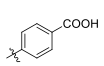 |  | 0.39 |

[a]Bioisosteric replacement of nitro and sulfonic acid moieties. [b]To evaluate the $IC_{50}$ of compounds **17**−**27**, a DiFMUP concentration of 10 $\mu$M was used. For full assay details, see the Experimental Section. Reference cmpd values: PHPS1 $IC_{50}$ = 0.06 $\mu$M; PTP II-B08 $IC_{50}$ = 12 $\mu$M; NSC-87877 $IC_{50}$ = 0.41 $\mu$M; PTP1B inhibitor $IC_{50}$ = 3.1 $\mu$M.

used for bioisosteric substitution of the nitro functionality.[61,62] In addition, the incorporation of oxygen- and nitrogen-containing heterocycles such as oxazolines and oxadiazoles was found to be beneficial in several reports.[63−67] Guided by these observations, we prepared several analogues of **17** and **18**, replacing the nitro group (Table 2) and tested their ability to inhibit SHP2. Several azaindoles demonstrated good activity with $IC_{50}$ values below 1 $\mu$M, among the analogues containing a trifluoromethyl group **21** and **22**, nitrile-bearing analogue **27**, and the benzoxadiazoles **19** and **20**, the latter being particularly promising, because of their lower lipophilicity. The good inhibitory effect of these derivatives aligns well with previous findings, showing the ability of the small molecules bearing nitro-benzoxadiazole to inhibit the closely related PTP1B enzyme.[68] Moreover, the benzoxadiazole moiety is highly fluorescent, and it provides an additional useful feature for the intended cellular permeability studies. Compounds **23**−**26**, however, demonstrated only moderate activity, compared to the nitro analogue **17**. A dioxolane-bearing derivative **26** supported the assumption that a strong electron-withdrawing group might be required for the successful replacement of the nitro moiety. Along these lines, pyridines **23**−**24** and the pyrimidine **25** analogue indicated that the presence of a protruding substituent is indispensable to establish these


https://dx.doi.org/10.1021/acs.jmedchem.0c01265
J. Med. Chem. XXXX, XXX, XXX−XXX

important interactions with the binding cavity. At this point by comparing the activity of several pairs of the meta−para benzoic acid isomers, we had sufficient evidence to conclude that the para-derivative outperforms the meta-analogue, and we therefore decided to utilize para-**19** as a platform for the next optimization step exploring the *N1*-azaindole substitution.

Despite their good biological activity, the novel compounds showed only limited aqueous solubility because of the flat aromatic, hence highly lipophilic structure. Consequently, we introduced variations at $R^1$ aiming for a higher solubility while maintaining or improving the activity (Table 3). Our previous

**Table 3. Investigation of the Scope for a Broader R1 Variation toward Improved Solubility**

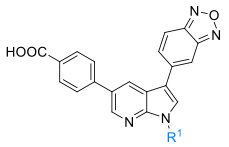


| Compound | Het | $R^1$ | SHP2 $IC_{50}$ (μM) [a] |
|---|---|---|---|
| **28** |  |  | >10[b] |
| **29** |  | 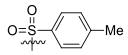 | 6.7 |
| **30** |  |  | 1.1 |
| **31** |  | 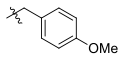 | 1.2 |
| **32** |  | 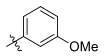 | 3.2 |
| **33** |  |  | 0.14 |
| **34** |  | 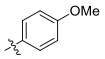 | >10[b] |
| **35** |  |  | >10 |

[a]To evaluate the $IC_{50}$ of compounds **28**-**33**, a DiFMUP concentration of 10 μM was used. For full assay details, see the Experimental Section. Reference cmpd values: PHPS1 $IC_{50}$ = 0.06 μM; PTP II-B08 $IC_{50}$ = 12 μM; NSC-87877 $IC_{50}$ = 0.41 μM; PTP1B inhibitor $IC_{50}$ = 3.1 μM. [b]To evaluate the $IC_{50}$ of compounds **34**−**35**, a DiFMUP concentration of 20 μM was used.

docking studies of the parent pyrazolone[37] indicated that this aromatic ring is not engaged in hydrogen bond interactions with the SHP2 enzyme, and thus, we assumed a higher degree of freedom for the modification of this moiety. For example, we synthesized isopropyl-bearing derivative **28**, a known bioisostere for aromatic rings. However, despite this assumption, analogue **28** was lacking any significant activity. We then attempted to outbalance affinity versus solubility by the introduction of a bulky but hydrophilic tosylate group, but the compound **29** showed considerably reduced inhibition of SHP2. Even small changes such as introducing a methylene spacer to enhance conformational flexibility in compounds **30** and **31** resulted in a decrease of activity, indicating detrimental interactions with the protein environment at the catalytic site. The same trend was observed with the meta-methoxy analogue **32**. Installation of a simple unsubstituted phenyl group (compound **33**) resulted in improved activity, but as expected, the solubility was further reduced. In an additional effort to circumvent the solubility limitations, we synthesized azaindazole congener **34** of the most promising compound **19**. We speculated that an azaindazole with an auxiliary nitrogen on the heterocyclic scaffold may enhance solubility and cellular permeability. Unfortunately, the solubility of azaindazole **34** was low, which was reflected in the absence of activity because of precipitation under assay conditions. We further tried to increase the solubility of the azaindazole by incorporating the tetrahydropyran (THP) ether instead of the $R^1$ aromatic ring, but the corresponding azaindazole **35** was only weakly active. Overall, the first iteration in this SAR study again confirmed compound **19** as the best template for the subsequent second optimization round.

Here, we focused our attention on the $R^3$ residue, bearing the carboxylic group (Table 4). This functionality was found to

**Table 4. Second Iteration of SAR Studies**

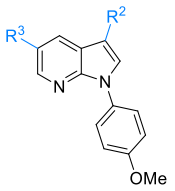


| Compound | $R^3$ | $R^2$ | SHP2 $IC_{50}$ (μM) [a] |
|---|---|---|---|
| **36** |  |  | 6.7 |
| **37** |  |  | 3.4 |
| **38** |  |  | 1.6 |
| **39** |  |  | 2.3 |
| **40** |  |  | 0.075 |
| **41** |  |  | 0.065 |
| **42** |  |  | >10 |
| **43** |  |  | 0.58[b] |
| **44** |  |  | >10[b] |
| **45** |  | 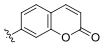 | 0.031[c] |

[a]To evaluate the $IC_{50}$ of the compounds **36**−**42** and **45**, a DiFMUP concentration of 10 μM was used. Reference cmpd values: PHPS1 $IC_{50}$ = 0.062 μM; PTP II-B08 $IC_{50}$ = 12 μM; NSC-87877 $IC_{50}$ = 0.41 μM; PTP1B inhibitor $IC_{50}$ = 3.1 μM. [b]To evaluate the $IC_{50}$ of the compounds **43**-**44**, a DiFMUP concentration of 20 μM was used. [c]PTP1B inhibitor $IC_{50}$ reference value for **45** is 2.5 μM.


https://dx.doi.org/10.1021/acs.jmedchem.0c01265
J. Med. Chem. XXXX, XXX, XXX−XXX

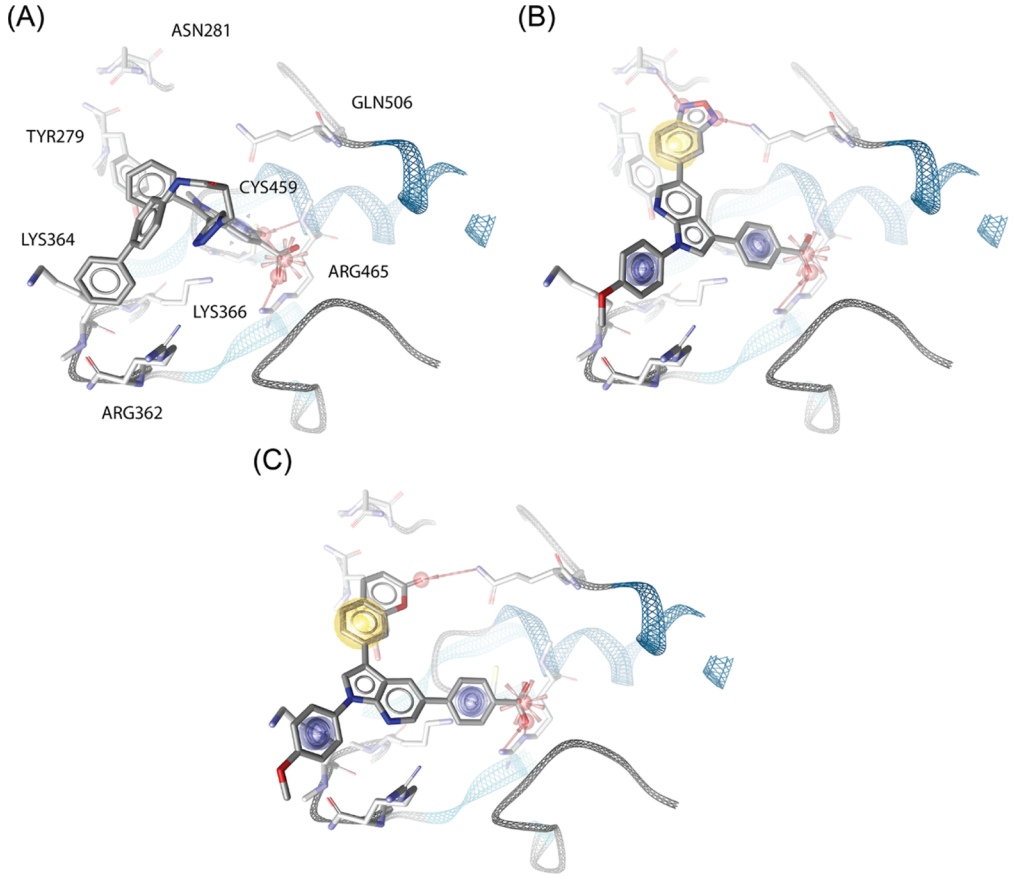


**Figure 2.** Binding mode of cocrystalized ligand (II-B08) of 3O5X[24] (A) and of compounds **41** (B) and **45** (C) observed in docking studies targeting the catalytic domain of SHP2 (PDB entry 3O5X[24]). Yellow sphere—hydrophobic interaction, red arrow—hydrogen bond acceptor, red asterisk—negative ionizable, blue ring—aromatic interaction. Figure produced using LigandScout 4.4.[72]

be pivotal in previous and current studies.[24,25] Therefore, we hypothesized that finding the optimal position in the catalytic pocket addressing ARG465 by salt-bridge formation may be most beneficial for enhanced activity. More flexible and shorter nonaromatic moieties were therefore tethered to provide compounds **36**–**38**. Here, we observed the strong trend of the inhibitor activity improvement with the increase in length and rigidity of the $R^3$ substituent. Thus, the aromatic ring as a spacer was confirmed to have favorable properties for achieving the optimal position and interactions of the carboxylic acid. To validate the importance of a negatively charged carboxylic acid and the flexibility to a further bioisosteric replacement, we constructed ester **39** and sulfonamide **40**. As expected, deletion of the charged carboxylic acid by an ester moiety (**39**) decreased the inhibitor activity significantly. Intriguingly, the sulfonamide acid analogue **40** was highly active, which indicates that a sulfonamide moiety may serve as an appropriate bioisostere of the sulfonic and carboxylic acid in this context.[25,69] Next, taking into consideration the pseudo symmetrical "propeller" nature of the decorated azaindoles, we anticipated that our small-molecule inhibitor may have various possible orientations for occupying the catalytic pocket. To test our hypothesis, we synthesized the analogue **41**, in which the critical affinity generating moieties, that is, the carboxylic acid and the benzoxadiazole at $R^2$ and $R^3$ were inverted. In line with our expectation, **41** was able to inhibit SHP2 with a remarkable $IC_{50}$ = 0.065 $\mu$M. This supported our assumption that the benzoxadiazole and carboxylic groups could be swapped. We speculated that the azaindole bearing two carboxylic acids may exhibit superior activity and may possess synthetic advantages such as one-pot functionalization of 3- and 5-positions. However, the corresponding analogue **42** exhibited surprisingly low inhibitory activity. Replacement of the carboxylic acid at $R^2$ by an aromatic lactone **43** restored the activity; however, the compound was highly unstable and underwent fast hydrolysis to its inactive open carboxylic acid analogue **44** under any storage and assay conditions. To overcome this stability issue and in search for an isomorphic noncharged hybrid moiety, resembling the benzoxadiazole and a hydrolysis-resistant lactone group, we replaced the benzo lactone at residue $R^2$ by a stable coumarine lactone. Gratifyingly, the corresponding compound **45** was found to have the highest inhibitory activity on SHP2 within the entire SAR study with an $IC_{50}$ = 0.031 $\mu$M. We therefore proceeded to investigate the most active azaindole of the series with regard to phosphatase and kinase selectivity and studies in advanced cellular models of metastasis and drug resistance. We also performed docking and molecular dynamic experiments to validate the SAR study findings.

**Structural Basis of Inhibition—Docking and Molecular Dynamics.** To rationalize the SAR of the presented ligand series, compounds were docked into the SHP2 catalytic domain of PDB entry 3O5X[24] using the OpenEye Python Toolkit.[70] The cocrystalized ligand of 3O5X was employed in the hybrid docking method[71] implemented in OEDocking to guide the ligand placement because it contains a benzoic acid similar to the majority of compounds of the investigated ligand series (**17**–**45**).


https://dx.doi.org/10.1021/acs.jmedchem.0c01265
J. Med. Chem. XXXX, XXX, XXX−XXX

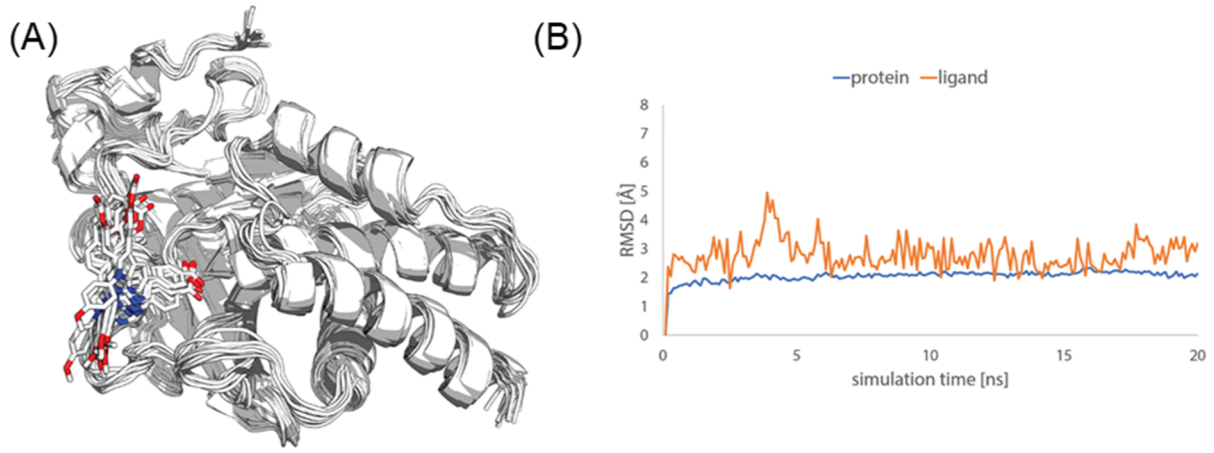


**Figure 3.** Results from a 20 ns MD simulation of SHP2 in complex with the most active compound **45**. (A) Depiction of 10 snapshots taken every 2 ns. (B) rmsd plot for ligand and protein atoms. Figures produced using PyMOL 1.8.6[75] and Microsoft Excel.

Similar to the cocrystalized inhibitor of 3O5X, the most consistent binding mode of docked compounds involves a charge interaction with ARG465 and a $\pi$−cation interaction with LYS366 as identified with LigandScout 4.4[72] (see Figure 1). The hydrogen bonds with the backbone nitrogen of ARG465 and the thiol of CYS459 are only observed in case of the cocrystalized inhibitor of 3O5X, which is consistent with the lack of a hydroxyl group at the benzoic acid moiety of the investigated compound series. Additionally, the identified binding mode involves a hydrophobic contact with TYR279, a further $\pi$−cation interaction with LYS364 and hydrogen bonds with ASN281 and GLN506. This binding mode could be observed for compounds **17**−**21**, **27**, **33**, **41**, and **45**, which all show an $IC_{50}$ below 1 $\mu$M (Supporting Information, Figure S2). Interestingly, albeit the azaindole moiety of the two most active compounds **41** and **45** is placed in two different orientations, the docking poses allow almost identical interactions (see Figure 2). This symmetric behavior can also be observed for compound **19**, in which $R^2$ and $R^3$ are inverted compared to compound **41**, but compound **19** still shows considerable inhibitory potency. The lower potency of compound **19** could thereby be explained by less favorable hydrogen bond interactions formed by the benzoxadiazole moiety, which is perfectly embedded between ASN281 and GLN506 in case of compound **41**. The importance of hydrogen bonds with these two residues is also supported by the decreased activity of compounds **23**, **24**, and **25**, which contain either a pyridine or a pyrimidine group at $R^2$ that are too limited in size to perform suitable hydrogen bonding interactions. In line with that, docking poses indicate an acceptor-like interaction formed by the fluorine atoms of the trifluoromethyl groups of active compounds **21** and **22** with ASN281 and GLN506. However, the lower activity of compound **26** cannot be easily explained with this binding mode because it contains a benzodioxolane that would allow for favorable hydrogen bond interactions similar to the benzoxadiazole moiety of compound **19**. Possibly, the more flexible nonplanar nature of the dioxolane ring prevents the formation of the optimal interactions.

Switching the carboxyl group of $R^3$ from para- (compounds **17**, **19**, **21**, and **23**) to meta-position (compounds **18**, **20**, **22**, and **24**) results in all pairs in a drop of inhibitory potency, which can be rationalized by a less favorable position of the aromatic ring not allowing $\pi$−cation interactions with LYS366 (see Figure 2, Supporting Information Figure S2). The absence of suitable interactions with LYS366 and ARG465 could also explain the reduced activity of compounds **36**, **37**, **38**, and **39** that are either too limited in size, miss the aromatic character needed for $\pi$−cation interactions, or cannot participate in a charged interaction with ARG465. The high activity of compound **40** can be attributed to the relatively low $pK_a$ of the aryl-sulfonamide moiety, making the sulfonamide proton sufficiently acidic for effective hydrogen bond interaction.[69]

The activity results from compounds **28**−**33** clearly indicate a strong preference for rigid structures with an aromatic moiety at $R^3$. Compound **28** lacks any aromatic character on the $R^1$ position and was inactive at a testing concentration of 10 $\mu$M. Compounds **29**−**31** introduce a rotatable bond that may result in an entropic penalty when binding to the catalytic domain of SHP2. Compound **32** was synthesized with the methoxy group in meta-position that may either clash with the protein or point into the solvent, which could explain its reduced activity compared to compound **19** with a methoxy group in para-position. Interestingly, compound **33** with an unsubstituted benzene moiety shows improved inhibitory potency compared to its para-methoxy-substituted counterpart **19**, which is supported by the observation that the methoxy group is not involved in any critical interactions.

The docking poses of compounds **41** and **45** present the most favorable interaction pattern observed within the investigated ligand series, which is also reflected by their superior inhibitory potency. To evaluate the identified binding mode further, the docking pose of the most active compound **45** was subjected to unbiased MD Simulation using Desmond 6.1.[73] An analysis of the root-mean-squared deviation (rmsd) of ligand and protein atoms in VMD 1.9.3[74] revealed a similar behavior for protein and ligand motions (see Figure 3). Although the ligand appears to leave the position after 4 ns, it returns to the initial binding mode quickly. In conclusion, the binding pose stayed stable over 20 ns of MD simulation, which underlines the validity of the identified binding mode.

**Phosphatase Selectivity.** Selective active-site inhibition of PTPs, including SHP2, has proven to be an extremely challenging task, primarily because of the highly conserved and positively charged nature of the PTP active site. We therefore tested the most potent azaindole **45** against a panel of 10 representative PTPs. Selectivity was high and greater than 35-fold for PP1B, PP1A, PTPRC/CD45, DUSP22/MKPX, and


https://dx.doi.org/10.1021/acs.jmedchem.0c01265
J. Med. Chem. XXXX, XXX, XXX−XXX

PTPN2/TC-PTP and satisfyingly good for PTP1B (13-fold) but, however, only moderate with a 4-fold selectivity for the closely related phosphatase SHP1 (Table 5).

**Table 5. Phosphatase Selectivity Evaluation for Compound 45**[a]

| target | $IC_{50}$ ($\mu$M) | selectivity ratio |
|---|---|---|
| SHP2 | 0.031 | |
| PP1B | >100 | >1000 |
| PP1A | >100 | >1000 |
| PP2A alpha/PP2R1A complex | 0.20 | 6 |
| PTPN6/SHP1 | 0.13 | 4.5 |
| PTPRC/CD45 | 1.1 | 35 |
| DUSP22/MKPX | 2.1 | 68 |
| PTPN2/TC-PTP | 1.3 | 41 |
| PTPN7/LC-PTP | 0.13 | 4.5 |
| PTPN12/PTP-PEST | 0.13 | 4.5 |
| PTPN1/PTP1B-CD | 0.41 | 13 |

[a]For full experimental conditions, see Supporting Information, Table S1.

**Evaluation of Kinase Activity.** As the rescaffolding studies of our SHP2 inhibitor yielded the azaindole core as a highly abundant and privileged kinase inhibitor motif in drug discovery,[52,53] we wanted to exclude any off-target kinase activity. The crucial feature for kinase inhibition, in particular when decorated with aromatic moieties at the 3- and 5-positions, is the hydrogen bond donor−acceptor pattern of the unsubstituted NH donor at *N1* and the pyrrolidine nitrogen at the 7-position of azaindoles with the hinge region of kinases.[76] Albeit, in principle, the installation of any functional group at this *N1* nitrogen should abolish off-target kinase activity, we wanted to examine and confirm this against a representative panel of kinases. For comparison, we used the benzofurazan-bearing molecule **46**, which is the truncated analogue of **19** without the crucial substituent at *N1* of the azaindole. Interestingly, several kinase inhibitors incorporate such a benzofurazan moiety.[77−79] Both compounds were tested against a general panel of ten house-keeping kinases at high concentration (100 $\mu$M) and low ATP concentration (10 $\mu$M). As expected, N-substituted azaindoles showed only negligible inhibition of the kinases (Table 6). In contrast, the *N1*-truncated derivative **46** when tested against the same kinase panel was significantly more prone to kinase recognition and showed compelling kinase inhibition for CDK1, AKT1, KDR, RSK1, and TRKA. Moreover, **46** was tested against SHP2 and was 26-fold less active than parent **19** ($IC_{50}$ = 6.1 $\mu$M), highlighting again the significance of the *N1* aryl substitution. Thus, despite apparent structural similarity between inhibitors **46** and **19**, the *N1* aryl moiety turned out to be a prominent selectivity switch driving inhibition toward the desired enzyme class of either phosphatase or kinase. The most active compound **45** was tested against the same panel of kinases and showed low interference (for detailed results see Supporting Information, Table S3).

**Evaluation of Azaindole Inhibitor 45 in Cellular Models of Metastasis and Tumor Resistance.** We next turned our attention to the evaluation of our most active inhibitor **45** in more advanced cellular models of metastasis and drug resistance. First, we investigated if **45** was able to block HGF-induced cell scattering and branching morphogenesis of the human pancreatic adenocarcinoma cell line

**Table 6. Structural Differences and Similarities of Kinase and Phosphatase Inhibitors**[a]

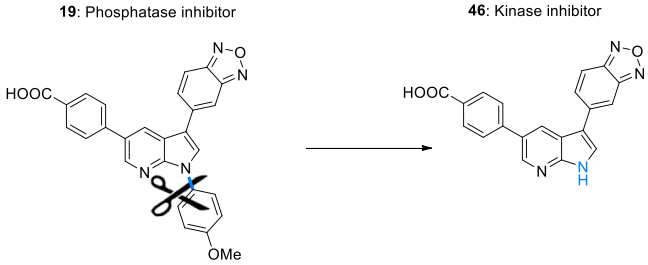


| target | % enzyme inhibition | |
|---|---|---|
| | **19** (100 $\mu$M) | **46** (100 $\mu$M) |
| AKT1 | 35 | 89 |
| c-Src | 35 | 47 |
| CDK1/cyclin B | 13 | 99 |
| EGFR | −35[b] | −95[b] |
| KDR/VEGFR2 | 33 | 92 |
| PDGFRb | 4 | 43 |
| PKA | −43[b] | 51 |
| RIPK2 | −3 | 60 |
| RSK2 | 35 | 95 |
| TRKA | 40 | 97 |

[a]For full experimental conditions, see Supporting Information, Table S2. [b]Negative values might indicate precipitation under assay conditions.

HPAF-II. This cellular system recapitulates the metastatic process of cell spreading and outgrowth and has been shown to be strongly dependent on SHP2 activation.[4,80,81] Compound **45** was tested against HPAF-II pancreatic cancer cells in different concentrations and clearly showed a dose-dependent ability of the azaindole **45** to block the HGF-induced scattering phenotype (Figure 4A,B). Concentration-dependent quantification of the inhibitory effect by analysis of minimum neighbor distances of proximal Hoechst stained nuclei revealed an $IC_{50}$ = 2.6 $\mu$M, while the previous reference pyrazolone GS493 showed an $IC_{50}$ of 3.4 $\mu$M. Blocking of the cell scattering and reversal of this phenotype was further confirmed by impedance measurements as a second independent readout (Figure 4D,E). In addition, **45** showed good cell permeability and intracellular enrichment in the absence of any signs of cell toxicity over 24 h (see Supporting Information, Figure S3). To further confirm and preclude any interference of these results with a perturbation of the cellular viability or any other nonspecific effect, we proceeded to investigate cytotoxicity of **45** in HPAF-II and HepG2 cells in a long-term incubation of 72 h at high concentration of up to 40 $\mu$M. Again, no significant cytotoxic effects could be observed in the relevant concentration range in both cell lines, even under these prolonged incubation times (Figure 4C).

**Compound 45 Blocks Proliferation in Two Drug-Resistant Cancer Cell Lines and Inhibits ERK Signaling.** Previous investigations have shown that simultaneous inhibition of SHP2 and MEK have a synergistic effect and allow for superior tumor growth control in RAS-mutant tumors.[8,9] In addition, cooperative inhibition of BRAF and SHP2 can overcome resistance to BRAF inhibitors mediated by EGFR activation in colon cancer cells.[7] We therefore investigated if **45** in combination with BRAF inhibitor PLX4032 could also block proliferation of BRAF inhibitor-resistant VACO432 colon cancer cells in a colony formation assay. While both


https://dx.doi.org/10.1021/acs.jmedchem.0c01265
J. Med. Chem. XXXX, XXX, XXX−XXX

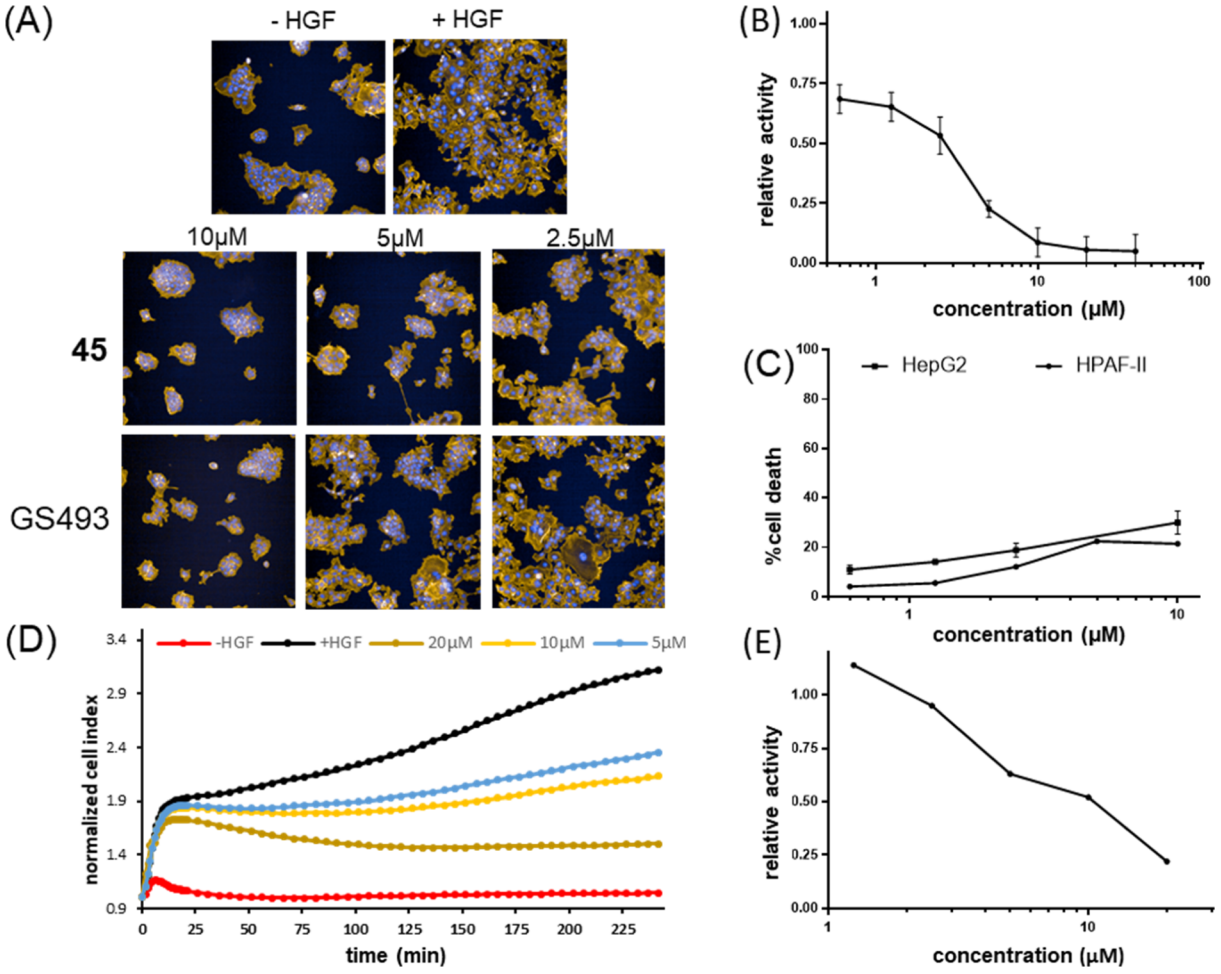


**Figure 4.** Azaindoles inhibit HGF-induced cell separation in scatter and impedance assays in HPAF-II pancreatic cancer cells. (A) The HPAF-II cell colonies were dissociated because of stimulation with HGF in the control cells (−HGF/+HGF). Treatment with compound **45** causes inhibition of cell scattering. (B) Quantification of changes in cell scattering was done by analysis of minimum neighbor distances. The mean ± SD values are shown, representing the relative activity compared to control conditions (+HGF/1, −HGF/0). (C) HPAF-II and HepG2 cells were exposed with different concentrations of compounds for 72 h. Cytotoxicity was determined by fluorescence microscopy using TO-PRO-3 staining for dead cell quantification. Mean values ± SD of damaged cells are indicated. (D) Impedance assay displays the changes in cell attachment and spreading because of HGF stimulation during the first 4 h, where the maximum cell index value was reached for the positive control (+HGF). The normalized cell index curves show a clear dose-dependent inhibition by the compound **45**. (E) Impedance assay dose−response curve. The graph shows the result of the end-point analysis after 4 h HGF exposure and treatment with compound **45**, demonstrating the inhibitory effect. The relative activity of normalized cell index values compared to control conditions (+HGF/1, −HGF/0) are displayed.

PLX4032 and **45** exhibited only a small effect when applied as single compounds, VACO432 cell proliferation was markedly inhibited by **45**/PLX4032 cotreatment (Figure 5A). A similar result was obtained in HCC1806 breast cancer cells, which are resistant to PI3K inhibition by BYL719 (Figure 5B). In this model, **45** sensitized HCC1806 cells considerably to BYL719 treatment, while monotreatment with these compounds was not as effective.

To evaluate the biochemical effect on ERK signaling of **45** and PLX4032 treatment, we subjected treated VACO432 cell lysates to western blotting. Cells treated with PLX4032 alone retained considerable phosphorylated ERK levels after 24 and 48 h. This explains the BRAF inhibitor-resistant phenotype because ERK activity is essential for the proliferation of these cells. In contrast, cotreatment with **45** and PLX4032 led to a substantial decrease in ERK phosphorylation compared to PLX4032 monotreatment (Figure 5C). Taken together, these results show that **45** is capable of preventing a BRAF inhibitor-resistant phenotype in a colon cancer cell line model and a PI3K inhibitor-resistant phenotype in a breast cancer cell line. In VACO432 cells, this is explained by the ability of **45** to effectively inhibit ERK signaling, when used in combination with PLX4032.

## CONCLUSIONS

We identified a novel class of azaindole SHP2 inhibitors, based on scaffold hopping of a previously reported pyrazolone framework and subsequent refinement by SAR optimization. Successful replacement of all physiologically incompatible functionalities provided a much more drug-like lead platform, which incorporates a privileged azaindole core, as well as coumarine and benzofurazan moieties, present in numerous approved drugs. The novel azaindole inhibitors showed high activity against SHP2, with an $IC_{50}$ of 0.031 $\mu$M for **45**. Docking studies aligned well with the observed SAR trends and provided a structural rationalization for the inhibitor binding mode. This could be further supported by molecular dynamic


https://dx.doi.org/10.1021/acs.jmedchem.0c01265
J. Med. Chem. XXXX, XXX, XXX−XXX

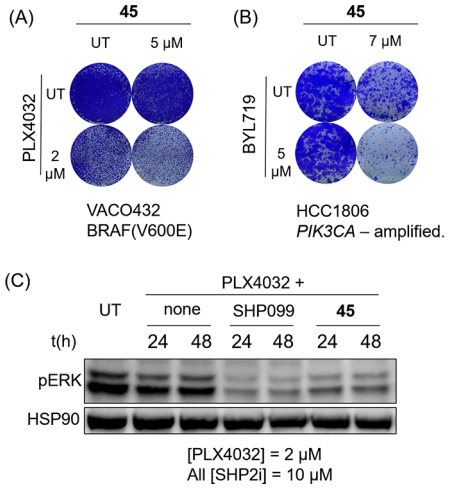


**Figure 5.** Synergistic combination of **45** with BYL719 and PLX4032 in VACO432 and HCC1806 cell lines. (A) *In vitro* coinhibition by PLX4032 (vemurafenib) and SHP2 (**45**) in colony formation experiments with the VACO432 human colorectal cancer cell line. (B) *In vitro* coinhibition by BYL719 (alpelisib) and SHP2 (**45**) in colony formation experiments with the HCC1806 human breast cancer cell line. Three independently repeated experiments were performed with similar results. (C) Blocking of ERK phosphorylation by PLX4032 and **45** cotreatment. Inhibition of ERK feedback reactivation is sustained after 48 h compared to PLX4032 monotreatment.

studies for the most active azaindole **45** showing that the identified binding poses were stable.

SHP2 activity was further cross-validated in advanced cellular assays recapitulating metastatic tumor outgrowth and drug-resistant tumor cells. In impedance and scatter assay treatment of HPAF-II pancreatic cancer cells with **45** led to almost full reversion of an HGF-induced scattering phenotype. Compound **45** exhibited synergistic activity in combination with BYL719 and PLX4032 and was able to inhibit cell proliferation in drug-resistant VACO432 colorectal cancer and HCC1806 breast cancer cells. Remarkably, the azaindole-based inhibitor showed no signs of unspecific cytotoxicity and was not active against a panel of representative kinases, distinguishing it from the parent pyrazolone. In view of recently increased interest toward SHP2 and the urge of finding adequate therapeutic approaches for drug resistance and tumor relapse, we believe that our compounds can serve as a platform for further lead optimization and as a valuable chemical tool for unraveling the (patho-)physiological role of SHP2 in cancer.

## EXPERIMENTAL SECTION

**Chemistry.** All chemicals were purchased from commercial suppliers: Fluorochem, Sigma-Aldrich, and Alfa Aesar and used as received unless otherwise specified. NMR spectra were recorded at either 295 K (300 MHz) or 300 K (600 MHz) at either Bruker AV 300 (300, 75 MHz) or Bruker AV 600 (600, 151 MHz) spectrometers. Chemical shifts are reported in ppm ($\delta$) referenced to TMS ($\delta$ = 0.00 ppm), dimethylsulfoxide (DMSO) (2.50 ppm), and $CHCl_3$ (7.26 ppm). LC/MS analysis was performed on an Agilent LC/MS 1260 analytical HPLC with DAD coupled to an Agilent 6120 single quadrupole mass spectrometer (ESI-SQ) equipped with a Thermo Fisher Scientific Accucore C18 column, 2.1 × 30 mm, 2.6 $\mu$m. Method: ESI$^+$, flux: 0.8 mL/min, 5−95% $CH_3CN$ in $H_2O$ + 0.1% FA, total runtime: 2.5 min. High-resolution mass spectra were recorded on an Agilent 6220A accurate-mass time-of-flight mass spectrometer (ESI-TOF) with Agilent 1200 HPLC/DAD front-end. The HPLC was equipped with an Agilent Poroshell 120, C18 column, 2.1 × 100 mm, 1.8 $\mu$m. Method: ESI$^+$, flux: 0.6 mL/min, 5−99% $CH_3CN$ in $H_2O$ + 0.1% FA, total runtime: 4.5 min. Unless otherwise stated, all compounds were purified using an Isolera one Biotage flash chromatography system utilizing silica gel-packed columns RediSep Rf from Teledyne Isco. Purity and characterization of all final compounds was established by a combination of LC−MS, LC−HRMS, and NMR analytical techniques. All compounds were found to be >95% pure by LC−MS and LC−HRMS analysis unless otherwise stated.

**Synthesis of Carboxamido-indazole 8.** *Methyl 3-(4-Nitrophenyl)-2,3-dioxopropanoate (**47**).* Methyl 3-(4-nitrophenyl)-2,3-dioxopropanoate (**47**) was synthesized according to previously reported procedure.[82] Briefly, methyl 3-(4-nitrophenyl)-3-oxo-2-(triphenyl-l5-phosphaneylidene)propanoate (2.0 g, 4.14 mmol, 1.0 equiv) was dissolved in 10 mL dichloromethane (DCM) and added to a stirred solution of DMSO in acetone (0.1 M, 103 mL). The mixture was stirred for 1 h at room temperature after which the solvent was evaporated. The crude product was purified by column chromatography ($SiO_2$, cyclohexane/ethylacetate 100:0 → 40:60) to obtain **47** in 83% yield (878 mg).

*Methyl 4-(4-Nitrophenyl)-2-phenyl-1H-imidazole-5-carboxylate (**48**).* **47** (878 mg, 3.44 mmol, 1 equiv) and benzaldehyde (0.702 mL, 6.88 mmol, 2 equiv) were added to a slurry of ammonium acetate (2.65 g) in acetic acid (10 mL). The mixture was stirred 2 h at 70 °C, then cooled to room temperature, and concentrated *in vacuo*. The crude mixture was redissolved in ethylacetate and washed with water, $NaHCO_3$, and brine. The ethylacetate layer was dried with $MgSO_4$ and concentrated *in vacuo*. The crude was purified by flash chromatography using EtOAc in cyclohexane as the eluent to obtain **48** in 9% yield (110.2 mg, 0.340 mmol, yellow amorphous solid). LCMS (pos. ESI-TOF): $m/z$ calcd for $C_{17}H_{13}N_3O_4$ 323.30 $(M + H)^+$; found, 323.95 $(M + H)^+$.

*4-(4-Nitrophenyl)-2-phenyl-1H-imidazole-5-carboxylic Acid (**49**).* **48** (110.2 mg, 0.34 mmol, 1 equiv) was dissolved in MeOH (4 mL), and LiOH (2 mL, 1 M) was added. The mixture was stirred for 3 h under microwave irradiation at 90 °C. The progress of the reaction was monitored by LCMS (3.3 min; $M + H^+$ = 309.95). After reaction completion, the mixture was diluted with water and acidified with HCl to a pH = 2−3. The precipitated product was collected by suction filtration. The filter cake was washed with sufficient water and dried in vacuum to yield **49** in 95% (102 mg, 0.329 mmol). The crude product was taken to the next step without further purification.

*4-(4-(4-Nitrophenyl)-2-phenyl-1H-imidazole-5-carboxamido)-benzenesulfonic Acid (**8**).* **49** (100.0 mg, 0.32 mmol, 1 equiv), *p*-sulfanilic acid (56.0 mg, 0.32 mmol, 1 equiv), EDCI (43.7 mg, 0.32 mmol, 1 equiv), HOBT (62.0 mg, 0.32 mmol, 1 equiv), and DMAP (4.0 mg, 0.032 mmol, 0.1 equiv) were stirred in dimethylformamide (DMF) (3 mL) at room temperature for 72 h. The solution was poured to 1 M HCl (5 mL) and extracted with EtOAc 2 × 10 mL. The product was precipitated, and the solids were collected by suction filtration. The filter cake was washed with little EtOAc and dried *in vacuo*, yielding **8** in 27% (40 mg, 0.08 mmol, yellow amorphous solid). $^1$H NMR (300 MHz, DMSO-$d_6$): $\delta$ 10.23 (s, 1H), 8.35 (d, $J$ = 8.8 Hz, 2H), 8.25−8.13 (m, 4H), 7.76 (d, $J$ = 8.5 Hz, 2H), 7.65−7.38 (m, 5H).

**Synthesis of Pyrazolo-triazole 9.** *tert-Butyl 2-Cyano-3-(4-nitrophenyl)-3-oxopropanoate (**50**).* To a stirred suspension of sodium hydride (60%, 400 mg, 10.0 mmol) in tetrahydrofuran (THF) *tert*-butyl-cyano acetate (0.77 mL, 5.39 mmol) was added dropwise at 0 °C, and the reaction mixture was stirred for 30 min. After addition of 4-nitro-benzoic acid chloride (1.00 g, 5.39 mmol), the reaction mixture was allowed to warm to room temperature over a period of 6 h and was brought to pH = 3 by treatment with concentrated HCl. After extraction with $CH_2Cl_2$ (3 × 50 mL), the combined organic layers were dried ($MgSO_4$) and filtered, and the solvent was removed under reduced pressure. *tert*-Butyl 2-cyano-3-(4-nitrophenyl)-3-oxopropanoate (1.56 g, 100%) was obtained as a yellow amorphous solid and used in the next step without further purification. The crude product *tert*-butyl 2-cyano-3-(4-nitrophenyl)-3-oxopropanoate (1.55


https://dx.doi.org/10.1021/acs.jmedchem.0c01265
J. Med. Chem. XXXX, XXX, XXX−XXX

g, 5.34 mmol) was dissolved in AcCN (10 mL), treated with trifluoroacetic acid (TFA) (5 mL) and pyridine (3 mL), and heated under reflux for 22 h. The reaction solution was concentrated in vacuum, the residue was diluted with $H_2O$ and extracted with $CH_2Cl_2$ (4 × 20 mL). The combined organic layers were dried ($MgSO_4$) and filtered, and the solvent was removed under reduced pressure to give **50** (635 mg, 3.34 mmol, 62% over 2 steps) as a yellow amorphous solid. Compound **50** was used in the next step without further purification.

*3-(4-Nitrophenyl)-1-phenyl-1H-pyrazol-5-amine (**51**).* A mixture of nitrile **50** (300 mg, 1.58 mmol) and phenylhydrazine hydrochloride (228 mg, 1.58 mmol) in MeOH (2 mL) was heated at 120 °C for 45 min in a microwave. Filtering of the resulting precipitate and washing with MeOH yield pyrazole **51** (484 mg, 1.53 mmol, 97%) as a colorless amorphous solid. $^1$H NMR (300 MHz, DMSO-$d_6$): $\delta$ 8.27 (d, $J$ = 8.6 Hz, 2H, Ar−H), 8.05 (d, $J$ = 8.7 Hz, 2H, Ar−H), 7.69 (d, $J$ = 7.9 Hz, 2H, Ar−H), 7.55 (t, $J$ = 7.7 Hz, 2H, Ar−H), 7.41 (t, $J$ = 7.3 Hz, 1H, Ar−H), 6.10 (s, 1H, Ar−H), 5.62 (s, 2H, −$NH_2$) ppm. $^{13}$C NMR (75 MHz, DMSO-$d_6$): $\delta$ 149.3, 148.4, 146.8, 140.5, 139.4, 129.7, 127.3, 126.3, 124.5, 123.7, 88.3. HRMS (pos. ESI-TOF): $m/z$ calcd for $C_{15}H_{13}N_4O_2$ 281.1033 $(M + H)^+$; found, 281.1032 $(M + H)^+$.

*(E)-4-((5-Amino-3-(4-nitrophenyl)-1-phenyl-1H-pyrazol-4-yl)-diazenyl)benzenesulfonic Acid (**52**).* Phenylsulfonic acid (570 mg, 3.33 mmol) was dissolved in 2 M HCl (1 mL), and the solution was cooled to 0 °C, followed by addition of $NaNO_2$ (215 mg, 3.12 mmol) in $H_2O$ (2.5 mL). Amine **51** (583 mg, 2.0 mmol) and NaOAc (850 mg) were suspended in EtOH (11 mL) and added dropwise to the reaction mixture. After warming to room temperature, the precipitate was filtered off and washed with $H_2O$. Drying in high vacuum gave **52** (366 mg, 0.75 mmol, 40%) as orange amorphous solid, which was used directly in the next step without further purification. LCMS (pos. ESI-TOF): $m/z$ calcd for $C_{21}H_{16}N_6O_5S^+$ 465.10 $(M + H)^+$; found, 465.03 $(M + H)^+$.

*4-(6-(4-Nitrophenyl)-4-phenylpyrazolo[3,4-d][1,2,3]triazol-2(4H)-yl)benzenesulfonic Acid (**9**).* Diazene **52** (200 mg, 0.39 mmol) was dissolved in anhydrous DMF (8 mL), and $CuSO_4 \cdot 5H_2O$ (96 mg, 0.39 mmol) as well as $K_2CO_3$ (320 mg, 2.32 mmol) was added subsequently. After heating under reflux for 5 h, the solvent was removed, and the solid was washed with $H_2O$ and dried in high vacuum to give **9** (140 mg, 0.30 mmol, 78%) as a brown oily solid. $^1$H NMR (600 MHz, DMSO-$d_6$): $\delta$ 8.51 (d, $J$ = 8.9 Hz, 2H), 8.47 (d, $J$ = 8.8 Hz, 2H), 8.30 (d, $J$ = 8.6 Hz, 2H), 8.15 (d, $J$ = 7.9 Hz, 2H), 7.91 (d, $J$ = 8.7 Hz, 2H), 7.68 (t, $J$ = 7.9 Hz, 2H), 7.39 (t, $J$ = 7.4 Hz, 1H) ppm. HRMS (neg. ESI-TOF): $m/z$ calcd for $C_{21}H_{13}N_6O_5S^-$ 461.0674 $[M - H]^-$; found, 461.0682 $[M - H]^-$.

**Synthesis of Indazole 10.** *tert*-Butyl 5-bromo-3-(4-nitrophenyl)-1*H*-indazole-1-carboxylate (**53**) was prepared utilizing *tert*-butyl 5-bromo-3-iodo-1*H*-indazole-1-carboxylate (29.1 mg, 0.305 mmol, 1 equiv), Pd(dppf)$Cl_2 \cdot CH_2Cl_2$ (29 mg, 0.04 equiv), 4-nitrophenylboronic acid pinacol ester (76.0 mg, 0.305 mmol, 1.0 equiv), and $K_2CO_3$ (1.22 mmol, 0168.9 g, 4 equiv) in degassed dioxane/water (1:3, 0.06 M) at 80 °C for 1 h. The solution was allowed to cool to room temperature, diluted with EtOAc and $H_2O$, and extracted with EtOAc. The combined organic layers were dried with $MgSO_4$ and concentrated *in vacuo*. The crude product was checked by LCMS and contained product **53** (LCMS (ESI$^+$): $m/z$ 440.1/442.0 $(M + Na)^+$, $R_t$ = 1.44 min), and boc-deprotected product (318.1/320.1 $(M + H)^+$, $R_t$ = 1.23 min), and the mixture was taken to the next step without further purification.

5-(4-((Neopentyltrioxidaneyl)thio)phenyl)-3-(4-nitrophenyl)-1*H*-indazole (**54**) was prepared utilizing **53** (ca. 0.305 mmol, 1 equiv, crude, mixture of boc-protected and deprotected azaindole), Pd(dppf)$Cl_2 \cdot CH_2Cl_2$ (30 mg, 0.038 mmol, 0.12 equiv), neopentyl 4-(4,4,5,5-tetramethyl-1,3,2-dioxaborolan-2-yl)benzenesulfonate (134 mg, 0.380 mmol, 1.24 equiv), and $K_2CO_3$ (1.21 mmol, 210 mg, 5 equiv) in degassed dioxane/water (1:3, 0.06 M) at 80 °C for 1 h. The solution was allowed to cool to room temperature, diluted with EtOAc and $H_2O$, and extracted with EtOAc. The combined organic layers were dried with $MgSO_4$ and concentrated *in vacuo*. The crude product was purified by column chromatography to provide title compound **54** (20 mg, 14% for 2 steps, yellow amorphous solid). LCMS: $m/z$ 440.1/442.0 $(M + Na)^+$, $R_t$ = 1.38 min. Alternatively, collected *tert*-butyl 5-(4-((neopentyltrioxidaneyl)thio)phenyl)-3-(4-nitrophenyl)-1*H*-indazole-1-carboxylate may be submitted to a Boc deprotection with TFA in DCM for 2 h to provide **54** in quantitative yield. $^1$H NMR (300 MHz, $CDCl_3$): $\delta$ 8.50−8.36 (m, 2H), 8.29−8.14 (m, 3H), 8.06−7.98 (m, 2H), 7.90−7.67 (m, 4H), 3.77 (s, 2H), 0.96 (s, 11H). LCMS (ESI$^+$): $m/z$ 466.2 $(M + H)^+$.

4-(1-(4-Methoxyphenyl)-3-(4-nitrophenyl)-1*H*-indazol-5-yl)-benzenesulfonic acid (**10**) was prepared as follows: **54** (90 mg, 0.19 mmol, 1 equiv) was dissolved in dioxane (12 mL), and then *trans*-1,2-cyclohexanediamine (21.6 mg, 0.096 mmol, 0.5 equiv), CuI (3.6 mg, 0.0096 mmol, 0.05 equiv), $K_3PO_4$ (84 mg, 0.38 mmol, 2 equiv), and 4-methoxy-1-iodobenzene (9 mg, 0.038 mmol, 1.2 equiv) were added sequentially. The reaction was heated to 100 °C and stirred for 24 h, then solution was allowed to cool to room temperature, diluted with EtOAc and $H_2O$, and extracted with EtOAc. The crude product was dissolved in DMF (2 mL), TBAF (75 mg, 0.69 mmol, 4 equiv) was added, and the reaction stirred for 2 h. The mixture was concentrated *in vacuo* and purified by HPLC (30−100% ACN in water) to yield 4-(1-(4-methoxyphenyl)-3-(4-nitrophenyl)-1*H*-indazol-5-yl)-benzenesulfonic acid **10** (17 mg, 0.034 mmol, 18% for 2 steps, light-orange amorphous solid). $^1$H NMR (300 MHz, DMSO-$d_6$): $\delta$ 8.53−8.37 (m, 4 H), 7.94−7.85 (m, 2H), 7.85−7.68 (m, 6H), 3.92−3.84 (m, 2H), 3.88 (s, 3H). HRMS (pos. ESI-TOF): $m/z$ calcd for $C_{26}H_{19}N_3O_6S$, 502.1067 $[M + H]^+$; found, 502.1054 $[M + H]^+$.

**Synthesis of the Compounds 11 and 17−46.** *General Procedure A: Cham−Lam Coupling of Azaindoles.* To a stirred suspension of 5-bromo-3-iodo-1*H*-pyrrolo[2,3-*b*]pyridine, boronic acid (2.5−3.0 equiv) and $Cu(OAc)_2$ (2.5−3.0 equiv) in DCM (0.026 M), DIPEA (2.5−4.5 equiv) was added in one portion. After stirring for 48 h at room temperature, the mixture was filtered and concentrated *in vacuo*. The crude product was purified by column chromatography ($SiO_2$, cyclohexane/DCM) to yield N-arylated 5-bromo-3-iodo azaindoles.

*5-Bromo-3-iodo-1-(4-methoxyphenyl)-1H-pyrrolo[2,3-b]pyridine (**55**).* General procedure A was applied using 5-bromo-3-iodo-1*H*-pyrrolo[2,3-*b*]pyridine (1.0 g, 3.1 mmol), (4-methoxyphenyl)boronic acid (1.18 g, 7.75 mmol), $Cu(OAc)_2$ (1.41 g, 7.75 mmol) and DIPEA (1.4 mL, 7.75 mmol). The crude product was purified by column chromatography ($SiO_2$, cyclohexane/DCM, 26−50% DCM) to give **55** in 21% yield (270.0 mg, 0.63 mmol, white amorphous solid). $^1$H NMR (300 MHz, $CDCl_3$): $\delta$ 8.39−8.32 (m, 1H), 7.94−7.88 (m, 1H), 7.56−7.47 (m, 3H), 7.08−7.00 (d, $J$ = 8.9 Hz, 2H), 3.87 (s, 3H). $^{13}$C NMR (75 MHz, $CDCl_3$): $\delta$ 158.9, 145.8, 145.4, 133.7, 131.8, 130.3, 125.9 (2C), 125.4, 114.9 (2C), 113.3, 55.8, 54.5. HRMS (pos. ESI-TOF): $m/z$ calcd for $C_{14}H_{11}BrIN_2O$, 428.9094/430.9075 $[M + H]^+$; found, 428.9072/430.9054 $[M + H]^+$.

*5-Bromo-3-iodo-1-isopropyl-1H-pyrrolo[2,3-b]pyridine (**56**).* NaH (60% in oil, 84 mg, 1.36 mmol) was added to a stirred solution of 5-bromo-3-iodo-1*H*-pyrrolo[2,3-*b*]pyridine (400 mg, 1.24 mmol, 1 equiv) in DMF (50 mL) at 0 °C. After stirring of the reaction mixture for 5 min, 2-bromopropane (174 $\mu$L, 1.86 mmol, 1.5 equiv) was added. The mixture was stirred for 1 h at room temperature and then quenched with 50 mL water. The water layer was extracted three times with 50 mL of DCM, and the combined organic layers were dried over $MgSO_4$ and concentrated *in vacuo*. The crude product was extracted two times with 150 mL of hot $Et_2O$. The organic layers were combined, filtered, and evaporated to dryness to give **56** in 88% yield (400 mg, 1.096 mmol). The compound was used directly for the next reaction step without further purification. LCMS (pos. ESI-TOF): $m/z$ calcd for $C_{10}H_{11}BrIN_2$, 364.9/366.9 $[M + H]^+$; found, 364.8/366.8 $[M + H]^+$.

*5-Bromo-3-iodo-1-tosyl-1H-pyrrolo[2,3-b]pyridine (**57**).* To a stirred solution of 5-bromo-3-iodo-1*H*-pyrrolo[2,3-*b*]pyridine (4.00 g, 12.4 mmol) in DMF was added NaH (60%, 573 mg, 14.3 mmol) in small portions. Then, TosCl was added, and the solution was stirred at room temperature for 3 h. After addition of $H_2O$, the precipitate was filtered off, the water layer was extracted three times with 50 mL


https://dx.doi.org/10.1021/acs.jmedchem.0c01265
J. Med. Chem. XXXX, XXX, XXX−XXX

of DCM, and the combined organic layers were dried over $MgSO_4$ and concentrated *in vacuo*. The crude product was purified by column chromatography ($SiO_2$, cyclohexane/DCM, 26−50% DCM) to give **57** (3.23 g, 54%, white amorphous solid). $^1$H NMR (300 MHz, DMSO-$d_6$): $\delta$ 8.55−8.45 (1H, m), 8.22 (s, 1H), 8.04−7.95 (m, 3H), 7.46−7.34 (m, 2H), 2.34 (s, 3H). $^{13}$C NMR (151 MHz, DMSO-$d_6$): $\delta$ 146.1, 146.0, 144.4, 133.9, 132.4, 131.9, 130.2 (2C), 127.7 (2C), 126.6, 115.7, 63.1, 21.1. HRMS (pos. ESI-TOF): $m/z$ calcd for $C_{14}H_{11}BrIN_2O_2S$, 476.8764/478.8744 $[M + H]^+$; found, 476.8743/478.8722 $[M + H]^+$.

*1-Benzyl-5-bromo-3-iodo-1H-pyrrolo[2,3-b]pyridine (**58**).* NaH (60% in oil, 180 mg, 4.5 mmol, 3 equiv) was added to a stirred solution of 5-bromo-3-iodo-1*H*-pyrrolo[2,3-*b*]pyridine (500 mg, 1.5 mmol, 1 equiv) in DMF (50 mL). After stirring of the reaction mixture for 30 min, benzyl bromide (267 $\mu$L, 2.25 mmol, 1.5 equiv) was added. The mixture was stirred for 12 h at room temperature and then quenched with water. The water layer was extracted three times with DCM, and the combined organic layers were dried over $Na_2SO_4$ and concentrated *in vacuo*. The crude product **58** (650 mg) was pure enough as judged by NMR and used for the next reaction step without further purification.

*5-Bromo-3-iodo-1-(4-methoxybenzyl)-1H-pyrrolo[2,3-b]pyridine (**59**).* NaH (60% in oil, 84 mg, 1.36 mmol) was added to a stirred solution of 5-bromo-3-iodo-1*H*-pyrrolo[2,3-*b*]pyridine (400 mg, 1.24 mmol, 1 equiv) in DMF (50 mL) at 0 °C. After stirring of the reaction mixture for 5 min, 4-methoxylbenzyl bromide (267 $\mu$L, 1.86 mmol, 1.5 equiv) was added. The mixture was stirred for 1 h at room temperature and then quenched with 50 mL water. The water layer was extracted three times with 50 mL of DCM, and the combined organic layers were dried over $MgSO_4$ and concentrated *in vacuo*. The crude was extracted two times with 150 mL of $Et_2O$ under reflux. The hot solutions were combined, filtered, and evaporated to dryness. The residue was triturated with 8 mL of $Et_2O$, sonicated for 5 min, filtered, and dried *in vacuo* to give **59** in 49% yield (292 mg, 0.659 mmol). The compound was used directly for the next step without further purification LCMS (pos. ESI-TOF): $m/z$ calcd for $C_{15}H_{13}BrIN_2O$; 442.9/444.9 $[M + H]^+$; found, 442.9/444.8 $[M + H]^+$.

*5-Bromo-3-iodo-1-(3-methoxyphenyl)-1H-pyrrolo[2,3-b]pyridine (**60**).* General procedure A was applied using 5-bromo-3-iodo-1*H*-pyrrolo[2,3-*b*]pyridine (2.0 g, 6.2 mmol), (3-methoxyphenyl)boronic acid (2.36 g, 15.5 mmol), $Cu(OAc)_2$ (2.8 g, 15.5 mmol), and DIPEA (2.72 mL, 15.5 mmol). The crude product was purified by column chromatography ($SiO_2$, cyclohexane/DCM, 26−50% DCM) to give 5-bromo-3-iodo-1-(3-methoxyphenyl)-1*H*-pyrrolo[2,3-*b*]pyridine **60** in 21% yield (535 mg, 1.2 mmol, white amorphous solid). $^1$H NMR (300 MHz, $CDCl_3$): $\delta$ 8.43−8.38 (m, 1H), 7.97−7.89 (m, 1H), 7.63 (s, 1H), 7.43 (d, $J$ = 8.1 Hz, 1H), 7.28−7.16 (m, 2H), 6.94 (ddd, $J$ = 8.4, 2.5, 0.9 Hz, 1H), 3.89 (s, 3H). $^{13}$C NMR (75 MHz, $CDCl_3$): $\delta$ 160.3, 145.5, 145.3, 138.3, 133.2, 131.7, 130.2, 125.6, 116.0, 113.5, 112.7, 110.0, 55.5, 55.3. HRMS (pos. ESI): $m/z$ calcd for $C_{14}H_{11}BrIN_2O$, 428.9094/430.9075 $[M + H]^+$; found, 428.9116/430.9098 $[M + H]^+$.

*5-Bromo-3-iodo-1-phenyl-1H-pyrrolo[2,3-b]pyridine (**61**).* General procedure A was adapted using 5-bromo-3-iodo-1*H*-pyrrolo[2,3-*b*]pyridine (1.5 g, 4.6 mmol), phenylboronic acid (1.7 g, 13.8 mmol, 3 equiv), $Cu(OAc)_2$ (2.5 g, 13.8 mmol, 3 equiv), and DIPEA (3.6 mL, 22.5 mmol, 4.5 equiv) that was added in one portion. After stirring for 48 h at room temperature, the mixture was filtered and concentrated *in vacuo*. The crude product was purified by column chromatography ($SiO_2$, cyclohexane/DCM, 26−50% DCM) to give **61** in 18% yield (340 mg, 0.85 mmol, beige amorphous solid). $^1$H NMR (300 MHz, $CDCl_3$): $\delta$ 8.42−8.32 (m, 1H), 7.95−7.89 (m, 1H), 7.74−7.62 (m, 2H), 7.62 (s, 1H), 7.57−7.45 (m, 2H), 7.46−7.34 (m, 1H). LCMS (pos. ESI-TOF): $m/z$ calcd for $C_{13}H_9BrIN_2$, 398.9/400.9 $[M + H]^+$; found, 398.8/400.8 $[M + H]^+$.

*Methyl 3-Iodo-1-(4-methoxyphenyl)-1H-pyrrolo[2,3-b]pyridine-5-carboxylate (**62**).* General procedure A was applied using methyl 3-iodo-1*H*-pyrrolo[2,3-*b*]pyridine-5-carboxylate (2.22 g, 7.3 mmol), *p*-methoxyphenylboronic acid (2.8 g, 18.0 mmol), $Cu(OAc)_2$ (3.34 g, 18 mmol), and DIPEA (3.6 mL, 18 mmol) that was added in one portion. After stirring for 48 h at room temperature, the mixture was filtered and concentrated *in vacuo*. The crude product was purified by column chromatography ($SiO_2$, cyclohexane/DCM, 26−50% DCM) to give methyl 3-iodo-1-(4-methoxyphenyl)-1*H*-pyrrolo[2,3-*b*]-pyridine-5-carboxylate **62** in 20% yield (588 mg, 1.44 mmol, white amorphous solid). $^1$H NMR (300 MHz, $CDCl_3$): $\delta$ 9.02−8.95 (m, 1H), 8.45−8.37 (m, 1H), 7.59 (s, 1H), 7.58−7.50 (m, 2H), 7.13−7.69 (m, 2H), 3.97 (s, 3H), 3.85 (s, 3H). LCMS (pos. ESI-TOF): $m/z$ calcd for $C_{16}H_{14}IN_2O_3$, 409.0 $[M + H]^+$; found, 408.9 $[M + H]^+$.

*5-Bromo-3-iodo-1-(4-methoxyphenyl)-1H-pyrazolo[3,4-b]-pyridine (**63**).* 5-Bromo-3-iodo-1*H*-pyrazolo[3,4-*b*]pyridine (2.1 g, 6.5 mmol), (4-methoxyphenyl)boronic acid (1.10 g, 7.2 mmol, 1.2 equiv), and $Cu(OAc)_2$ (1.17 g, 6.5 mmol, 1 equiv) were mixed in MeOH (170 mL). After stirring for 48 h at room temperature, the mixture was filtered and concentrated *in vacuo*. The crude product was purified by column chromatography ($SiO_2$, cyclohexane/DCM 74:26 → 50:50) to obtain **63** (590.0 mg, 0.13 mmol, 21%, yellowish amorphous solid). $^1$H NMR (300 MHz, $CDCl_3$): $\delta$ 8.44−8.36 (m, 1H), 7.96−7.92 (m, 1H), 7.60−7.50 (m, 3H), 7.11−7.03 (d, $J$ = 8.9 Hz, 2H), 3.88 (s, 3H). LCMS (pos. ESI-TOF): $m/z$ calcd for $C_{13}H_{10}BrIN_3O$, 429.9/431.9 $[M + H]^+$; found, 429.8/431.8 $[M + H]^+$.

*5-Bromo-3-iodo-1-(tetrahydro-2H-pyran-2-yl)-1H-pyrazolo[3,4-b]pyridine (**64**).* 5-Bromo-3-iodo-1*H*-pyrazolo[3,4-*b*]pyridine (500.0 mg, 1.54 mmol, 1 equiv) was dissolved in EtOAc (9 mL), and then catalytic amounts of *p*-TSA and DHP (260.0 mg, 2.09 mmol, 2 equiv) were added sequentially at room temperature. The mixture was heated to 60 °C and stirred for 12 h. The solution was allowed to cool and concentrated *in vacuo*. The crude product was purified by column chromatography ($SiO_2$, cyclohexane/DCM 74:26 → 50:50) to give 5-bromo-3-iodo-1*H*-pyrazolo[3,4-*b*]pyridine **64** in 80% yield (500 mg, 1.23 mmol, yellowish oily solid). $^1$H NMR (300 MHz, $CDCl_3$): $\delta$ 8.62 (d, $J$ = 2.1 Hz, 1H), 7.98 (d, $J$ = 2.1 Hz, 1H), 6.05 (dd, $J$ = 10.5, 2.5 Hz, 1H), 4.17−4.02 (m, 1H), 3.85−3.65 (m, 1H), 3.57−3.32 (m, 1H), 2.73−2.50 (m, 1H), 2.00 (ddd, $J$ = 15.6, 5.0, 2.8 Hz, 1H), 1.67−1.56 (m, 3H). LCMS (pos. ESI-TOF): $m/z$ calcd for $C_{13}H_{10}BrIN_3O$, 407.9/409.9 $[M + H]^+$; found, 407.9/409.9 $[M + H]^+$.

*General Procedure B: Suzuki Coupling Using Pd(PPh$_3$)$_4$.* Pd-$(PPh_3)_4$ (0.075 equiv) was added to a stirred solution of heterocyclic halide (1 equiv), boronic acid or boronate ester (1.2 equiv), and $NaHCO_3$ (3 equiv) in degassed $H_2O$/MeCN (1:3, 0.02 M) at 100 °C. The resulting reaction mixture was stirred for 12−16 h under $N_2$. The solution was allowed to cool to room temperature, diluted with DCM and $H_2O$, and extracted with DCM. The combined organic layers were dried with $Na_2SO_4$ or $MgSO_4$ and concentrated *in vacuo*. The crude product was purified by column chromatography to yield the substituted product or recrystallization and silica filtration to yield the substituted product or used directly as a crude for the further step.

*General Procedure C: Suzuki Coupling Using Pd(dppf)Cl$_2$.* Heterocyclic halide (1 equiv), $Pd(dppf)Cl_2$ (0.025 equiv), boronic acid or boronate ester (1.0−1.2 equiv), and $K_2CO_3$ (3 equiv) were dissolved in degassed $H_2O$/dioxane (1:3, 0.06 M), and the resulting reaction mixture was stirred for 3−12 h at 80 °C under $N_2$. The solution was allowed to cool to room temperature, diluted with DCM and $H_2O$, and extracted with DCM. The combined organic layers were dried with $Na_2SO_4$ or $MgSO_4$ and concentrated *in vacuo*. The crude product was purified by column chromatography or recrystallization and silica filtration to yield the product. In some cases, the product was pure enough and used without further purification in the subsequent reaction step.

*5-Bromo-(1-(4-methoxyphenyl)-3-(4-nitrophenyl)-1H-pyrrolo-[2,3-b]pyridine) (**65**).* General B was applied using halide **55** (770 mg, 1.795 mmol), 4,4,5,5-tetramethyl-2-(4-nitrophenyl)-1,3-dioxolane (541 mg, 2.153 mmol), $NaHCO_3$ (453.7 mg, 5.38 mmol), and $Pd(PPh_3)_4$ (156 mg, 0.134 mmol) in 70 mL of 3:1 MeCN/$H_2O$. The reaction mixture was diluted with DCM (25 mL) and water (25 mL). The aqueous phase was extracted three times with DCM (25 mL). The organic phases were combined, dried over $MgSO_4$, and evaporated to dryness. The crude residue was boiled with 10 mL of MeOH, sonicated, and filtered to yield crude 5-bromo-1-(4-


https://dx.doi.org/10.1021/acs.jmedchem.0c01265
J. Med. Chem. XXXX, XXX, XXX−XXX

methoxyphenyl)-3-(4-nitrophenyl)-1*H*-pyrrolo[2,3-*b*]pyridine **65** (300 mg, 0.131 mmol, amorphous orange solid). The compound was directly used in the next reaction step without further purification. LCMS (ESI): *m*/*z* calcd for $C_{20}H_{15}BrN_3O_3$, 424.0/426.0[M + H]$^+$; found, 423.9/425.9 [M + H]$^+$.

*5-(5-Bromo-1-(4-methoxyphenyl)-1H-pyrrolo[2,3-b]pyridin-3-yl)-benzo[c][1,2,5]oxadiazole (**66**).* General procedure B was applied using halide **55** (300 mg, 0.7 mmol), benzo[*c*][1,2,5]oxadiazole-5-boronic acid pinacol ester (206 mg, 0.84 mmol), $NaHCO_3$ (176 mg, 2.1 mmol), $Pd(PPh_3)_4$ (61 mg, 0.05 mmol), and 35 mL of 3:1 MeCN/$H_2O$. Purification of the crude by flash column chromatography ($SiO_2$, 0−30% ethyl acetate in cyclohexane) yielded 5-(5-bromo-1-(4-methoxyphenyl)-1*H*-pyrrolo[2,3-*b*]pyridin-3-yl)benzo-[*c*][1,2,5]oxadiazole **66** in 51% yield (150 mg, 0.36 mmol, yellow amorphous solid). $^1$H NMR (300 MHz, $CDCl_3$): $\delta$ 8.49−8.43 (m, 2H), 8.02 (s, 1H), 7.94 (dd, *J* = 9.5 Hz, 1.0, 1H), 7.83 (s, 1H), 7.74 (dd, *J* = 9.4, 1.4 Hz, 1H), 7.66−7.54 (m, 2H), 7.15−7.06 (m, 2H), 3.92 (s, 3H). $^{13}$C NMR (75 MHz, DMSO-$d_6$): $\delta$ 158.2, 149.7, 148.1, 146.1, 144.3, 136.9, 133.7, 131.2, 129.9, 129.5, 125.6 (2C), 119.7, 116.4, 114.4, 113.4 (2C), 112.6, 109.3, 55.5. HRMS (pos. ESI-TOF): *m*/*z* calcd for $C_{20}H_{14}BrN_4O_2$, 421.0295/423.0277 [M + H]$^+$; found, 421.0272/423.0252 [M + H]$^+$.

*5-Bromo-1-(4-methoxyphenyl)-3-(4-(trifluoromethyl)phenyl)-1H-pyrrolo[2,3-b]pyridine (**67**).* General procedure C was applied using halide **55** (300 mg, 0.69 mmol), 4-trifluorohenylboronic acid (146 mg, 0.77 mmol), $K_2CO_3$ (290 mg, 2.1 mmol), and $Pd(dppf)Cl_2$ (13 mg, 0.017 mmol) in 13 mL of 3:1 dioxane/$H_2O$. Purification of the crude product by flash column chromatography ($SiO_2$, 0−40% ethyl acetate in cyclohexane, slow gradient) provided 5-bromo-1-(4-methoxyphenyl)-3-(4-(trifluoromethyl)phenyl)-1*H*-pyrrolo[2,3-*b*]-pyridine **67** in 39% yield (122 mg, 0.27 mmol, white amorphous solid). $^1$H NMR (300 MHz, $CDCl_3$): $\delta$ 8.47−8.39 (m, 1H), 8.38−8.29 (m, 1H), 7.76−7.70 (m, 4H), 7.62 (s, 1H), 7.60 (d, *J* = 8.5 Hz, 2H), 7.07 (d, *J* = 8.3 Hz, 2H), 3.88 (s, 3H). LCMS (pos. ESI-TOF): *m*/*z* calcd for $C_{21}H_{15}BrF_3N_2O$, 447.0/449.0 [M + H]$^+$; 447.1/449.1 [M + H]$^+$.

*5-Bromo-1-(4-methoxyphenyl)-3-(pyridin-4-yl)-1H-pyrrolo[2,3-b]pyridine (**68**).* General procedure C was applied using halide **55** (280 mg, 0.65 mmol), 3,4-pyridinylboronic acid (79 mg, 0.65 mmol), $K_2CO_3$ (269 mg, 1.95 mmol), and $Pd(dppf)Cl_2$ (11 mg, 0.015 mmol) in 8 mL of 3:1 dioxane/$H_2O$. Purification of the crude product by flash column chromatography ($SiO_2$, 0−100% EtOAc in cyclohexane) yielded 5-bromo-1-(4-methoxyphenyl)-3-(pyridin-4-yl)-1*H*-pyrrolo-[2,3-*b*]pyridine **68** in 34% yield (85 mg, 0.22 mmol, white amorphous solid). $^1$H NMR (300 MHz, $CDCl_3$): $\delta$ 8.79−8.65 (m, 2H), 8.54−8.37 (m, 2H), 7.82 (s, 1H), 7.69−7.53 (m, 4H), 7.20−7.01 (m, 2H), 3.89 (s, 3H). LCMS (ESI): *m*/*z* calcd for $C_{19}H_{15}BrN_3O$, 380.0/382.0 [M + H]$^+$; found, 380.0/382.0 [M + H]$^+$.

*5-Bromo-1-(4-methoxyphenyl)-3-(pyrimidin-5-yl)-1H-pyrrolo-[2,3-b]pyridine (**69**).* General procedure C was applied using halide **55** (200 mg, 0.46 mmol), 3-5,5-pyrimidinboronic acid (57 mg, 0.46 mmol), $K_2CO_3$ (192 mg, 1.3 mmol), and $Pd(dppf)Cl_2$ (9 mg, 0.012 mmol) in 6 mL of 6:2 dioxane/$H_2O$. Purification of the crude product by flash column chromatography ($SiO_2$, 0−100% EtOAc in cyclohexane) yielded 5-bromo-1-(4-methoxyphenyl)-3-(pyrimidin-5-yl)-1*H*-pyrrolo[2,3-*b*]pyridine in an inseparable mixture with triphenylphosphine oxide. The impure product **69** was used for the next reaction step without further purification.

*3-(Benzo[d][1,3]dioxol-5-yl)-5-bromo-1-(4-methoxyphenyl)-1H-pyrrolo[2,3-b]pyridine (**70**).* General procedure B was applied using halide **55** (300 mg, 0.69 mmol), benzo[*d*][1,3]dioxol-5-ylboronic acid (138 mg, 0.82 mmol), $NaHCO_3$ (174 mg, 2.0 mmol), and $Pd(PPh_3)_4$ (60 mg, 0.05 mmol) in 40 mL of 3:1 MeCN/$H_2O$. Purification of the crude product by flash column chromatography ($SiO_2$, 0−40% ethyl acetate in cyclohexane, slow gradient) yielded 3-(benzo[*d*][1,3]-dioxol-5-yl)-5-bromo-1-(4-methoxyphenyl)-1*H*-pyrrolo[2,3-*b*]-pyridine **70** in 42% yield (124 mg, 0.29 mmol, white amorphous solid). $^1$H NMR (300 MHz, $CDCl_3$): $\delta$ 8.47−8.38 (m, 1H), 8.38−8.27 (m, 1H), 7.68−7.60 (m, 2H), 7.53 (s, 1H), 7.16−7.03 (m, 4H), 7.01−6.89 (m, 1H), 6.02 (s, 2H), 3.87 (s, 3H), $^{13}$C NMR (75 MHz, $CDCl_3$): $\delta$ 158.6, 148.4, 146.7, 146.3, 144.5, 130.9, 130.3, 127.8, 126.3, 125.7 (2C), 121.0, 120.7, 116.0, 114.8 (2C), 112.8, 109.1, 107.9, 101.3, 55.7. LCMS (pos. ESI-TOF): *m*/*z* calcd for $C_{21}H_{16}BrN_2O_3$, 423.0/425.0 [M + H]$^+$; found, 423.07425.0 [M + H]$^+$.

*4-((5-(4-Bromophenyl)-1-(4-methoxyphenyl)-1H-pyrrolo[2,3-b]-pyridin-3-yl)benzonitrile) (**71**).* General procedure C was applied using halide **55** (300 mg, 0.69 mmol), 4-cyanophenylboronic acid (112 mg, 0.77 mmol), $K_2CO_3$ (290 mg, 2.1 mmol), and $Pd(dppf)Cl_2$ (13 mg, 0.017 mmol) in 13 mL of 3:1 dioxane/$H_2O$. After extraction of the water layer with DCM and drying with $Na_2SO_4$, the solution was concentrated under vacuum until the formation of a precipitate. The precipitate was collected by filtration and dried under vacuum to give 4-(5-(4-bromophenyl)-1-(4-methoxyphenyl)-1*H*-pyrrolo[2,3-*b*]-pyridin-3-yl)benzonitrile **71** in 28% yield (78 mg, 0.19 mmol, white amorphous solid). This solid was taken to the next reaction step without further purification as NMR and LCMS analysis revealed that the compound was pure enough.

*5-(5-Bromo-1-isopropyl-1H-pyrrolo[2,3-b]pyridin-3-yl)benzo[c]-[1,2,5]oxadiazole (**72**).* General procedure C was applied using halide **56** (250 mg, 0.564 mmol), benzo[*c*][1,2,5]oxadiazole-5-boronic acid (167 mg, 0.677 mmol), $K_2CO_3$ (233 mg, 1.692 mmol), and $Pd(dppf)Cl_2$ (10.3 mg, 0.014 mmol) in 10 mL of 3:1 dioxane/$H_2O$, and the reaction was stirred at 55 °C. The mixture was diluted with DCM (30 mL) and extracted two times with 10% $K_2CO_3$ solution, followed by brine. The combined organic phases were dried over $MgSO_4$, filtered, and evaporated. The residue was stirred with 10 mL of $Et_2O$ under sonication for 5 min. The supernatant was removed (repeated twice), and the remaining solid was dried *in vacuo*. Purification of the crude product by flash column chromatography ($SiO_2$, 0% to 40% ethyl acetate in cyclohexane, slow gradient) provided 5-(5-bromo-1-isopropyl-1*H*-pyrrolo[2,3-*b*]pyridin-3-yl)-benzo[*c*][1,2,5]oxadiazole **72** in 71% yield (280 mg, 0.784 mmol, yellow amorphous solid). LCMS (pos. ESI-TOF): *m*/*z* calcd for $C_{16}H_{14}BrN_4O$, 357.03/359.03 [M + H]$^+$; found, 357.0/359.0 [M + H]$^+$.

*5-(5-Bromo-1-tosyl-1H-pyrrolo[2,3-b]pyridin-3-yl)benzo[c]-[1,2,5]oxadiazole (**73**).* General procedure B was applied using halide **57** (1.00 g, 2.10 mmol), benzo[*c*][1,2,5]oxadiazole-5-boronic acid pinacol ester (619 mg, 2.520 mmol), $NaHCO_3$ (528 mg, 6.29 mmol), $Pd(PPh_3)_4$ (174 mg, 0.151 mmol) in 100 mL of MeCN, and 33.3 mL of $H_2O$. Purification of the crude product by flash column chromatography ($SiO_2$, 0−100% ethyl acetate in cyclohexane) yielded 5-(5-bromo-1-tosyl-1*H*-pyrrolo[2,3-*b*]pyridin-3-yl)benzo[*c*][1,2,5]-oxadiazole **73** in 69% yield (630 mg, 0.13 mmol, yellow amorphous solid). $^1$H NMR (300 MHz, $CDCl_3$): $\delta$ 8.57−8.52 (m, 1H), 8.34−8.27 (m, 1H), 8.18−8.05 (m, 3H), 7.98 (d, *J* = 9.6 Hz, 2H), 7.72−7.61 (m, 1H), 7.34 (d, *J* = 8.2 Hz, 2H), 2.41 (s, 3H). $^{13}$C NMR (75 MHz, $CDCl_3$): $\delta$ 149.5, 148.5, 146.7, 146.3, 145.8, 135.5, 134.6, 132.2, 131.1, 129.9 (2C), 128.6 (2C), 126.0, 122.2, 117.8, 117.3, 116.1, 112.8, 21.8. HRMS (pos. ESI-TOF): *m*/*z* calcd for $C_{20}H_{14}BrN_4O_3S$, 468.9965 [M + H]$^+$; found, 468.9936 [M + H]$^+$.

*5-(1-Benzyl-5-bromo-1H-pyrrolo[2,3-b]pyridin-3-yl)benzo[c]-[1,2,5]oxadiazole (**74**).* General procedure C was applied using halide **58** (334 mg, 0.809 mmol), benzo[*c*][1,2,5]oxadiazole-5-boronic acid (238 mg, 0.970 mmol), $K_2CO_3$ (336 mg, 2.43 mmol), and $Pd(dppf)Cl_2$ (15 mg, 0.020 mmol) in 13 mL of 3:1 dioxane/$H_2O$. The mixture was diluted with DCM and extracted two times with water, followed by brine. The combined organic phases were dried over $MgSO_4$, filtered, and evaporated. The residue was stirred with $Et_2O$ under sonication for 5 min. The supernatant was removed, and the remaining solid was dried *in vacuo* to give 5-(1-benzyl-5-bromo-1*H*-pyrrolo[2,3-*b*]pyridin-3-yl)benzo[*c*][1,2,5]oxadiazole **74** in 57% yield (188 mg, 0.464 mmol, brown oily solid). The product was used in the next reaction step without further purification. LCMS (pos. ESI-TOF): *m*/*z* calcd for $C_{20}H_{14}BrN_4O$, 405.03/407.03 [M + H]$^+$; found, 404.9/406.9 [M + H]$^+$.

*5-(5-Bromo-1-(4-methoxybenzyl)-1H-pyrrolo[2,3-b]pyridin-3-yl)-benzo[c][1,2,5]oxadiazole (**75**).* General procedure C was applied using halide **59** (250 mg, 0.564 mmol), benzo[*c*][1,2,5]oxadiazole-5-


https://dx.doi.org/10.1021/acs.jmedchem.0c01265
J. Med. Chem. XXXX, XXX, XXX−XXX

boronic acid (167 mg, 0.677 mmol), $K_2CO_3$ (233 mg, 1.692 mmol), and Pd(dppf)$Cl_2$ (10.3 mg, 0.014 mmol) in 10 mL of 3:1 dioxane/$H_2O$. The mixture was diluted with DCM (30 mL) and extracted two times with 10% $K_2CO_3$ solution, followed by brine. The combined organic phases were dried over $MgSO_4$, filtered, and evaporated. The residue was stirred with 10 mL of $Et_2O$ under sonication for 5 min. The supernatant was removed (repeated twice), and the remaining solid was dried *in vacuo* to give 5-(5-bromo-1-(4-methoxybenzyl)-1*H*-pyrrolo[2,3-*b*]pyridin-3-yl)benzo[*c*][1,2,5]oxadiazole **75** in quantitative yield (272 mg, 0.625 mmol, brown amorphous solid). The product was taken for the next step without further purification. LCMS (pos. ESI-TOF): *m*/*z* calcd for $C_{21}H_{16}BrN_4O_2$, 435.04/437.04 $[M + H]^+$; found, 434.9/437.0 $[M + H]^+$.

*5-(5-Bromo-1-(3-methoxyphenyl)-1H-pyrrolo[2,3-b]pyridin-3-yl)-benzo[c][1,2,5]oxadiazole (**76**).* General procedure C was applied using halide **60** (535 mg, 1.24 mmol), benzo[*c*][1,2,5]oxadiazole-5-boronic acid pinacol ester (307 mg, 1.24 mmol), $K_2CO_3$ (513 mg, 2.1 mmol), and Pd(dppf)$Cl_2$ (18 mg, 0.05 mmol) in 24 mL of 3:1 dioxane/$H_2O$. Purification of the crude product by flash column chromatography ($SiO_2$, 0−40% ethyl acetate in hexane) yielded 5-(5-bromo-1-(3-methoxyphenyl)-1*H*-pyrrolo[2,3-*b*]pyridin-3-yl)benzo-[*c*][1,2,5]oxadiazole **76** in 43% yield (210 mg, 0.53 mmol, yellow amorphous solid). $^1$H NMR (300 MHz, $CDCl_3$): $\delta$ 8.49 (s, 1H), 8.45 (s, 1H), 8.02 (s, 1H), 7.95 (d, $J$ = 9.3 Hz, 1H), 7.87 (s, 1H), 7.75 (d, $J$ = 9.3 Hz, 1H), 7.53−7.42 (m, 1H), 7.38−7.27 (m, 2H), 6.97 (d, $J$ = 8.3 Hz, 1H), 3.90 (s, 3H). $^{13}$C NMR (75 MHz, $CDCl_3$): $\delta$ 160.6, 149.9, 148.5, 146.6, 145.5, 138.4, 136.9, 132.7, 130.6, 130.5, 128.3, 120.7, 117.4, 116.5, 114.4, 114.0, 113.1, 111.0, 110.7, 55.7. LCMS (pos. ESI-TOF): *m*/*z* calcd for $C_{20}H_{14}BrN_4O_2$, 421.0/423.0 $[M + H]^+$; found, 420.9/423.1 $[M + H]^+$.

*5-(5-Bromo-1-phenyl-1H-pyrrolo[2,3-b]pyridin-3-yl)benzo[c]-[1,2,5]oxadiazole (**77**).* General procedure C was applied using halide **61** (200 mg, 0.5 mmol), benzo[*c*][1,2,5]oxadiazole-5-boronic acid pinacol ester (123 mg, 0.5 mmol), $K_2CO_3$ (207 mg, 1.5 mmol), and Pd(dppf)$Cl_2$ (9.2 mg, 0.0125 mmol) in 10 mL of 3:1 dioxane/$H_2O$. The obtained crude product (117 mg) was analyzed by LCMS and NMR and was pure enough for the next reaction step without further purification.

*5-(5-Bromo-1-(4-methoxyphenyl)-1H-pyrazolo[3,4-b]pyridin-3-yl)benzo[c][1,2,5]oxadiazole (**78**).* General procedure B was applied using halide **63** (300 mg, 0.70 mmol), benzo[*c*][1,2,5]oxadiazole-5-boronic acid pinacol ester (205 mg, 0.84 mmol), $NaHCO_3$ (180 mg, 2.14 mmol), and $Pd(PPh_3)_4$ (59 mg, 0.052 mmol) in 40 mL of 3:1 MeCN/$H_2O$. Purification of the crude product by flash column chromatography (0−50% ethyl acetate in cyclohexane) gave 5-(5-bromo-1-(4-methoxyphenyl)-1*H*-pyrazolo[3,4-*b*]pyridin-3-yl)benzo-[*c*][1,2,5]oxadiazole **78** in 38% yield (110 mg, 0.26 mmol, yellow amorphous solid). $^1$H NMR (300 MHz, $CDCl_3$): $\delta$ 8.74−8.68 (m, 1H), 8.70−8.57 (m, 1H), 8.41−8.27 (m, 2H), 8.19−8.09 (m, 2H), 8.07−7.94 (m, 1H), 7.16−7.07 (m, 2H), 3.90 (s, 3H). $^{13}$C NMR (75 MHz, $CDCl_3$): $\delta$ 158.8, 150.6, 149.6, 149.5, 149.0, 140.2, 135.8, 132.1, 131.9, 131.8, 123.6 (2C), 117.4, 116.2, 114.7, 114.6 (2C), 112.9, 77.2, 55.8.

*5-(5-Bromo-1-(tetrahydro-2H-pyran-2-yl)-1H-pyrazolo[3,4-b]-pyridin-3-yl)benzo[c][1,2,5]oxadiazole (**79**).* General procedure B was applied using halide **64** (385 mg, 0.94 mmol), benzo[*c*][1,2,5]-oxadiazole-5-boronic acid pinacol ester (280 mg, 1.1 mmol), $NaHCO_3$ (235 mg, 2.8 mmol), and $Pd(PPh_3)_4$ (81 mg, 0.07 mmol) in 55 mL of 3:1 MeCN/$H_2O$. Purification of the crude product by flash column chromatography (0−40% ethylacetate in cyclohexane) gave 5-5-(5-bromo-1-(tetrahydro-2*H*-pyran-2-yl)-1*H*-pyrazolo[3,4-*b*]pyridin-3-yl)benzo[*c*][1,2,5]oxadiazole **79** in 54% yield (200 mg, 0.5 mmol, yellow amorphous solid). $^1$H NMR (300 MHz, $CDCl_3$): $\delta$ 8.67 (d, $J$ = 2.1 Hz, 1H), 8.57 (d, $J$ = 2.1 Hz, 1H), 8.37−8.20 (m, 2H), 7.96 (dd, $J$ = 9.7, 0.8 Hz, 1H), 6.20 (dd, $J$ = 10.4, 2.6 Hz, 1H), 4.28−4.09 (m, 1H), 4.00−3.78 (m, 1H), 2.85−2.62 (m, 1H), 2.30−2.14 (m, 1H), 2.11−1.98 (m, 1H), 1.93−1.57 (m, 3H).

*Methyl 4-(5-Bromo-1-(4-methoxyphenyl)-1H-pyrrolo[2,3-b]-pyridin-3-yl)benzoate (**80**).* General procedure C was applied using halide **55** (304 mg, 0.71 mmol), 4-methoxycarbonylphenylboronic acid (127 mg, 0.71 mmol), $K_2CO_3$ (293 mg, 2.11 mmol), and 13 mg (0.017 mmol) of Pd(dppf)$Cl_2$, 13 mL of 3:1 dioxane/$H_2O$. Purification of the crude product by flash column chromatography ($SiO_2$, 0−50% EtOAc in cyclohexane) yielded methyl 4-(5-bromo-1-(4-methoxyphenyl)-1*H*-pyrrolo[2,3-*b*]pyridin-3-yl)benzoate **80** in 22% yield (65 mg, 0.15 mmol, white amorphous solid). $^1$H NMR (300 MHz, $CDCl_3$): $\delta$ 8.45−8.34 (m, 2H), 8.15 (d, $J$ = 8.2 Hz, 2H), 7.77−7.66 (m, 3H), 7.61 (d, $J$ = 8.4 Hz, 2H), 7.07 (d, $J$ = 8.2 Hz, 2H), 3.96 (s, 3H), 3.88 (s, 3H). LCMS (ESI): *m*/*z* calcd for $C_{22}H_{18}BrN_2O_3$, 437.1/439.1 $[M + H]^+$; found, 436.9/438.9 $[M + H]^+$.

*6-(5-Bromo-1-(4-methoxyphenyl)-1H-pyrrolo[2,3-b]pyridin-3-yl)-isobenzofuran-1(3H)-one (**81**).* General procedure B coupling was applied using **55** (200 mg, 0.47 mmol), 6-(4,4,5,5-tetramethyl-1,3,2-dioxaborolan-2-yl)isobenzofuran-1(3*H*)-one (145 mg,0.56 mmol), $NaHCO_3$ (117 mg, 1.4 mmol) $Pd(PPh_3)_4$ (38 mg, 0.034 mmol), and 35 mL of 3:1 MeCN/$H_2O$. The crude mixture was cooled to room temperature and filtrated. The resulted filtrate was dissolved in DCM and extracted with water. The organic phase was concentrated *in vacuo* to provide crude 6-(5-bromo-1-(4-methoxyphenyl)-1*H*-pyrrolo[2,3-*b*]pyridin-3-yl)isobenzofuran-1(3*H*)-one **81** in 25% yield. Because of a rapid hydrolysis of the lactone, the crude product was taken to the next step without further purification.

*7-(5-Bromo-1-(4-methoxyphenyl)-1H-pyrrolo[2,3-b]pyridin-3-yl)-2H-chromen-2-one (**82**).* General procedure C was applied using halide **55** (159.6 mg, 0.373 mmol), 7-(4,4,5,5-tetramethyl-1,3,2-dioxaborolan-2-yl)-2*H*-chromen-2-one (121.8 mg, 0.447 mmol), $K_2CO_3$ (154.6 mg, 1.119 mmol), and Pd(dppf)$Cl_2$ (6.8 mg, 0.009 mmol) in 7.5 mL of 3:1 dioxane/$H_2O$, and the reaction was stirred at 55 °C. The mixture was diluted with DCM (30 mL) and extracted two times with 5% $K_2CO_3$ solution, followed by brine. The combined organic phases were dried over $MgSO_4$, filtered, and evaporated. Purification of the crude product by flash column chromatography ($SiO_2$, 0−50%) THF in DCM provided 7-(5-bromo-1-(4-methoxyphenyl)-1*H*-pyrrolo[2,3-*b*]pyridin-3-yl)-2*H*-chromen-2-one **82** in 30% yield (50 mg, 0.111 mmol, yellow amorphous solid). LCMS (pos. ESI-TOF): *m*/*z* calcd for $C_{23}H_{16}BrN_2O_3$, 447.03/449.02 $[M + H]^+$; found, 446.9/449.0 $[M + H]^+$.

*4-(1-(4-Methoxyphenyl)-3-(4-nitrophenyl)-1H-pyrrolo[2,3-b]-pyridin-5-yl)benzenesulfonic Acid (**11**).* Compound **11** was synthesized according to general procedure B using halide **65** (100 mg, 0.236 mmol), (4-((neopentyloxy)sulfonyl)phenyl)boronic acid (354.3 mg, 0.377 mmol), $NaHCO_3$ (79.3 mg, 0.944 mmol), and $Pd(PPh_3)_4$ (20.5 mg, 0.018 mmol) in 10 mL of 3:1 MeCN/$H_2O$. The reaction mixture was diluted with DCM (30 mL), more water (25 mL) was added, and the solution was extracted four times with 30 mL of 4:1 DCM/THF. The combined organic layers were dried over $MgSO_4$, filtered, and evaporated *in vacuo*. The crude residue was sonicated with 10 mL of 9:1 $Et_2O$/DCM for 5 min, and centrifuged. The supernatant was removed, and the remaining was solid dried *in vacuo*. The compound was dissolved in 2.5 mL of DMF, 130 mg (1.186 mmol) of tetramethylammonium chloride was added, and the solution was refluxed overnight. After cooling to room temperature, a yellow precipitate was formed, isolated by filtration, and refluxed in 1 mL of DMF. After cooling to room temperature, the yellow suspension was filtered through a Buchner funnel. The solid was washed with 5 mL of EtOH, 10 mL of EtOAc, and 10 mL of $Et_2O$ and dried *in vacuo* to give 4-(1-(4-methoxyphenyl)-3-(4-nitrophenyl)-1*H*-pyrrolo[2,3-*b*]pyridin-5-yl)benzenesulfonic acid **11** in 10% yield (12 mg, 0.024 mmol, amorphous yellow solid). $^1$H NMR (300 MHz, DMSO-$d_6$): $\delta$ 8.90−8.76 (m, 2H), 8.73−8.64 (m, 1H), 8.46−8.28 (m, 4H), 8.24 (d, $J$ = 8.8 Hz, 2H), 8.18 (d, $J$ = 8.7 Hz, 2H), 7.87 (d, $J$ = 8.8 Hz, 2H), 7.18 (d, $J$ = 8.9 Hz, 2H), 3.86 (s, 3H). HRMS (pos. ESI-TOF): *m*/*z* calcd for $C_{26}H_{20}N_3O_6S$, 502.1067 $[M + H]^+$; found, 502.1054 $[M + H]^+$.

*4-(1-(4-Methoxyphenyl)-3-(4-nitrophenyl)-1H-pyrrolo[2,3-b]-pyridin-5-yl)benzoic Acid (**17**).* Compound **17** was synthesized according to general procedure B using 75 mg (0.177 mmol) of halide **65** (75 mg, 0.177 mmol), 4-carboxyphenylboronic acid (35.2 mg, 0.212 mmol), $NaHCO_3$ (44.6 mg, 0.531 mmol), and $Pd(PPh_3)_4$


https://dx.doi.org/10.1021/acs.jmedchem.0c01265
J. Med. Chem. XXXX, XXX, XXX−XXX

(25.3 mg, 0.013 mmol) in 7.5 mL of 3:1 MeCN/$H_2O$. The reaction mixture was diluted with DCM (30 mL), more water (25 mL) was added, and the solution was extracted once with dichlormethane. Then, the water layer was acidified until the formation of an orange precipitate and extracted four times with 30 mL of 4:1 DCM/THF. The combined organic layers were dried over $MgSO_4$, filtered, and evaporated *in vacuo*. The crude product was purified by column chromatography ($SiO_2$, THF in DCM, 0−50% + 0.01% AcOH). The combined fractions were evaporated, and the residue was sonicated with 1 mL of DCM for 5 min and centrifuged. The supernatant was removed, and the remaining solid was dried *in vacuo* to give 4-(1-(4-methoxyphenyl)-3-(4-nitrophenyl)-1*H*-pyrrolo[2,3-*b*]pyridin-5-yl)-benzoic acid **17** in 36% yield (30 mg, 0.064 mmol, orange amorphous solid). $^1$H NMR (600 MHz, DMSO-$d_6$): $\delta$ 8.81−8.76 (m, 2H), 8.64 (s, 1H), 8.32 (d, $J$ = 8.9 Hz, 2H), 8.23 (d, $J$ = 8.9 Hz, 2H), 8.07 (d, $J$ = 8.4 Hz, 2H), 7.99 (d, $J$ = 8.3 Hz, 2H), 7.87 (d, $J$ = 8.9 Hz, 2H), 7.17 (d, $J$ = 8.9 Hz, 2H), 3.86 (s, 3H). $^{13}$C NMR (151 MHz, DMSO-$d_6$): $\delta$ 167.2, 158.2, 147.5, 145.2, 143.1, 142.5, 141.2, 130.4, 130.0, 130.0 (2C), 129.5, 127.4 (2C), 127.2 (2C), 126.9, 125.5 (2C), 124.3 (2C), 118.3, 114.4 (2C), 113.6, 55.6. HRMS (pos. ESI-TOF): $m/z$ calcd for $C_{27}H_{20}N_3O_5$, 465.1325 [M+]$^+$; found, 465.1296 [M+]$^+$.

*3-(1-(4-Methoxyphenyl)-3-(4-nitrophenyl)-1H-pyrrolo[2,3-b]-pyridin-5-yl)benzoic Acid (**18**).* Compound **18** was synthesized according to general procedure B using halide **65** (75 mg, 0.177 mmol), 4-carboxyphenylboronic acid (35.2 mg, 0.212 mmol), $NaHCO_3$ (44.6 mg, 0.531 mmol), and $Pd(PPh_3)_4$ (25.3 mg, 0.013 mmol) in 7.5 mL of 3:1 MeCN/$H_2O$. The reaction mixture was diluted with DCM (30 mL), more water (25 mL) was added, and the solution was extracted with DCM. The water layer was acidified until the formation of an orange precipitate and extracted four times with 30 mL of 4:1 DCM/THF. The combined organic layers were dried over $MgSO_4$, filtered, and evaporated *in vacuo*. The crude residue was purified by column chromatography (THF in DCM, 0−50% + 0.01% AcOH). The combined fractions were evaporated, and the residue was sonicated with 1 mL of DCM for 5 min and centrifuged. The supernatant was removed, and the remaining solid was dried *in vacuo* to give 3-(1-(4-methoxyphenyl)-3-(4-nitrophenyl)-1*H*-pyrrolo[2,3-*b*]pyridin-5-yl)benzoic acid **18** in 34% yield (28 mg, 0.060 mmol, amorphous orange solid). $^1$H NMR (600 MHz, DMSO-$d_6$): $\delta$ 8.75−8.67 (m, 2H), 8.62 (s, 1H), 8.37−8.27 (m, 3H), 8.24−8.19 (m, 2H), 8.12−8.04 (m, 1H), 8.01−7.96 (m, 1H), 7.90−7.81 (m, 2H), 7.66 (t, $J$ = 7.7 Hz, 1H), 7.17 (d, $J$ = 9.0 Hz, 2H), 3.86 (s, 3H). $^{13}$C NMR (151 MHz, DMSO-$d_6$): $\delta$ 167.2, 158.0, 147.3, 145.1, 142.9, 141.2, 138.8, 132.0, 131.6, 130.3, 129.9, 129.8, 129.4, 128.2, 128.0, 127.1 (2C), 126.7, 125.5 (2C), 124.3 (2C), 118.2, 114.4 (2C), 113.5, 55.5. HRMS (pos. ESI-TOF): $m/z$ calcd for $C_{27}H_{20}N_3O_5$, 466.1397 [M + H]$^+$; found, 466.1376 [M + H]$^+$.

*4-(3-(Benzo[c][1,2,5]oxadiazol-5-yl)-1-(4-methoxyphenyl)-1H-pyrrolo[2,3-b]pyridin-5-yl)benzoic Acid (**19**).* General procedure B was applied using halide **66** (100 mg, 0.24 mmol), 4-carboxyphenylboronic acid (47 mg, 0.28 mmol), $NaHCO_3$ (60 mg, 0.72 mmol), and $Pd(PPh_3)_4$ (21 mg, 0.018 mmol) in 10 mL of 3:1 MeCN/$H_2O$. Purification of the crude product by flash column chromatography ($SiO_2$, 0−10% methanol in DCM) yielded 4-(3-(benzo[*c*][1,2,5]-oxadiazol-5-yl)-1-(4-methoxyphenyl)-1*H*-pyrrolo[2,3-*b*]pyridin-5-yl)-benzoic acid **19** in 30% yield (33 mg, 0.07 mmol, orange amorphous solid). $^1$H NMR (300 MHz, DMSO-$d_6$): $\delta$ 8.90−8.80 (m, 1H), 8.78−8.66 (m, 2H), 8.52 (s, 1H), 8.30 (d, $J$ = 9.0 Hz, 1H), 8.16 (m, 5H), 8.16−7.92 (m, 2H), 7.24−7.07 (m, 2H), 3.87 (s, 3H). $^{13}$C NMR (151 MHz, DMSO-$d_6$): $\delta$ 167.3, 158.1, 149.8, 148.1, 147.5, 143.2, 142.4, 137.4, 133.9, 130.5, 130.3, 129.9 (2C), 129.5, 128.0, 127.5 (2C), 127.3, 125.5 (2C), 118.2, 116.3, 114.4 (2C), 113.5, 109.2, 55.5. HRMS (pos. ESI-TOF): $m/z$ calcd for $C_{27}H_{19}N_4O_4$, 463.1401 [M + H]$^+$; found, 463.1421 [M + H]$^+$.

*3-(3-(Benzo[c][1,2,5]oxadiazol-5-yl)-1-(4-methoxyphenyl)-1H-pyrrolo[2,3-b]pyridin-5-yl)benzoic Acid (**20**).* General procedure B was applied using halide **66** (50 mg, 0.12 mmol), 3-carboxyphenylboronic acid (24 mg, 0.14 mmol), $NaHCO_3$ (30 mg, 0.36 mmol), and $Pd(PPh_3)_4$ (11 mg, 0.009 mmol) in 5 mL of 3:1 MeCN/$H_2O$. Purification of the crude product by flash column chromatography ($SiO_2$, 30−100% ethyl acetate in cyclohexane) yielded 3-(3-(benzo[*c*][1,2,5]oxadiazol-5-yl)-1-(4-methoxyphenyl)-1*H*-pyrrolo-[2,3-*b*]pyridin-5-yl)benzoic acid **20** in 30% yield (14 mg, 0.035 mmol, orange amorphous solid). $^1$H NMR (300 MHz, DMSO-$d_6$): $\delta$ 8.87−8.83 (m, 1H), 8.74−8.68 (m, 2H), 8.52 (s, 1H), 8.34 (s, 1H), 8.29−8.25 (m, 1H), 8.16−8.11 (m, 2H), 8.02−7.97 (m, 1H), 7.90−7.86 (m, 2H), 7.67 (t, $J$ = 7.7 Hz, 1H), 7.22−7.13 (m, 2H), 3.86 (s, 3H) ppm. $^{13}$C NMR (151 MHz, DMSO-$d_6$): $\delta$ 167.3, 158.1, 149.8, 148.1, 147.3, 143.1, 138.7, 137.4, 134.0, 132.0, 131.6, 130.4, 130.3, 129.9, 129.3, 128.2, 128.1, 127.3, 125.5 (2C), 118.2, 116.3, 114.4 (2C), 113.5, 109.2, 55.5. HRMS (pos. ESI-TOF): $m/z$ calcd for $C_{27}H_{19}N_4O_4$, 463.1401 [M + H]$^+$; found, 463.1378 [M + H]$^+$.

*4-(1-(4-Methoxyphenyl)-3-(4-(trifluoromethyl)phenyl)-1H-pyrrolo[2,3-b]pyridin-5-yl)benzoic Acid (**21**).* General procedure B was applied using halide **67** (70 mg, 0.156 mmol), 4-carboxyphenylboronic acid (31.6 mg, 0.190 mmol), $NaHCO_3$ (39.5 mg, 0.470 mmol), $Pd(PPh_3)_4$ (13.5 mg, 0.012 mmol) in 10 mL of 3:1 MeCN/$H_2O$. The reaction mixture was diluted with DCM (50 mL), more water (25 mL) was added, and the solution was extracted one time with DCM. Then, the water layer was acidified until the formation of a precipitate and then extracted four times with 30 mL of a mixture of DCM/THF 4:1. The combined organic layer was dried over $MgSO_4$, filtered, and evaporated *in vacuo*. The crude residue was absorbed on isolute and purified by column chromatography ($SiO_2$, THF in DCM, 0−50%) to obtain 4-(1-(4-methoxyphenyl)-3-(4-(trifluoromethyl)-phenyl)-1*H*-pyrrolo[2,3-*b*]pyridin-5-yl)benzoic acid **21** in 84% yield (64.3 mg, 0.131 mmol, pale pink amorphous solid). $^1$H NMR (600 MHz, DMSO-$d_6$): $\delta$ 8.80−8.74 (m, 1H), 8.74−8.68 (m, 1H), 8.49 (s, 1H), 8.15 (d, $J$ = 8.1 Hz, 2H), 8.06 (d, $J$ = 8.4 Hz, 2H), 7.97 (d, $J$ = 8.4 Hz, 2H), 7.87 (d, $J$ = 8.9 Hz, 2H), 7.83 (d, $J$ = 8.2 Hz, 2H), 7.17 (d, $J$ = 9.0 Hz, 2H), 3.85 (s, 3H). $^{19}$F NMR (564 MHz, DMSO-$d_6$): $\delta$ −60.7. HRMS (pos. ESI-TOF): $m/z$ calcd for $C_{28}H_{20}F_3N_2O$, 489.1421 [M + H]$^+$; found, 489.1441[M + H]$^+$.

*3-(1-(4-Methoxyphenyl)-3-(4-(trifluoromethyl)phenyl)-1H-pyrrolo[2,3-b]pyridin-5-yl)benzoic Acid (**22**).* General procedure B was applied using halide **67** (43 mg, 0.096 mmol), 3-carboxyphenylboronic acid (19.4 mg, 0.117 mmol), $NaHCO_3$ (24.2 mg, 0.288 mmol), and $Pd(PPh_3)_4$ (9.6 mg, 0.008 mmol) in 6 mL of 3:1 MeCN/$H_2O$. The reaction mixture was diluted with DCM (50 mL), more water (25 mL) was added, and the solution was extracted one time with DCM. Then, the water layer was acidified until the formation of a pale yellow precipitate and extracted four times with 30 mL of a mixture of DCM/THF 4:1. The combined organic layers were dried over $MgSO_4$, filtered, and evaporated *in vacuo*. The crude residue was purified by column chromatography ($SiO_2$, THF in DCM, 0−50%) to give 3-(1-(4-methoxyphenyl)-3-(4-(trifluoromethyl)phenyl)-1*H*-pyrrolo[2,3-*b*]pyridin-5-yl)benzoic acid **22** in 98% yield (46.0 mg 0.094 mmol, pale yellow amorphous solid). $^1$H NMR (600 MHz, DMSO-$d_6$): $\delta$ 8.74−8.69 (m, 1H), 8.66−8.63 (m, 1H), 8.50 (s, 1H), 8.37−8.27 (m, 1H), 8.14 (d, $J$ = 8.0 Hz, 2H), 8.10−8.04 (m, 1H), 8.02.-7.98 (m, 1H), 7.92−7.87 (m, 2H), 7.83 (d, $J$ = 8.1 Hz, 2H), 7.64 (t, $J$ = 7.7 Hz, 1H), 7.17 (d, $J$ = 8.9 Hz, 2H), 3.86 (s, 3H). $^{19}$F NMR (564 MHz, DMSO-$d_6$): $\delta$ −60.7. HRMS (pos. ESI-TOF): $m/z$ calcd for $C_{28}H_{20}F_3N_2O$, 489.1421 [M + H]$^+$; found, 489.1438 [M + H]$^+$.

*4-(1-(4-Methoxyphenyl)-3-(pyridin-4-yl)-1H-pyrrolo[2,3-b]-pyridin-5-yl)benzoic Acid (**23**).* Compound **23** was synthesized according to general procedure B using halide **68** (122 mg, 0.321 mmol), 4-carboxyphenylboronic acid (63.9 mg, 0.385 mmol), $NaHCO_3$ (80.9 mg, 0.963 mmol), and $Pd(PPh_3)_4$ (27.8 mg, 0.024 mmol) in 7.5 mL of 3:1 MeCN/$H_2O$. The reaction mixture was diluted with DCM (30 mL), more water (25 mL) was added, and the solution was extracted once with DCM. The organic layer was discarded, and the water layer was acidified and extracted four times with 30 mL of 4:1 DCM/THF. The combined organic layers were dried over $MgSO_4$, filtered, and evaporated *in vacuo*. The crude residue was purified by column chromatography ($SiO_2$, THF in DCM, 0−50%). The combined fractions were evaporated, and the residue was sonicated with 5 mL of $Et_2O$ for 5 min, and then centrifuged. The supernatant was removed, and the remaining was


https://dx.doi.org/10.1021/acs.jmedchem.0c01265
J. Med. Chem. XXXX, XXX, XXX−XXX

solid dried *in vacuo* to give 4-(1-(4-methoxyphenyl)-3-(pyridin-4-yl)-1*H*-pyrrolo[2,3-*b*]pyridin-5-yl)benzoic acid **23** in 23% yield (31 mg, 0.074 mmol, yellow amorphous solid). $^1$H NMR (300 MHz, DMSO-$d_6$): $\delta$ 8.80−8.71 (m, 2H), 8.71−8.55 (m, 3H), 8.10−8.03 (m, 2H), 8.03−7.95 (m, 4H), 7.91−7.80 (m, 2H), 7.23−7.10 (m, 2H), 3.85 (s, 3H). $^{13}$C NMR (151 MHz, DMSO-$d_6$): $\delta$ 167.1, 158.1, 149.6, 147.5, 143.0, 142.5, 141.8, 130.3, 129.9, 129.9 (3C), 129.5, 129.3, 127.4 (2C), 126.8, 125.5 (2C), 121.0 (2C), 118.2, 114.4 (2C), 112.6, 55.5. HRMS (pos. ESI-TOF): $m/z$ calcd for $C_{26}H_{19}N_3O_3$, 421.1426 $[M]^+$; found, 421.1459 $[M]^+$.

*3-(1-(4-Methoxyphenyl)-3-(pyridin-4-yl)-1H-pyrrolo[2,3-b]-pyridin-5-yl)benzoic Acid (**24**).* General procedure C was applied using halide **68** (85 mg, 0.22 mmol), 3-carboxyphenylboronic acid (44 mg, 0.26 mmol), $K_2CO_3$ (91 mg, 0.66 mmol), and Pd(dppf)$Cl_2$ (4 mg, 0.006 mmol) in 4 mL of 3:1 dioxane/$H_2O$. Purification of the crude product by flash column chromatography ($SiO_2$, 0−25% MeOH in DCM) yielded 4-(1-(4-methoxyphenyl)-3-(pyridin-4-yl)-1*H*-pyrrolo[2,3-*b*]pyridin-5-yl)benzoic acid **24** in 10% yield (9.5 mg, 0.022 mmol, white amorphous solid). $^1$H NMR (600 MHz, DMSO-$d_6$): $\delta$ 8.81−8.68 (m, 2H), 8.67−8.62 (m, 3H), 8.32 (s, 1H), 8.10 (d, $J$ = 7.7 Hz, 1H), 8.01 (d, $J$ = 7.7 Hz, 1H), 7.96 (d, $J$ = 5.2 Hz, 2H), 7.87 (d, $J$ = 8.6 Hz, 2H), 7.68 (t, $J$ = 7.7 Hz, 1H), 7.19 (d, $J$ = 8.6 Hz, 2H), 3.88 (s, 3H). $^{13}$C NMR (151 MHz, DMSO-$d_6$): $\delta$ 167.4, 158.1, 150.1 (2C), 142.9, 142.9, 141.4, 138.7, 131.9, 130.4, 129.8, 129.5, 129.4, 128.2, 127.9, 126.8, 125.5 (2C), 120.9 (2C), 118.2, 114.5 (2C), 112.6, 55.5. HRMS (pos. ESI-TOF): $m/z$ calcd for $C_{26}H_{20}N_3O_3$, 422.1499 $[M + H]^+$; found, 422.1489 $[M + H]^+$.

*4-(1-(4-Methoxyphenyl)-3-(pyrimidin-5-yl)-1H-pyrrolo[2,3-b]-pyridin-5-yl)benzoic Acid (**25**).* General procedure B was applied using halide **69** (30 mg, 0.08 mmol), 4-carboxyphenylboronic acid (17 mg, 0.09 mmol), $NaHCO_3$ (21 mg, 0.24 mmol), and Pd(PPh3)$_4$ (6 mg, 0.005 mmol) in 7 mL of 3:1 MeCN/$H_2O$. Purification of the crude product by flash column chromatography ($SiO_2$, 0−25% MeOH in DCM) yielded 4-(1-(4-methoxyphenyl)-3-(pyrimidin-5-yl)-1*H*-pyrrolo[2,3-*b*]pyridin-5-yl)benzoic acid **25** in 25% yield (8.4 mg, 0.019 mmol, white amorphous solid). $^1$H NMR (600 MHz, DMSO-$d_6$): $\delta$ 9.43−9.34 (m, 2H), 9.17 (s, 1H), 8.81−8.73 (m, 2H), 8.63 (s, 1H), 8.12−7.99 (m, 4H), 7.88 (d, $J$ = 8.9 Hz, 2H), 7.20 (d, $J$ = 8.9 Hz, 2H), 3.88 (s, 3H). $^{13}$C NMR (151 MHz, DMSO-$d_6$): $\delta$ 167.2, 158.0, 156.1, 154.3 (2C), 147.2, 143.0, 142.4, 130.4, 129.9 (2C), 129.6, 129.2, 128.8, 128.3, 127.4 (2C), 126.9, 125.4 (2C), 118.2, 114.5 (2C), 108.9, 55.5. HRMS (pos. ESI-TOF): $m/z$ calcd for $C_{25}H_{19}N_4O_3$, $[M + H]^+$ 423.1463; found, $[M + H]^+$ 423.1452.

*4-(3-(Benzo[d][1,3]dioxol-5-yl)-1-(4-methoxyphenyl)-1H-pyrrolo-[2,3-b]pyridin-5-yl)benzoic Acid (**26**).* General procedure B was applied using halide **70** (50 mg, 0.12 mmol), 4-carboxyphenylboronic acid (23 mg, 0.14 mmol), $NaHCO_3$ (30 mg, 0.30 mmol), and $Pd(PPh_3)_4$ (10 mg, 0.009 mmol) in 5 mL of 3:1 MeCN/$H_2O$. Purification of the crude product by flash column chromatography (30−100% ethyl acetate in cyclohexane) yielded 4-(3-(benzo[*d*]-[1,3]dioxol-5-yl)-1-(4-methoxyphenyl)-1*H*-pyrrolo[2,3-*b*]pyridin-5-yl)benzoic acid **26** in 22% yield (12 mg, 0.026 mmol, white amorphous solid). $^1$H NMR (600 MHz, DMSO-$d_6$): $\delta$ 8.74−8.67 (m, 1H), 8.57−8.52 (m, 1H), 8.24 (s, 1H), 8.06 (d, $J$ = 8.3 Hz, 2H), 7.96 (d, $J$ = 8.3 Hz, 2H), 7.89−7.83 (m, 2H), 7.49−7.44 (m, 1H), 7.41−7.33 (m, 1H), 7.19−7.13 (m, 2H), 7.05 (d, $J$ = 8.0 Hz, 1H), 6.09 (s, 2H), 3.86 (s, 3H). $^{13}$C NMR (151 MHz, DMSO-$d_6$): $\delta$ 167.2, 157.6, 147.8, 147.0, 146.0, 142.8, 142.4, 130.8, 130.0 (2C), 129.4, 128.5, 127.8, 127.2 (2C), 126.7, 126.4, 125.0 (2C), 120.3, 118.6, 115.7, 114.3 (2C), 108.8, 107.5, 100.9, 55.4. HRMS (pos. ESI-TOF): $m/z$ calcd for $C_{28}H_{21}N_2O_5$, 465.1445 $[M + H]^+$; found, 465.1449 $[M + H]^+$.

*4-(3-(4-Cyanophenyl)-1-(4-methoxyphenyl)-1H-pyrrolo[2,3-b]-pyridin-5-yl)benzoic Acid (**27**).* General procedure B was applied using halide **71** (73 mg, 0.18 mmol), 4-carboxyphenylboronic acid (33 mg, 0.2 mmol), $NaHCO_3$ (45 mg, 0.54 mmol), and $Pd(PPh_3)_4$ (16 mg, 0.014 mmol) in 8 mL of 3:1 MeCN/$H_2O$. Purification of the crude product by recrystallization from cold DCM, redissolving in EtOAc, and filtration on short plug of silica yielded 4-(3-(4-cyanophenyl)-1-(4-methoxyphenyl)-1*H*-pyrrolo[2,3-*b*]pyridin-5-yl)-benzoic acid **27** in 34% yield (27 mg, 0.035 mmol, white amorphous solid). $^1$H NMR (600 MHz, DMSO-$d_6$): $\delta$ 8.76−8.73 (m, 1H), 8.72−8.69 (m, 1H), 8.57 (s, 1H), 8.16 (d, $J$ = 8.3 Hz, 2H), 8.09 (d, $J$ = 8.3 Hz, 2H), 7.99 (d, $J$ = 8.0 Hz, 2H), 7.94 (d, $J$ = 8.3 Hz, 2H), 7.88 (d, $J$ = 8.9 Hz, 2H), 7.18 (d, $J$ = 8.9 Hz, 2H), 3.86 (s, 3H). $^{13}$C NMR (151 MHz, DMSO-$d_6$): $\delta$ 167.1, 158.0, 147.3, 142.9, 142.5, 138.9, 132.8 (2C), 130.4, 129.9 (2C), 129.5, 129.2, 128.9, 127.3 (2C), 127.1 (2C), 126.7, 125.4 (2C), 119.2, 118.2, 114.4 (2C), 113.9, 108.2, 55.5. HRMS (pos. ESI-TOF): $m/z$ calcd for $C_{28}H_{20}N_3O_3$, 446.1499 $[M + H]^+$; found, 446.1480 $[M + H]^+$.

*4-(3-(Benzo[c][1,2,5]oxadiazol-5-yl)-1-isopropyl-1H-pyrrolo[2,3-b]pyridin-5-yl)benzoic Acid (**28**).* Compound **28** was synthesized according to general procedure B using halide **72** (114 mg, 0.319 mmol), 4-carboxyphenylboronic acid (80.0 mg, 0.383 mmol), $NaHCO_3$ (80 mg, 0.957 mmol), and $Pd(PPh_3)_4$ (27.6 mg, 0.020 mmol) in 10 mL of 3:1 MeCN/$H_2O$. The reaction mixture was diluted with DCM (30 mL), more water (25 mL) was added, and the solution was extracted with DCM. The organic layer was discarded, and the water layer was acidified and extracted four times with 30 mL of 4:1 DCM/THF. The combined organic layers were dried over $MgSO_4$, filtered, and evaporated *in vacuo*. The crude residue was purified by column chromatography ($SiO_2$, THF in DCM, 0−15%). The combined fractions were evaporated, and the residue was sonicated with 5 mL of *n*-pentane for 5 min and centrifuged. The supernatant was removed, and the remaining solid was dried *in vacuo* to give 4-(3-(benzo[*c*][1,2,5]oxadiazol-5-yl)-1-isopropyl-1*H*-pyrrolo-[2,3-*b*]pyridin-5-yl)benzoic acid **28** in 28% yield (36 mg, 0.090 mmol, amorphous yellow solid). $^1$H NMR (600 MHz, DMSO-$d_6$): $\delta$ 8.84−8.77 (m, 1H), 8.74−8.72 (m, 1H), 8.61 (s, 1H), 8.45−8.40 (m, 1H), 8.22 (dd, $J$ = 9.4, 1.5 Hz, 1H), 8.11 (dd, $J$ = 9.4, 0.9 Hz, 1H), 8.08−8.04 (m, 2H), 8.04−7.99 (m, 2H), 5.22 (p, $J$ = 6.8 Hz, 1H), 1.59 (d, $J$ = 6.7 Hz, 6H). $^{13}$C NMR (151 MHz, DMSO-$d_6$): $\delta$ 167.3, 149.9, 148.1, 147.1, 142.4, 139.1, 138.0, 133.9, 132.0, 131.5, 129.3, 129.2, 128.2, 128.1, 128.0, 127.0, 117.5, 116.1, 112.2, 107.9, 45.9, 22.4 (2C). HRMS (pos. ESI-TOF): $m/z$ calcd for $C_{23}H_{19}N_4O_3$, 399.1480 $[M + H]^+$; found, 399.1452 $[M + H]^+$.

*4-(3-(Benzo[c][1,2,5]oxadiazol-5-yl)-1-tosyl-1H-pyrrolo[2,3-b]-pyridin-5-yl)benzoic Acid (**29**).* General procedure B was applied using halide **73** (58 mg, 0.12 mmol), 4-carboxyphenylboronic acid (24 mg, 0.15 mmol), $NaHCO_3$ (30 mg, 0.36 mmol), and $Pd(PPh_3)_4$ (10 mg, 0.008 mmol) in 7 mL of 3:1 MeCN/$H_2O$. Purification of the crude product by flash column chromatography ($SiO_2$, 30−100% ethyl acetate in cyclohexane, with 5% MeOH for complete elution of the product) yielded 4-(3-(benzo[*c*][1,2,5]oxadiazol-5-yl)-1-tosyl-1*H*-pyrrolo[2,3-*b*]pyridin-5-yl)benzoic acid **29** in 11% yield (7 mg, 0.014 mmol, white amorphous solid). $^1$H NMR (300 MHz, DMSO-$d_6$): $\delta$ 8.88−8.81 (m, 1H), 8.81−8.74 (m, 1H), 8.74−8.65 (m, 1H), 8.65−8.57 (m, 1H), 8.28−8.16 (m, 2H), 8.16−8.10 (m, 2H), 8.08−8.02 (m, 2H), 8.03−7.93 (m, 2H), 7.51−7.42 (m, 2H), 2.36 (s, 3H). HRMS (pos. ESI-TOF): $m/z$ calcd for $C_{27}H_{19}N_4O_5S$, 511.1071 $[M + H]^+$; found, 511.1070 $[M + H]^+$.

*4-(3-(Benzo[c][1,2,5]oxadiazol-5-yl)-1-benzyl-1H-pyrrolo[2,3-b]-pyridin-5-yl)benzoic Acid (**30**).* Compound **30** was synthesized according to general procedure B using halide **74** (80 mg, 0.197 mmol), 4-carboxyphenylboronic acid (40.0 mg, 0.236 mmol), $NaHCO_3$ (50.0 mg, 0.591 mmol), and $Pd(PPh_3)_4$ (16.5 mg, 0.014 mmol) in 10 mL of 3:1 MeCN/$H_2O$. The reaction mixture was diluted with DCM (30 mL), more water (25 mL) was added, and the solution was extracted once with DCM. Then, the water layer was acidified and extracted four times with 30 mL of 4:1 DCM/THF. The organic layer was dried over $MgSO_4$, filtered, and evaporated *in vacuo*. The crude residue was purified by column chromatography ($SiO_2$, THF in DCM, 0−50%). The combined fractions were evaporated, and the residue was sonicated with 5 mL of $Et_2O$ for 5 min, and then centrifuged. The supernatant was removed, and the remaining solid was dried *in vacuo* to give 4-(3-(benzo[*c*][1,2,5]oxadiazol-5-yl)-1-benzyl-1*H*-pyrrolo[2,3-*b*]pyridin-5-yl)benzoic acid **30** in 65% yield (57 mg, 0.127 mmol yellow amorphous solid). $^1$H NMR (600 MHz, DMSO-$d_6$): $\delta$ 8.85 (d, $J$ = 2.0 Hz, 1H), 8.76 (d, $J$ = 2.0 Hz, 1H), 8.60 (s, 1H), 8.45 (t, $J$ = 1.2 Hz, 1H), 8.16−8.08 (m, 2H), 8.07 (d, $J$ = 8.4


https://dx.doi.org/10.1021/acs.jmedchem.0c01265
J. Med. Chem. XXXX, XXX, XXX−XXX

Hz, 2H), 8.02 (d, $J$ = 8.4 Hz, 2H), 7.39−7.32 (m, 4H), 7.31−7.25 (m, 1H), 5.61 (s, 2H). $^{13}$C NMR (151 MHz, DMSO-$d_6$): $\delta$ 170.4, 153.0, 151.3, 150.9, 146.2, 145.9, 140.8, 140.8, 136.9, 134.4, 133.1 (2C), 132.6, 132.2, 131.9 (2C), 130.8, 130.7 (2C), 130.6 (2C), 130.5, 120.6, 119.5, 115.7, 111.7, 70.2. HRMS (pos. ESI-TOF): $m/z$ calcd for $C_{27}H_{19}N_4O_3$, 447.1452 [M + H]$^+$; found, 447.1481 [M + H]$^+$.

*4-(3-(Benzo[c][1,2,5]oxadiazol-5-yl)-1-(4-methoxybenzyl)-1H-pyrrolo[2,3-b]pyridin-5-yl)benzoic Acid (**31**).* Compound **31** was synthesized according to general procedure B using halide **75** (117 mg, 0.245 mmol), 4-carboxyphenylboronic acid (50.0 mg, 0.295 mmol), $NaHCO_3$ (61.7 mg, 0.735 mmol), and $Pd(PPh_3)_4$ (21.0 mg, 0.018 mmol) in 10 mL of 3:1 MeCN/$H_2O$. The reaction mixture was diluted with DCM (30 mL), more water (25 mL) was added, and the solution was extracted with DCM. The organic layer was discarded, and the water layer was acidified and extracted four times with 30 mL of 4:1 DCM/THF. The combined organic layers were dried over $MgSO_4$, filtered, and evaporated *in vacuo*. The crude residue was purified by column chromatography ($SiO_2$, THF in DCM, 0−50%). The combined fractions were evaporated, and the residue was sonicated with 5 mL of $Et_2O$ for 5 min and then centrifuged. The supernatant was removed, and the remaining solid was dried *in vacuo* to give 4-(3-(benzo[$c$][1,2,5]oxadiazol-5-yl)-1-(4-methoxybenzyl)-1$H$-pyrrolo[2,3-$b$]pyridin-5-yl)benzoic acid **31** in 2% yield (3 mg, 0.006 mmol, yellow amorphous solid). $^1$H NMR (600 MHz, DMSO-$d_6$): $\delta$ 8.84−8.81 (m, 1H), 8.78−8.75 (m, 1H), 8.57 (s, 1H), 8.46−8.42 (m, 1H), 8.13−8.09 (m, 2H), 8.07 (d, $J$ = 8.3 Hz, 2H), 8.02 (d, $J$ = 8.4 Hz, 2H), 7.36 (d, $J$ = 8.7 Hz, 2H), 6.90 (d, $J$ = 8.7 Hz, 2H), 5.52 (s, 2H), 3.71 (s, 3H). $^{13}$C NMR (151 MHz, DMSO-$d_6$): $\delta$ 167.2, 158.8, 149.8, 148.1, 147.6, 142.9, 142.7, 137.6, 133.7, 131.1, 129.9 (2C), 129.6, 129.4, 129.1, 129.0 (2C), 127.5 (2C), 127.2, 117.4, 116.3, 114.0 (2C), 112.4, 108.4, 55.1, 47.3. HRMS (pos. ESI-TOF): $m/z$ calcd for $C_{28}H_{21}N_4O_4$, 477.1564 [M + H]$^+$; found, 477.1557 [M + H]$^+$.

*4-(3-(Benzo[c][1,2,5]oxadiazol-5-yl)-1-(3-methoxyphenyl)-1H-pyrrolo[2,3-b]pyridin-5-yl)benzoic Acid (**32**).* General procedure C was applied using halide **76** (210 mg, 0.50 mmol), 4-carboxyphenylboronic acid (90 mg, 0.55 mmol), $K_2CO_3$ (206 mg, 0.54 mmol), and Pd(dppf)$Cl_2$ (9 mg, 0.014 mmol) in 8 mL of 3:1 dioxane/$H_2O$. The reaction was stirred for 5 h and then allowed to cool down to room temperature. The mixture was acidified until the formation of a yellow precipitate (pH = 4.5) and extracted three times with DCM. The combined organic layers were dried with $Na_2SO_4$ and concentrated *in vacuo*. The crude product was purified by column chromatography to 4-(3-(benzo[$c$][1,2,5]oxadiazol-5-yl)-1-(3-methoxyphenyl)-1$H$-pyrrolo[2,3-$b$]pyridin-5-yl)benzoic acid **32** in 2.5% yield (6 mg, 0.015 mmol, yellow solid). The solid residue in the aqueous layer was boiled with addition of acetic acid, filtrated, and lyophilized. The NMR of the solid showed that the product coprecipitated with acetic acid. The yield of 4-(3-(benzo[$c$][1,2,5]-oxadiazol-5-yl)-1-(3-methoxyphenyl)-1$H$-pyrrolo[2,3-$b$]pyridin-5-yl)-benzoic acid acetate is 48% yield (125 mg, 0.24 mmol, yellow amorphous solid). $^1$H NMR (600 MHz, DMSO-$d_6$): $\delta$ 8.91−8.88 (m, 1H), 8.85−8.76 (m, 2H), 8.57 (s, 1H), 8.30 (dd, $J$ = 9.4, 1.5 Hz, 1H), 8.17 (d, $J$ = 9.4, 1H), 8.11−8.06 (m, 2H), 8.04−7.98 (m, 2H), 7.68−7.63 (m, 2H), 7.54 (t, $J$ = 8.1 Hz, 1H), 7.05−7.02 (m, 1H), 3.91 (s, 3H). $^{13}$C NMR (151 MHz, DMSO-$d_6$): $\delta$ 167.1, 159.9, 149.7, 148.1, 147.4, 143.2, 142.3, 138.3, 137.2, 134.0, 130.2 (2C), 130.0, 129.9, 129.7, 127.5 (2C), 127.4, 118.6, 116.3, 115.9, 114.1, 112.2, 109.7, 109.6, 55.5. HRMS (pos. ESI-TOF): $m/z$ calcd for $C_{27}H_{19}N_4O_4$, 463.1401 [M + H]$^+$; found, 463.1404 [M + H]$^+$.

*4-(3-(Benzo[c][1,2,5]oxadiazol-5-yl)-1-phenyl-1H-pyrrolo[2,3-b]-pyridin-5-yl)benzoic Acid (**33**).* General procedure B was applied using halide **77** (32 mg, 0.08 mmol), 4-carboxyphenylboronic acid (16 mg, 0.1 mmol), $NaHCO_3$ (20 mg, 0.24 mmol), and $Pd(PPh_3)_4$ (7 mg, 0.006 mmol) in 10 mL of 3:1 MeCN/$H_2O$. The crude product was concentrated *in vacuo*, more water was added, and the solution was extracted with DCM. Then, the water layer was acidified until the formation of a yellow precipitate and extracted one more time with DCM. The organic layer was discarded (albeit containing traces of product), and the major portion of the water was decanted. The crude precipitate was lyophilized, and the dry product was dissolved in ACN/MeOH, absorbed on isolute, and purified by column chromatography ($SiO_2$, MeOH in DCM, 0−25%) to give 4-(3-(benzo[$c$][1,2,5]oxadiazol-5-yl)-1-phenyl-1$H$-pyrrolo[2,3-$b$]pyridin-5-yl)benzoic acid **33** in 14% yield (5.3 mg, 0.011 mmol, yellow amorphous solid). $^1$H NMR (600 MHz, DMSO-$d_6$): $\delta$ 8.91−8.85 (m, 1H), 8.84−8.80 (m, 1H), 8.81−8.77 (m, 1H), 8.57 (s, 1H), 8.30 (d, $J$ = 9.4 Hz, 1H), 8.17 (d, $J$ = 9.4 Hz, 1H), 8.12−8.06 (m, 2H), 8.06−8.01 (m, 2H), 8.01−7.94 (m, 2H), 7.70−7.60 (m, 2H), 7.46 (t, $J$ = 7.5 Hz, 1H). HRMS (pos. ESI-TOF): $m/z$ calcd for $C_{26}H_{17}N_4O_3$, 434.1326 [M + H]$^+$; found, 434.1341 [M + H]$^+$.

*Methyl 4-(3-(Benzo[c][1,2,5]oxadiazol-5-yl)-1-(4-methoxyphenyl)-1H-pyrazolo[3,4-b]pyridin-5-yl)benzoate (**83**).* General procedure B was applied using halide **78** (66 mg, 0.16 mmol), 4-methoxycarbonylphenylboronic acid (36 mg, 0.20 mmol), $NaHCO_3$ (41 mg, 0.48 mmol), and $Pd(PPh_3)_4$ (14 mg, 0.012 mmol) in 10 mL of 3:1 MeCN/$H_2O$. Purification of the crude product by flash column chromatography (0−100% DCM in cyclohexane) yielded 4-(3-(benzo[$c$][1,2,5]oxadiazol-5-yl)-1-(4-methoxyphenyl)-1$H$-pyrazolo-[3,4-$b$]pyridin-5-yl)benzoate **83** in 37% (28 mg, 0.058 mmol, yellow amorphous solid). $^1$H NMR (300 MHz, $CDCl_3$): $\delta$ 9.08−8.87 (m, 1H), 8.74−8.61 (m, 1H), 8.50−8.35 (m, 2H), 8.30−8.15 (m, 4H), 8.11−7.94 (m, 1H), 7.89−7.73 (m, 2H), 7.23−7.07 (m, 2H), 3.99 (s, 3H), 3.91 (s, 3H). HRMS (pos. ESI-TOF): $m/z$ calcd for $C_{27}H_{20}N_5O_4$, [M + H]$^+$, 478.1510; found, 478.1522.

*4-(3-(Benzo[c][1,2,5]oxadiazol-5-yl)-1-(4-methoxyphenyl)-1H-pyrazolo[3,4-b]pyridin-5-yl)benzoic Acid (**34**).* Corresponding indazol ester **83** (26 mg, 0.06 mmol, 1 equiv) was dissolved in dioxane (1.5 mL), and an aqueous solution of NaOH (5 equiv, 2 M) was added. The mixture was stirred at 60 °C for 12 h. The crude product was concentrated *in vacuo*, more water was added, and the solution was extracted one time with DCM. Then, the water layer was acidified until the formation of a yellow precipitate and extracted one more time with DCM. The organic layer was discarded, and the major portion of the water was decanted. A yellow solid was washed with DCM and acetone and lyophilized to give 4-(3-(benzo[$c$][1,2,5]-oxadiazol-5-yl)-1-(4-methoxyphenyl)-1$H$-pyrazolo[3,4-$b$]pyridin-5-yl)benzoic acid **34** in 68% yield (18 mg, 0.04 mmol, yellow amorphous solid). $^1$H NMR (600 MHz, DMSO-$d_6$): $\delta$ 9.22−9.11 (m, 1H), 9.10−8.97 (m, 1H), 8.94 (m, 1H), 8.54−8.37 (m, 1H), 8.29−8.14 (m, 3H), 8.14−7.87 (m, 4H), 7.23−7.07 (m, 2H), 3.87 (s, 3H). HRMS (pos. ESI-TOF): $m/z$ calcd for $C_{26}H_{18}N_5O_4$ [M + H]$^+$, 464.1353; found, 464.1379. $IC_{50}$ > 100 $\mu$M (DiFMUP assay, DiFMUP concentration = 20 $\mu$M).

*Methyl 4-(3-(Benzo[c][1,2,5]oxadiazol-5-yl)-1-(tetrahydro-2H-pyran-2-yl)-1H-pyrazolo[3,4-b]pyridin-5-yl)benzoate (**84**).* General procedure B coupling was applied using halide **79** (100 mg, 0.25 mmol), 4-methoxycarbonylphenylboronic acid (54 mg, 0.30 mmol), $NaHCO_3$ (63 mg, 0.75 mmol), and $Pd(PPh_3)_4$ (21 mg, 0.012 mmol) in 10 mL of 3:1 MeCN/$H_2O$. Purification of the crude product by flash column chromatography (0−50% ethylacetate in cyclohexane) gave methyl 4-(3-(benzo[$c$][1,2,5]oxadiazol-5-yl)-1-(tetrahydro-2$H$-pyran-2-yl)-1$H$-pyrazolo[3,4-$b$]pyridin-5-yl)benzoate **84** in 40% yield (45 mg, 0.10 mmol, white amorphous solid). $^1$H NMR (300 MHz, $CDCl_3$): $\delta$ 8.94−8.79 (m, 1H), 8.61−8.48 (m, 1H), 8.42−8.26 (m, 2H), 8.24−8.10 (m, 2H), 8.01−7.86 (m, 1H), 7.78−7.67 (m, 2H), 6.33−6.18 (m, 1H), 4.28−4.07 (m, 1H), 4.05−3.78 (m, 4H), 2.88−2.65 (m, 1H), 2.29−2.14 (m, 1H), 2.14−1.99 (m, 1H), 1.98−1.78 (m, 2H), 1.78−1.59 (m, 1H). HRMS (pos. ESI-TOF): $m/z$ calcd for $C_{25}H_{22}N_5O_4$ [M + H]$^+$, 456.2; found, 456.0.

*4-(3-(Benzo[c][1,2,5]oxadiazol-5-yl)-1-(tetrahydro-2H-pyran-2-yl)-1H-pyrazolo[3,4-b]pyridin-5-yl)benzoic Acid (**35**).* The corresponding azaindazole ester **84** (45 mg, 0.01 mmol, 1 equiv) was dissolved in dioxane (1.5 mL) and an aqueous solution of NaOH (5 equiv, 2 M) was added. The mixture was stirred at 60 °C for 12 h. The crude was concentrated *in vacuo*, more water was added, and the solution was extracted one time with DCM. Then, the water layer was acidified until the formation of a white precipitate and extracted one more time with DCM. The organic layer was discarded, and the major portion of the water was decanted. White solid was washed with


https://dx.doi.org/10.1021/acs.jmedchem.0c01265
J. Med. Chem. XXXX, XXX, XXX−XXX

DCM and acetone and lyophilized to give 4-(3-(benzo[*c*][1,2,5]-oxadiazol-5-yl)-1-(tetrahydro-2*H*-pyran-2-yl)-1*H*-pyrazolo[3,4-*b*]-pyridin-5-yl)benzoic acid **35** in 54% yield (24 mg, 0.054 mmol, white amorphous solid). $^1$H NMR (300 MHz, $CDCl_3$): $\delta$ 9.22−9.08 (m, 1H), 9.07−8.99 (m, 1H), 8.90 (s, 1H), 8.45−8.30 (m, 1H), 8.23−8.14 (m, 1H), 8.14−7.97 (m, 4H), 6.27−6.03 (m, 1H), 4.08−3.88 (m, 1H), 3.85−3.64 (m, 1H), 2.70−2.53 (m, 1H), 2.18−1.95 (m, 2H), 1.95−1.74 (m, 1H), 1.74−1.55 (m, 2H). $^{13}$C NMR (75 MHz, DMSO-$d_6$): $\delta$ 167.2, 150.7, 149.5, 149.0, 148.6, 141.5, 140.7, 135.4, 132.1, 130.6, 130.1, 129.9 (2C), 129.3, 127.8 (2C), 116.7, 113.3, 113.2, 82.1, 67.3, 39.5, 28.8, 24.7, 22.3. HRMS (pos. ESI-TOF): *m*/*z* calcd for $C_{24}H_{20}N_5O_4$, $[M + H]^+$, 443.1540; found, 443.1542. $IC_{50}$ > 100 $\mu$M (DiFMUP assay, DiFMUP concentration = 20 $\mu$M).

*Methyl 3-(Benzo[c][1,2,5]oxadiazol-5-yl)-1-(4-methoxyphenyl)-1H-pyrrolo[2,3-b]pyridine-5-carboxylate (**85**).* General procedure B was adapted using halide **62** (200 mg, 0.49 mmol), benzo[*c*][1,2,5]-oxadiazole-5-boronic acid pinacol ester (258 mg, 0.10 mmol), $K_2CO_3$ (430 mg, 3.14 mmol), and $Pd(PPh_3)_4$ (14 mg, 0.012 mmol) in 9 mL of 3:1 MeCN/$H_2O$. Purification of the crude product by flash column chromatography ($SiO_2$, 30−100% ethyl acetate in cyclohexane) yielded methyl 3-(benzo[*c*][1,2,5]oxadiazol-5-yl)-1-(4-methoxyphenyl)-1*H*-pyrrolo[2,3-*b*]pyridine-5-carboxylate **60** in 18% yield (33 mg, 0.08 mmol, yellow amorphous solid). $^1$H NMR (300 MHz, $CDCl_3$): $\delta$ 9.17−9.03 (m, 1H), 9.03−8.94 (m, 1H), 816−8.09 (m, 1H), 8.01−7.92 (m, 1H), 7.90 (s, 1H), 7.86−7.72 (m, 1H), 7.73−7.57 (m, 2H), 7.22−7.14 (m, 2H), 4.00 (s, 3H),3.89 (s, 3H). LCMS (pos. ESI-TOF): *m*/*z* calcd for $C_{22}H_{17}N_4O_4$, 401.1 $[M + H]^+$; found, 401.0 $[M + H]^+$.

*3-(Benzo[c][1,2,5]oxadiazol-5-yl)-1-(4-methoxyphenyl)-1H-pyrrolo[2,3-b]pyridine-5-carboxylic Acid (**36**).* Ester **85** (30 mg, 0.075 mmol, 1 equiv) was dissolved in dioxane (3 mL) and aqueous NaOH (5 equiv, 2 M) was added. The mixture was stirred at 60 °C for 12 h. The crude product was concentrated *in vacuo*, more water was added, and the solution was extracted one time with DCM. Then, the water layer was acidified until the formation of a yellow precipitate (pH = 4.0−4.5). The solid was collected by vacuum filtration, washed with DCM and ether, and lyophilized to give 3-(benzo[*c*][1,2,5]-oxadiazol-5-yl)-1-(4-methoxyphenyl)-1*H*-pyrrolo[2,3-*b*]pyridine-5-carboxylic acid **36** in 77% yield (24 mg, 0.057 mmol, yellow amorphous solid). $^1$H NMR (600 MHz, DMSO-$d_6$): $\delta$ = 9.02−8.98 (m, 1H), 8.98−8.89 (m, 1H), 8.76 (s, 1H), 8.39−8.35 (m, 1H), 8.23−8.15 (m, 2H), 7.88−7.80 (m, 2H), 7.22−7.14 (m, 2H), 3.87 (s, 3H). $^{13}$C NMR (151 MHz, DMSO-$d_6$): $\delta$ 166.9, 158.3, 149.6, 149.2, 148.2, 145.6, 137.2, 133.8, 131.2, 130.3, 129.9, 125.8 (2C), 117.5, 117.0, 116.7, 114.5 (2C), 114.0, 109.5, 55.5. HRMS (pos. ESI-TOF): *m*/*z* calcd for $C_{21}H_{15}N_4O_4$, 388.1118 $[M + H]^+$; found, $[M + H]^+$ 388.1121.

*Ethyl (E)-3-(3-(Benzo[c][1,2,5]oxadiazol-5-yl)-1-(4-methoxyphenyl)-1H-pyrrolo[2,3-b]pyridin-5-yl)acrylate (**86**).* **66** (117 mg, 0.28 mmol, 1 equiv), ethyl acrylate (83 mg, 0.83 mmol, 3.0 equiv), $Pd(OAc)_2$ (6.24 mg, 0.03 mmol, 0.1 equiv), and tris(2-methylphenyl)phosphine (16.9 mg, 0.06 mmol, 0.2 equiv) were dissolved in a mixture of TEA/DMF 2:5 (7 mL), and purged with $N_2$ prior to use. The mixture was heated to 120 °C and stirred for 12 h under $N_2$. The mixture was cooled to room temperature and water was added. The water layer was extracted three times with DCM, dried with $Na_2SO_4$, and evaporated under vacuum. The crude product was purified by silica gel chromatography ($SiO_2$, DCM in cyclohexane, 0−50%) to give ethyl (*E*)-3-(3-(benzo[*c*][1,2,5]oxadiazol-5-yl)-1-(4-methoxyphenyl)-1*H*-pyrrolo[2,3-*b*]pyridin-5-yl)acrylate **86** in 17% yield (21 mg, 0.05 mmol, yellow amorphous solid). $^1$H NMR (300 MHz, $CDCl_3$): $\delta$ 8.66−8.60 (m, 1H), 8.57−8.44 (m, 1H), 8.11−8.03 (m, 1H), 7.99−7.84 (m, 3H), 7.84−7.74 (m, 1H), 7.70−7.60 (m, 2H), 7.17−7.05 (m, 2H), 6.60 (d, *J* = 16.0 Hz, 1H), 4.32 (q, *J* = 7.1 Hz, 2H), 3.89 (s, 3H), 1.39 (t, *J* = 7.1 Hz, 3H) ppm. LCMS (pos. ESI-TOF): *m*/*z* calcd for $C_{25}H_{21}N_4O_4$, 441.2 $[M + H]^+$; found, 441.1 $[M + H]^+$.

*3-(3-(Benzo[c][1,2,5]oxadiazol-5-yl)-1-(4-methoxyphenyl)-1H-pyrrolo[2,3-b]pyridin-5-yl)acrylic Acid (**37**).* Ester **86** (20 mg, 0.045 mmol, 1 equiv) was dissolved in THF (1.5 mL), and an aqueous solution of LiOH (5 equiv, 2 M) was added. The mixture was stirred at room temperature for 24 h, then an additional portion of LiOH (5 equiv, 2 M) was added. The reaction was stirred for additional 24 h, then the crude product was concentrated *in vacuo*, more water was added, and the solution was extracted one time with DCM. The water layer was acidified until the formation of a yellow precipitate (pH = 4.0−4.5). The solid was collected by vacuum filtration, washed with DCM and ether, and lyophilized to give 3-(3-(benzo[*c*][1,2,5]-oxadiazol-5-yl)-1-(4-methoxyphenyl)-1*H*-pyrrolo[2,3-*b*]pyridin-5-yl)-acrylic acid **37** in 44% yield (8 mg, 0.02 mmol, yellow amorphous solid). $^1$H NMR (300 MHz, DMSO-$d_6$): $\delta$ 9.06−8.96 (m, 1H), 8.80−8.68 (m, 2H), 8.52 (s, 1H), 8.34−8.19 (m, 1H), 8.19−8.06 (m, 1H), 7.92−7.78 (m, 3H), 7.24−7.10 (m, 2H), 6.90 (d, *J* = 16.1 Hz, 1H), 3.87 (s, 3H). $^{13}$C NMR (75 MHz, DMSO-$d_6$): $\delta$ 167.8, 158.1, 149.8, 148.1, 144.9, 141.9, 137.1, 133.8, 130.9, 130.1, 128.5, 125.5 (3C), 124.8, 119.0, 118.2, 116.2, 114.4 (2C), 113.6, 109.2, 55.5. HRMS (pos. ESI-TOF): *m*/*z* calcd for $C_{23}H_{17}N_4O_4$ $[M + H]^+$, 414.1275; found, $[M + H]^+$ 414.1286.

*4-(3-(Benzo[c][1,2,5]oxadiazol-5-yl)-1-(4-methoxyphenyl)-1H-pyrrolo[2,3-b]pyridin-5-yl)cyclohex-3-ene-1-carboxylic Acid (**38**).* Compound **38** was synthesized according to general procedure B using halide **66** (43 mg, 0.102 mmol), 4-(4,4,5,5-tetramethyl-1,3,2-dioxaborolan-2-yl)cyclohex-3-ene-1-carboxylic acid (30.9 mg, 0.122 mmol), $NaHCO_3$ (25.7 mg, 0.306 mmol), and $Pd(PPh_3)_4$ (8.8 mg, 0.008 mmol) in 5 mL of 3:1 MeCN/$H_2O$. The reaction mixture was diluted with DCM (30 mL), more water (25 mL) was added, and the solution was extracted one time with DCM. The organic layer was discarded, and the water layer was acidified and extracted four times with 30 mL of 4:1 DCM/THF. The combined organic layers were dried over $MgSO_4$, filtered, and evaporated *in vacuo*. The crude residue was purified by column chromatography ($SiO_2$, THF in DCM, 0−25%). The combined fractions were evaporated, and the residue was sonicated with 5 mL of 1:1 *n*-pentane/$Et_2O$ for 5 min and then centrifuged. The supernatant was removed, and the remaining solid was dried *in vacuo* to give 4-(3-(benzo[*c*][1,2,5]oxadiazol-5-yl)-1-(4-methoxyphenyl)-1*H*-pyrrolo[2,3-*b*]pyridin-5-yl)cyclohex-3-ene-1-carboxylic acid **38** in 38% yield (18 mg, 0.036 mmol, amorphous yellow solid). $^1$H NMR (600 MHz, DMSO-$d_6$): $\delta$ 8.65 (s, 1H), 8.58−8.56 (m, 1H), 8.56−8.53 (m, 1H), 8.47−8.44 (m, 1H), 8.22 (dd, *J* = 9.4, 1.5 Hz, 1H), 8.13 (dd, *J* = 9.4, 0.9 Hz, 1H), 7.85 (d, *J* = 8.9 Hz, 2H), 7.16 (d, *J* = 8.9 Hz, 2H), 6.39−6.34 (m, 1H), 3.85 (s, 3H), 2.80−2.59 (m, 4H), 2.54−2.47 (m, 1H), 2.25−2.15 (m, 1H), 1.93−1.75 (m, 1H). $^{13}$C NMR (151 MHz, DMSO-$d_6$): $\delta$ 176.4, 157.9, 149.7, 148.1, 146.9, 142.1, 141.7, 137.6, 133.9, 131.7, 130.4, 129.9, 125.3 (2C), 124.7, 123.4, 117.7, 116.3, 114.3 (2C), 113.2, 108.7, 55.5, 38.0, 27.9, 26.5, 25.3. HRMS (pos. ESI-TOF): *m*/*z* calcd for $C_{27}H_{23}N_4O_4$, 467.1750 $[M + H]^+$; found, 467.1714 $[M + H]^+$.

*Ethyl-4-(3-(benzo[c][1,2,5]oxadiazol-5-yl)-1-(4-methoxyphenyl)-1H-pyrrolo[2,3-b]pyridin-5-yl)benzoate (**39**).* Compound **39** was synthesized according to general procedure B using halide **66** (100 mg, 0.237 mmol), 4-(ethoxycarbonyl)phenyl)boronic acid (55.3 mg, 0.284 mmol), $NaHCO_3$ (59.8 mg, 0.712 mmol), and $Pd(PPh_3)_4$ (20.6 mg, 0.018 mmol) in 10 mL of 3:1 MeCN/$H_2O$. The reaction mixture was diluted with DCM (30 mL), more water (25 mL) was added, and the solution was extracted four times with 30 mL of 4:1 DCM/THF. The organic layer was dried over $MgSO_4$, filtered, and evaporated *in vacuo*. The crude residue was dissolved in 5 mL of EtOH abs and cooled to 0 °C, and 18 $\mu$L of thionyl chloride was added. The mixture was refluxed for 4 h, concentrated *in vacuo*, and afterward submitted for flash column chromatography without further workup. The product was eluted with THF in DCM ($SiO_2$, 0−25%) to give impure ethyl-4-(3-(benzo[*c*][1,2,5]oxadiazol-5-yl)-1-(4-methoxyphenyl)-1*H*-pyrrolo[2,3-*b*]pyridin-5-yl)benzoate **39** in 43% yield over two steps (50 mg, 0.102 mmol, yellow amorphous solid, 70% purity, the byproduct is 5,5′-(1-(4-methoxyphenyl)-1*H*-pyrrolo[2,3-*b*]pyridine-3,5-diyl)bis(benzo[*c*][1,2,5]oxadiazole). $^1$H NMR (600 MHz, DMSO-$d_6$): $\delta$ 8.88 (dd, *J* = 5.1, 2.2 Hz, 1H), 8.78−8.74 (m, 1H), 8.72 (s, 1H), 8.54−8.50 (m, 1H), 8.30−8.22 (m, 1H), 8.13 (dd, *J* = 9.4, 1.0 Hz, 1H), 8.08 (d, *J* = 8.4 Hz, 2H), 8.06−8.03 (m, 2H), 7.90−7.83 (m, 2H), 7.17 (dd, *J* = 9.1, 2.3 Hz, 2H), 4.36 (q, *J* = 7.1 Hz, 2H),


https://dx.doi.org/10.1021/acs.jmedchem.0c01265
J. Med. Chem. XXXX, XXX, XXX−XXX

3.86 (s, 3H), 1.36 (t, $J$ = 7.1 Hz, 3H). $^{13}$C NMR (600 MHz, DMSO-$d_6$, representative peaks): $\delta$ 165.6, 158.1, 149.8, 148.1, 147.5, 143.2, 142.8, 137.4, 134.0, 130.6, 130.2, 129.7 (2C), 129.3, 127.6 (2C), 127.3, 125.5 (2C), 118.2, 116.3, 114.4 (2C), 113.6, 109.2, 60.8, 55.5, 14.2. HRMS (pos. ESI-TOF): $m/z$ calcd for $C_{29}H_{23}N_5O_4S$, $[M + H]^+$ 491.1714; found, 491.1743.

*N-(4-(3-(Benzo[c][1,2,5]oxadiazol-5-yl)-1-(4-methoxyphenyl)-1H-pyrrolo[2,3-b]pyridin-5-yl)phenyl)methanesulfonamide (**40**).* General procedure B was applied using halide **66** (150 mg, 0.35 mmol), 4-aminophenylboronic pinacol ester (93 mg, 0.42 mmol), $NaHCO_3$ (87 mg, 1.05 mmol), and $Pd(PPh_3)_4$ (27 mg, 0.026 mmol) in 20 mL of 3:1 MeCN/$H_2O$. After stirring the reaction overnight, the mixture was cooled to room temperature, and water was added. The water layer was extracted three times with DCM, and the combined organic layers were concentrated *in vacuo* to give 180 mg of crude amine intermediate. After analysis of the $^1$H NMR, the isolated product was taken to the next reaction step without further purification. Crude 4-(3-(benzo[$c$][1,2,5]oxadiazol-5-yl)-1-(4-methoxyphenyl)-1$H$-pyrrolo[2,3-$b$]pyridin-5-yl)aniline (60 mg) was dissolved in 4 mL of DCM, and 28 $\mu$L of pyridine (2.5 equiv, 0.34 mmol) and 26 $\mu$L of methanesulfonyl chloride (2.5 equiv, 0.34 mmol) were added at room temperature. The mixture was stirred for 16 h, concentrated *in vacuo*, and then submitted to flash column chromatography without further workup. The product was eluted with ethyl acetate in cyclohexane ($SiO_2$, 0−100%) to give pure *N*-(4-(3-(benzo[$c$][1,2,5]oxadiazol-5-yl)-1-(4-methoxyphenyl)-1$H$-pyrrolo-[2,3-$b$]pyridin-5-yl)phenyl)methanesulfonamide **40** in 40% yield over two steps (24 mg, 0.046 mmol, yellow amorphous solid). $^1$H NMR (300 MHz, DMSO-$d_6$): $\delta$ 9.97−9.81 (bs, 1H), 8.80−8.75 (m, 1H), 8.75−8.70 (m, 1H), 8.70−8.66 (m, 1H), 8.50 (s, 1H), 8.30−8.23 (m, 1H), 8.18−8.10 (m, 1H), 7.93−7.81 (m, 4H), 7.40−7.31 (m, 2H), 7.24−7.10 (m, 2H), 3.88 (s, 3H), 3.06 (s, 3H). $^{13}$C NMR (151 MHz, DMSO-$d_6$): $\delta$ 158.0, 149.8, 148.1, 147.1, 142.9, 137.5, 134.0, 133.6, 130.4, 130.3, 130.1, 128.3 (2C), 126.5, 125.4 (2C), 120.2 (3C), 118.2, 116.3, 114.4 (2C), 113.3, 109.0, 55.5, 40.1. HRMS (pos. ESI-TOF): $m/z$ calcd for $C_{27}H_{22}N_5O_4S$, $[M + H]^+$ 513.1416; found, $[M + H]^+$ 513.1419.

*Methyl 4-(5-(Benzo[c][1,2,5]oxadiazol-5-yl)-1-(4-methoxyphenyl)-1H-pyrrolo[2,3-b]pyridin-3-yl)benzoate (**87**).* General procedure B was applied using halide **80** (62 mg, 0.14 mmol), benzo[$c$][1,2,5]-oxadiazole-5-boronic acid pinacol ester (41 mg, 0.17 mmol), $NaHCO_3$ (35 mg, 0.42 mmol), and $Pd(PPh_3)_4$ (12 mg, 0.011 mmol) in 10 mL of 3:1 MeCN/$H_2O$. After the standard workup procedure, 65 mg of the crude mixture was obtained. NMR of the crude mixture showed clean product, 52 mg was taken for the next step without further purification, and the remaining 13 mg was subjected to further purification. Recrystallization from cold DCM, redissolving in EtOAc, and filtration over short plug of silica yielded methyl 4-(5-(benzo[$c$][1,2,5]oxadiazol-5-yl)-1-(4-methoxyphenyl)-1$H$-pyrrolo[2,3-$b$]pyridin-3-yl)benzoate **87** in 60% yield (8 mg, 0.017 mmol, yellow-orange amorphous solid). $^1$H NMR (300 MHz, DMSO-$d_6$): $\delta$ 8.76−8.71 (m, 1H), 8.56−8.50 (m, 1H), 8.24−8.17 (m, 2H), 8.07−7.96 (m, 2H), 7.86−7.76 (m, 4H), 7.75−7.66 (m, 2H), 7.16−7.09 (m, 2H), 3.96 (s, 3H), 3.91 (s, 3H). $^{13}$C NMR (75 MHz, DMSO-$d_6$): $\delta$ 167.0, 158.9, 149.8, 148.6, 148.4, 143.4, 142.5, 138.8, 133.2 (2C), 130.6, 130.6 (2C), 128.8, 128.4, 127.8, 127.1, 126.9 (2C), 126.0 (2C), 119.3, 117.3, 116.1, 114.9, 113.0, 55.8, 52.3. HRMS (pos. ESI-TOF): $m/z$ calcd for $C_{28}H_{21}N_4O_4$ 477.1557 $[M + H]^+$; found, 477.1556 $[M + H]^+$.

*4-(5-(Benzo[c][1,2,5]oxadiazol-5-yl)-1-(4-methoxyphenyl)-1H-pyrrolo[2,3-b]pyridin-3-yl)benzoic Acid (**41**).* Methylester **87** (52 mg, 0.11 mmol, 1 equiv) was dissolved in dioxane (2.6 mL) and MeOH (2.6 mL), and an aqueous solution of NaOH (0.35 mL, 12 equiv, 4 M) was added. The mixture was stirred at 60 °C for 1 h. The crude product was concentrated *in vacuo*, and more water was added. Then, the water layer was acidified until the formation of a yellow precipitate (pH = 4.5) and extracted three times with DCM. The combined organic layers were dried with $Na_2SO_4$ and concentrated *in vacuo*. The crude product was purified by column chromatography ($SiO_2$, 50−100% EtOAc in cyclohexane) to give 4-(5-(benzo[$c$]-[1,2,5]oxadiazol-5-yl)-1-(4-methoxyphenyl)-1$H$-pyrrolo[2,3-$b$]-pyridin-3-yl)benzoic acid **41** in 4% yield (2.6 mg, 0.056 mmol, yellow amorphous solid) for two steps. The remaining solid in the aqueous layer was refluxed upon addition of acetic acid, filtrated, and lyophilized. The NMR of the solid showed a pure compound identical to the product obtained by column chromatography. The yield of combined products was 37% (24 mg, 0.051 mmol) over 2 steps. $^1$H NMR (600 MHz, DMSO-$d_6$): $\delta$ 8.92−8.81 (m, 2H), 8.57−8.40 (m, 2H), 8.25−8.15 (m, 2H), 8.14−7.98 (m, 4H), 7.91−7.83 (m, 2H), 7.21−7.11 (m, 2H), 3.87 (s, 3H). $^{13}$C NMR (151 MHz, DMSO-$d_6$): $\delta$ 167.2, 157.9, 149.6, 148.3, 147.6, 143.0, 142.1, 138.2, 134.0, 130.4, 130.0 (2C), 128.8, 128.3, 127.8, 127.4, 126.6 (2C), 125.4 (2C), 118.3, 116.5, 114.8, 114.4 (2C), 112.3, 55.5. HRMS (pos. ESI-TOF): $m/z$ calcd for $C_{27}H_{19}N_4O_4$, 463.1401 $[M + H]^+$; found, 463.1401 $[M + H]^+$.

*4,4′-(1-(4-Methoxyphenyl)-1H-pyrrolo[2,3-b]pyridine-3,5-diyl)-dibenzoic Acid (**42**).* General procedure C was applied using halide **55** (100 mg, 0.233 mmol), 4-methoxycarbonyl-phenylboronic acid (125 mg, 0.694 mmol), $K_2CO_3$ (300 mg, 2.170 mmol), and $Pd(dppf)Cl_2$ (6 mg, 0.008 mmol) in 10 mL of 3:1 dioxane/$H_2O$. The reaction mixture was diluted with DCM (50 mL), more water (25 mL) was added, and the solution was extracted four times with 30 mL of DCM and THF 4:1. The combined organic layers were dried over $MgSO_4$, filtered, and evaporated *in vacuo*. The crude residue was purified by column chromatography ($SiO_2$, THF in DCM, 0−10%) to yield dimethyl 4,4′-(1-(4-methoxyphenyl)-1$H$-pyrrolo[2,3-$b$]pyridine-3,5-diyl)dibenzoate contaminated with 4-methoxycarbonyl-phenylboronic acid. The residue was dissolved in DCM (100 mL) and extracted three times with 10% $K_2CO_3$ solution (15 mL). The organic layer was dried over $MgSO_4$, filtered, and evaporated *in vacuo* to yield monosubstituted intermediate in 38% yield (44.5 mg, 0.090 mmol, white solid), which was used directly for the next reaction step. Dimethyl 4,4′-(1-(4-methoxyphenyl)-1$H$-pyrrolo [2,3-$b$] pyridine-3,5-diyl)dibenzoate (44.5 mg, 0.090 mmol) was dissolved in 6 mL of THF and 2 mL of MeOH after which a solution of 73 mg (1.8 mmol, 2 mL, 0.9 M) of NaOH in water was added, and the solution was stirred at room temperature for 8 h. The organic solvents were removed *in vacuo*. The remaining aqueous solution was diluted with DCM (10 mL), more water (15 mL) was added, and the solution was extracted one time with DCM. Then, the water layer was acidified until the formation of a white precipitate and extracted four times with 25 mL of DCM and THF 4:1. The combined organic layers were dried over $MgSO_4$, filtered, and evaporated *in vacuo*. The residue was boiled with DCM (3 mL) and after that sonicated. The supernatant was removed (repeated twice), and the solid was dried *in vacuo* to obtain 4,4′-(1-(4-methoxyphenyl)-1$H$-pyrrolo[2,3-$b$]pyridine-3,5-diyl)dibenzoic acid **42** in 10% yield (11 mg, 0.023 mmol) as a white amorphous solid. $^1$H NMR (300 MHz, DMSO-$d_6$): $\delta$ 8.75 (d, $J$ = 2.1 Hz, 1H), 8.70 (d, $J$ = 2.1 Hz, 1H), 8.49 (s, 1H), 8.09−8.03 (m, 6H), 7.98 (d, $J$ = 8.4 Hz, 2H), 7.87 (d, $J$ = 8.9 Hz, 2H), 7.17 (d, $J$ = 8.9 Hz, 2H), 3.86 (s, 3H). $^{13}$C NMR (151 MHz, DMSO-$d_6$): $\delta$ 167.2, 167.1, 157.9, 147.3, 142.8, 142.6, 138.4, 130.5, 130.1 (2C), 130.0 (2C), 129.4, 129.1, 128.6, 128.2, 127.3 (2C), 126.7, 126.6 (2C), 125.4 (2C), 118.4, 114.7, 114.4 (2C), 55.5. HRMS (pos. ESI-TOF): $m/z$ calcd for $C_{28}H_{21}N_2O_5$, 465.1478 $[M + H]^+$; found, 465.1445 $[M + H]^+$.

*4-(1-(4-Methoxyphenyl)-3-(3-oxo-1,3-dihydroisobenzofuran-5-yl)-1H-pyrrolo[2,3-b]pyridin-5-yl)benzoic Acid (**43**).* Compound **43** was synthesized according to general procedure B using halide **81** (45 mg, 0.103 mmol), 4-cabroxyphenyl boronic acid (20.59 mg, 0.124 mmol), $NaHCO_3$ (26.06 mg, 0.310 mmol), and $Pd(PPh_3)_4$ (8.60 mg, 0.0074 mmol) in 6 mL of 3:1 MeCN/$H_2O$. The crude mixture was cooled to room temperature and filtrated. The resulted filtrate was dissolved in ethyl acetate and extracted with water. The organic phase was concentrated *in vacuo* and purified by flash column chromatography (0−100% DCM in cyclohexane) to yield **43** in 6% (3 mg, 0.003 mmol, yellow amorphous solid). The product contained 10% of open form **44** and undergoes spontaneous further hydrolysis over time. $^1$H NMR (600 MHz, DMSO-$d_6$): $\delta$ 8.75 (q, $J$ = 2.2 Hz, 2H), 8.58 (s, 1H), 8.25 (s, 1H), 8.15 (d, $J$ = 9.0 Hz, 1H), 8.08 (d, $J$ = 12.0 Hz, 2H),


https://dx.doi.org/10.1021/acs.jmedchem.0c01265
J. Med. Chem. XXXX, XXX, XXX−XXX

7.98 (d, $J$ = 6.0 Hz, 2H), 7.93 (d, $J$ = 6.0 Hz, 1H), 7.89−7.86 (m, 2H), 7.18 (d, $J$ = 6.0 Hz, 2H), 5.50 (s, 2H), 3.86 (s, $3H_3$). HRMS (pos. ESI-TOF): $m/z$ calcd for $C_{29}H_{20}N_2O_5$, 477.1445 $[M + H]^+$; found, 477.1417 $[M + H]^+$. $IC_{50}$ = 0.58 $\mu$M (DiFMUP assay, DiFMUP concentration = 20 $\mu$M).

*5-(5-(4-Carboxyphenyl)-1-(4-methoxyphenyl)-1H-pyrrolo[2,3-b]-pyridin-3-yl)-2-(hydroxymethyl)benzoic Acid (**44**).* Compound **44** was synthesized according to general procedure B using halide **81** (45 mg, 0.103 mmol), 4-cabroxyphenyl boronic acid (20.59 mg, 0.124 mmol), $NaHCO_3$ (26.06 mg, 0.310 mmol), and $Pd(PPh_3)_4$ (8.60 mg, 0.0074 mmol) in 6 mL of 3:1 MeCN/$H_2O$. The crude mixture was cooled to room temperature and filtrated. The resulted filtrate was dissolved in ethylacetate and extracted with water. The organic phase was concentrated *in vacuo* and purified by flash column chromatography (0−100% DCM in cyclohexane) to give **44** in 20% yield (10 mg, 0.01 mmol, yellow amorphous solid). $^1$H NMR (600 MHz, DMSO-$d_6$): $\delta$ 8.74 (s, 1H), 8.67 (s, 1H), 8.42 (s, 1H), 8.19 (s, 1H), 8.06 (d, $J$ = 6.0 Hz, 2H), 8.01−7.98 (m, 1H), 7.93 (d, $J$ = 6.0 Hz, 2H), 7.91−7.84 (m, 3H), 7.17 (d, $J$ = 6.0 Hz, 2H), 4.94 (s, 2H), 3.85 (s, 3H) ppm. HRMS (pos. ESI-TOF): $m/z$ calcd for $C_{29}H_{23}N_2O_6$, 495.1551 $[M + H]^+$; found, 495.1525 $[M + H]^+$. $IC_{50}$ = 17.0 $\mu$M (DiFMUP assay, DiFMUP concentration = 20 $\mu$M).

*4-(1-(4-Methoxyphenyl)-3-(2-oxo-2H-chromen-7-yl)-1H-pyrrolo-[2,3-b]pyridin-5-yl)benzoic Acid (**45**).* Compound **45** was synthesized according to general procedure B using halide **82** (50 mg, 0.112 mmol), 4-carboxyphenylboronic acid (22 mg, 0.134 mmol), $NaHCO_3$ (28.2, 0.336 mmol), and $Pd(PPh_3)_4$ (3 mg, 0.003 mmol) in 8 mL of 3:1 MeCN/$H_2O$. The reaction mixture was diluted with DCM (30 mL), and more water (25 mL) was added, and the solution was extracted with DCM. Then, the water layer was acidified and extracted four times with 30 mL of 4:1 DCM/THF. The combined organic layer was dried over $MgSO_4$, filtered, and evaporated *in vacuo*. The crude residue was purified by column chromatography ($SiO_2$, THF in DCM, 0−35%). The combined fractions were evaporated, and the residue was sonicated with 5 mL of $Et_2O$ for 5 min, centrifuged, and the supernatant was removed. This procedure was repeated with *n*-pentane. The remaining solid was dried *in vacuo* to obtain 4-(1-(4-methoxyphenyl)-3-(2-oxo-2*H*-chromen-7-yl)-1*H*-pyrrolo[2,3-*b*]pyridin-5-yl)benzoic acid **45** in 11% yield (6 mg, 0.012 mmol, yellow amorphous solid). $^1$H NMR (600 MHz, DMSO-$d_6$): $\delta$ 8.76−8.70 (m, 2H), 8.56 (s, 1H), 8.11 (d, $J$ = 9.3 Hz, 1H), 8.07 (d, $J$ = 8.3 Hz, 2H), 8.00−7.97 (m, 2H), 7.97−7.93 (m, 2H), 7.87 (d, $J$ = 7.9, 1.0 Hz, 2H), 7.83−7.80 (m, 1H), 7.21−7.14 (m, 2H), 6.47 (d, $J$ = 9.6, 0.9 Hz, 1H), 3.86 (s, 3H). $^{13}$C NMR (151 MHz, DMSO-$d_6$): $\delta$ 167.2, 160.2, 157.9, 154.3, 147.3, 144.1, 142.9, 142.5, 137.9, 130.4, 129.9 (2C), 129.2, 129.1, 129.0, 127.4, 126.8, 125.3 (2C), 123.0 (2C), 118.3, 116.9, 115.0, 114.4 (2C), 114.2, 113.4, 55.5 ppm. HRMS (pos. ESI-TOF): $m/z$ calcd for $C_{30}H_{20}N_2O_5$, $[M + H]^+$ 489.1445; found, 489.1459.

*4-(3-(Benzo[c][1,2,5]oxadiazol-5-yl)-1H-pyrrolo[2,3-b]pyridin-5-yl)benzoic Acid (**46**).* Compound **46** was obtained as a byproduct in the preparation of **29** in 13% yield. Alternatively, **46** can be prepared from methyl 4-(3-(benzo[*c*][1,2,5]oxadiazol-5-yl)-1-tosyl-1*H*-pyrrolo-[2,3-*b*]pyridin-5-yl)benzoate by hydrolysis with 2 M NaOH. $^1$H NMR (300 MHz, DMSO-$d_6$): $\delta$ 12.55−12.42 (bs, 1H), 8.84−8.76 (m, 1H), 8.76−8.66 (m, 1H), 8.46−8.35 (m, 2H), 8.24−8.15 (m, 1H), 8.11−8.03 (m, 3H), 8.01−7.94 (m, 2H). HRMS (pos. ESI-TOF): $m/z$ calcd for $C_{20}H_{13}N_4O$, 357.0987 $[M + H]^+$; found, 357.0992 $[M + H]^+$.

Reference compounds PHPS1, GS493, II-B08, and NSC87877 were purchased from commercial suppliers Merck (Merck Millipore) and Merck (Sigma-Aldrich).

**Biochemical SHP2 Assay.** Biochemical assay for the determination of $IC_{50}$ values for compounds **1**−**5** and **43**−**44** was carried out according to the following DiFMUP protocol. Recombinant SHP2 (amino acids 262−532, produced in house) was utilized. Test compounds were dissolved in (DMSO) at a concentration of 10 or 100 mM, and the assay was carried out at a final concentration of below 1% DMSO. DiFMUP assay buffer contains a final concentration of 25 mM MOPSO (pH 7.0), 50 mM NaCl, 0.05% Tween 20, 0.1% bovine serum albumin (BSA), 1 mM dithiothreitol (DTT), freshly added prior to each measurement, and between 0.12 and 0.8 ng/$\mu$L SHP2 (final concentration, applied concentration adjusted to the activity of the enzyme batch used). The final assay volume was 30 $\mu$L. Enzyme and the test compound in buffer solution were incubated for 1 h at RT. The reaction was started by adding 20 $\mu$M DiFMUP. Measurements were performed on a plate reader (SAFIRE II, Tecan) with the following settings: fluorescence reading from top; excitation wavelength: 360 nm (bandwidth 20 nm); emission wavelength 460 nm (bandwidth 20 nm); and five readings with a time interval of 135 s. Measurements were performed in triplicate. $IC_{50}$ values were calculated with Prism 5 (for Windows, Version 5.01, Graph Pad Software, Inc.).

Biochemical assay for the determination of $IC_{50}$ values for compounds **17**−**42** and **45**−**46** was carried out by Reaction Biology Corp utilizing the DiFMUP assay protocol. Recombinant SHP2 (amino acids 246−593) was utilized. Briefly, test compounds were dissolved in DMSO at a concentration of 10 mM, and the assay was carried out at a final DMSO concentration <1%. The DiFMUP assay buffer contained a final concentration of 25 mM HEPES (pH 7.5), 5 mM $MgCl_2$, 0.01% Brij-35, 1 mM DTT, and 1% DMSO. Enzyme and the test compound were incubated in buffer solution for 20 min at room temperature. The reaction was started by adding DiFMUP with a final concentration of 10 $\mu$M. Measurements were performed in duplicate using a 10-dose response protocol (concentration 100 to 0.005 $\mu$M). The following compounds were used as a reference—PHPS1, NSC87877, PTP II-B08, PTP1B inhibitor. The enzyme activities were monitored (Ex/Em 355/460) as a time-course measurement of the increase in the fluorescence signal from the fluorescence substrate for 120 min at room temperature. Shown data represent the average of duplicate measurement.

**Docking and Binding Mode Investigations.** The catalytic domain of SHP2 from the protein data bank (PDB) entry 3O5X was employed for docking studies with the OpenEye Python toolkit [OpenEye Toolkits 2019.Oct.2; OpenEye Scientific Software: Santa Fe, NM, 2019].[70] The OEChem and OESpruce modules were used to add hydrogens and to prepare protein and cocrystalized ligand for docking. Docking of the investigated ligand series was performed with the hybrid method, which uses the goodness of shape and interaction overlap between the docked molecule and the cocrystalized ligand to bias the exhaustive search of the docking algorithm. Reasonable tautomeric states were generated for each ligand at pH 7.4 using the OEQuacpac module. Conformations were generated with OEOmega, and 20 docking poses were produced with high search resolution using the OEDocking module. Chemgauss4 was used as a scoring function. Finally, docking poses were analyzed in terms of pharmacophoric interaction patterns using LigandScout 4.4 [LigandScout 4.4, Inteligand: Vienna, Austria, 2019].[72]

**Molecular Dynamic Simulation.** The previously prepared catalytic domain of SHP2 in complex with the identified docking pose of the most active compound (**45**) was solvated in a cubic box with 10 Å padding with the SPC water model and 0.15 NaCl using Maestro 12.3 [Maestro 12.3, Schrödinger Release 2020-1; Schrödinger, LLC: New York, NY, 2020]. The solvated system was subjected to 20 ns of unbiased MD simulation with Desmond 6.1[73] [Desmond 6.1, Schrödinger Release 2020-1; Schrödinger, LLC: New York, NY, 2020] using the default equilibration and simulation settings. Coordinates were saved every 100 ps and analyzed using the molecular visualization program VMD 1.9.3 [VMD 1.9.3; University of Illinois at Urbana−Champaign: Urbana, IL, 2016].[74]

**Phosphatase Profiling.** Biochemical assay for the determination of $IC_{50}$ values was carried out by Reaction Biology Corp utilizing the DiFMUP assay protocol. Briefly, test compounds were dissolved in DMSO at a concentration of 10 mM, and the assay was carried out at a final DMSO concentration <1%. The DiFMUP assay buffer contained a final concentration of 25 mM HEPES (pH 7.5), 5 mM $MgCl_2$, 0.01% Brij-35, 1 mM DTT, and 1% DMSO. For PP2A alpha/PPP2R1A complex, PP1A, and PP1B, 1 mM $MnCl_2$ was added to reaction buffer. Enzymes and test compound were incubated in buffer solution for 20 min at room temperature. The reaction was started by


https://dx.doi.org/10.1021/acs.jmedchem.0c01265
J. Med. Chem. XXXX, XXX, XXX−XXX

adding DiFMUP with a final concentration of 2 μM for PTPN1/PTP1B-CD, 30 μM for PP1B, and 10 μM for all other PTPs. Measurements were performed in duplicate using a 10-dose response protocol (concentration 100 to 0.005 μM). Following compounds were used as a reference—PTP1B inhibitor and canthardic acid. The enzyme activities were monitored (Ex/Em 355/460) as a time-course measurement of the increase in the fluorescence signal from the fluorescence substrate for 120 min at room temperature. Shown data represent the average of duplicate measurement.

**Kinase Profiling.** Kinase activity assay was carried out by Reaction Biology Corp. Briefly, test compounds were dissolved in DMSO at a concentration of 10 mM, and the assay was carried out at a final DMSO concentration <1%. The reaction assay buffer contained a final concentration of 20 mM Hepes (pH 7.5), 10 mM $MgCl_2$, 1 mM EGTA, 0.02% Brij35, 0.02 mg/mL BSA, 0.1 mM $Na_3VO_4$, 2 mM DTT, and 1% DMSO. Required cofactors were added individually to each kinase reaction. Enzyme and the test compound (final concentration 100 μM) were incubated in buffer solution for 20 min at room temperature. The reaction was started by adding $^{33}$P-γ-ATP with a final concentration of 10 μM. Kinase reaction was incubated for 2 h at room temperature, and reactions were spotted onto P81 ion-exchange paper. Kinase activity was detected by the filter-binding method. Measurements were performed in duplicate using a single dose response protocol, and percentage of kinase activity was calculated. Shown data represent the average of duplicate measurement. Staurosporine was used as a reference.

**Cell Culture.** The human pancreatic adenocarcinoma cell line HPAF-II (ATCC CRL-1997) obtained from ATCC (American Type Culture Collection) was cultured in Dulbecco's modified Eagle's medium (Gibco BRL, Gaithersburg, MD, USA) containing 4.5 g/L glucose, supplemented with 10% (v/v) fetal bovine serum (FBS, Gibco BRL), and 100 U/mL penicillin−streptomycin (Gibco BRL).

The human hepatocellular carcinoma cell line HepG2, purchased from ATCC (HB-8065) was maintained in RPMI-1640 medium (Gibco BRL), supplemented with 10% (v/v) FBS (Gibco BRL), and 100 U/mL penicillin−streptomycin (Gibco BRL).

**Scatter Assay.** HPAF-II cells were plated at a density of 1000 cells per well in medium supplemented with 5% FBS into 384-well cell-bind microplates (Corning Life Sciences, Acton, MA, USA) and incubated for 24 h prior to treatment. The test compounds were dissolved and stored in DMSO at a concentration of 10 mM, and a 2-fold serial predilution was prepared yielding a final DMSO concentration of 0.4% (v/v). Compound medium solutions were added to the assay plates and incubated for 1 h. Subsequently, recombinant human hepatocyte growth factor (HGF, provided by W. Birchmeier) was added to a final concentration of 300 pM. The cells were further incubated for 20 h, fixed with 4% formaldehyde/phosphate-buffered saline, and the nuclei were stained with Hoechst 33342 (10 μM, Sigma-Aldrich).

An Array-Scan XTI Reader (Thermo Fisher Scientific Inc.) was used to acquire images in the Hoechst 33342-associated filter channel (BGRFR 386_23) with a 10× objective. For each well, four image fields were acquired, ensuring that typically 1000 cells or more could be analyzed using the morphology analysis bioapplication of the HCS Studio software. The cell scattering was quantified based on the analysis of nuclei minimum distances. Valid nuclei were identified applying thresholds for size, shape, and intensity. The percentage of nuclei showing a minimum neighbor distance above a defined threshold value was calculated.

**Impedance.** The scatterassay was additionally applied to label-free kinetic impedance measurements using the xCeLLigence RTCA SP System (ACEA Biosciences Inc., San Diego, CA, USA). This live-cell assay was performed with HPAF-II cells in a 96-well E-plate format. The electrical impedance was measured by the RTCA-integrated software as a dimensionless parameter termed CI.

After doing the background measurement of 50 μL medium per well, 12,000 cells were added in 40 μL of medium to each well of the E-plate 96. The attachment and growth of the cells was recorded by the xCELLigence system every 30 min for 20 h. Then, the cells were preincubated with the compounds for 1 h by transferring 5 μL of 20-fold concentrated compound medium solutions, followed by stimulation with recombinant human HGF by adding a predilution of 5 μL per well to achieve a final concentration of 300 pM. Controls received medium plus DMSO with a final concentration of 0.2%. The impedance was monitored every 5 min for 4 h.

**Cell Growth and Cytotoxicity.** The cells (HPAF-II and HepG2) were seeded in 384-well microplates at 750 cells in 40 μL medium per well (CellCarrier-384 ultra, PerkinElmer) and incubated for 20 h. Then, 10 μL per well of 5-fold concentrated serial compound dilutions were added into the plates (final concentration 40 −0.6 μM, 0.4% DMSO). Following further incubation for 72 h, a live-cell staining of nuclei was performed using Hoechst 33342 (1 μM, Sigma-Aldrich) and TO-PRO-3 (1 μM, Invitrogen) as the dead cell indicator. The Array-Scan XTI Reader (Thermo Fisher Scientific Inc.) was used to acquire images with a 10× objective in the Hoechst 33342-associated filter channel (BGRFR 386_23) and the TO-PRO-3-associated far-red filter channel (BGRFR 650_13). Cell proliferation was determined by counting of valid Hoechst 33342 fluorescent cell nuclei, whereas the number of TO-PRO-3 fluorescent nuclei was used for the cytotoxicity analysis.

**Colony Formation Assay.** VACO432 and HCC1806 cells were seeded at 5000 cells/well in 12-well plates (Sarstedt) and allowed to adhere overnight. The next day, compounds were added as indicated and treatments were refreshed every 3−4 days. When vehicle (DMSO)-treated cells (indicated as "UT" in all figures) reached confluence, all wells were fixed in 3.7% formaldehyde, stained with 0.1% crystal violet and subsequently scanned.

**Western Blotting.** Cell samples were lysed in RIPA buffer [50 mM Tris pH 7.4, 150 mM NaCl, 1% NP40, 0.1% sodium dodecyl sulfate (SDS) and 0.5% sodium deoxycholate] supplemented with protease inhibitor (Roche, #11836153001) and phosphatase inhibitor cocktails 2 and 3 (Sigma-Aldrich, #P57261 and #P0044). Protein concentrations were determined by Pierce BCA protein assay kit (Thermo Scientific, #23225). Proteins were separated by SDS-PAGE in Laemmli buffer (0.25 M Tris, 1.92 M glycine, 1% SDS), transferred to polyvinylidene difluoride membranes (Carl Roth, pore size 0.45 μM) in transfer buffer (25 mM Tris, 192 mM glycine, 20% methanol), and subsequently incubated overnight at 4 °C with indicated antibodies in 5% BSA in PBST. ECL (PerkinElmer, NEL104001EA) was used to detect antibodies in a Vilber Fusion FX. Antibodies against HSP90 (sc-13119) and p-ERK Y204 (sc-7383) were purchased from Santa Cruz Biotechnology..

## ■ ASSOCIATED CONTENT

### Supporting Information

The Supporting Information is available free of charge at https://pubs.acs.org/doi/10.1021/acs.jmedchem.0c01265.

Docking complexes in PDB format (ZIP)

Ligand alignment studies, alternative synthetic pathway for the preparation of the azaindoles, docking poses of the representative compounds, full-detailed phosphatase and kinase profiling, cell permeability experiments, and HRMS data of the key compounds (PDF)

Molecular formula strings of compounds **8**−**46** (CSV)

## ■ AUTHOR INFORMATION


### Corresponding Author

**Marc Nazaré** − *Leibniz-Forschungsinstitut für Molekulare Pharmakologie (FMP), Campus Berlin-Buch, 13125 Berlin, Germany*; orcid.org/0000-0002-1602-2330; Phone: +49 30 9406-3083; Email: nazare@fmp-berlin.de

### Authors

**Yelena Mostinski** − *Leibniz-Forschungsinstitut für Molekulare Pharmakologie (FMP), Campus Berlin-Buch, 13125 Berlin, Germany*




https://dx.doi.org/10.1021/acs.jmedchem.0c01265
J. Med. Chem. XXXX, XXX, XXX−XXX

**Guus J. J. E. Heynen** − *Max Delbrück Center for Molecular Medicine in the Helmholtz Association (MDC), Campus Berlin-Buch, 13125 Berlin, Germany*
**Maria Pascual López-Alberca** − *Leibniz-Forschungsinstitut für Molekulare Pharmakologie (FMP), Campus Berlin-Buch, 13125 Berlin, Germany*
**Jerome Paul** − *Leibniz-Forschungsinstitut für Molekulare Pharmakologie (FMP), Campus Berlin-Buch, 13125 Berlin, Germany*
**Sandra Miksche** − *Leibniz-Forschungsinstitut für Molekulare Pharmakologie (FMP), Campus Berlin-Buch, 13125 Berlin, Germany*
**Silke Radetzki** − *Leibniz-Forschungsinstitut für Molekulare Pharmakologie (FMP), Campus Berlin-Buch, 13125 Berlin, Germany*
**David Schaller** − *Charité–Universitätsmedizin Berlin, 10117 Berlin, Germany*
**Elena Shanina** − *Max-Planck-Institut für Kolloid- und Grenzflächenforschung, 14476 Potsdam, Germany*
**Carola Seyffarth** − *Leibniz-Forschungsinstitut für Molekulare Pharmakologie (FMP), Campus Berlin-Buch, 13125 Berlin, Germany*
**Yuliya Kolomeets** − *Leibniz-Forschungsinstitut für Molekulare Pharmakologie (FMP), Campus Berlin-Buch, 13125 Berlin, Germany*
**Nandor Ziebart** − *Leibniz-Forschungsinstitut für Molekulare Pharmakologie (FMP), Campus Berlin-Buch, 13125 Berlin, Germany*
**Judith de Schryver** − *Leibniz-Forschungsinstitut für Molekulare Pharmakologie (FMP), Campus Berlin-Buch, 13125 Berlin, Germany*
**Sylvia Oestreich** − *Leibniz-Forschungsinstitut für Molekulare Pharmakologie (FMP), Campus Berlin-Buch, 13125 Berlin, Germany*
**Martin Neuenschwander** − *Leibniz-Forschungsinstitut für Molekulare Pharmakologie (FMP), Campus Berlin-Buch, 13125 Berlin, Germany*
**Yvette Roske** − *Max Delbrück Center for Molecular Medicine in the Helmholtz Association (MDC), Campus Berlin-Buch, 13125 Berlin, Germany*
**Udo Heinemann** − *Max Delbrück Center for Molecular Medicine in the Helmholtz Association (MDC), Campus Berlin-Buch, 13125 Berlin, Germany*
**Christoph Rademacher** − *Max-Planck-Institut für Kolloid- und Grenzflächenforschung, 14476 Potsdam, Germany;* orcid.org/0000-0001-7082-7239
**Andrea Volkamer** − *Charité–Universitätsmedizin Berlin, 10117 Berlin, Germany;* orcid.org/0000-0002-3760-580X
**Jens Peter von Kries** − *Leibniz-Forschungsinstitut für Molekulare Pharmakologie (FMP), Campus Berlin-Buch, 13125 Berlin, Germany*
**Walter Birchmeier** − *Max Delbrück Center for Molecular Medicine in the Helmholtz Association (MDC), Campus Berlin-Buch, 13125 Berlin, Germany*

Complete contact information is available at: https://pubs.acs.org/10.1021/acs.jmedchem.0c01265

### Author Contributions

The manuscript was written through contributions of all authors. All authors have given approval to the final version of the manuscript.

### Notes

The authors declare no competing financial interest.

## ■ ACKNOWLEDGMENTS

M.N., Y.M., M.P.L.-A., J.d.S., S.M., and J.P. would like to thank Dr. Edgar Specker (FMP) and the NMR core facility of the FMP for their excellent support on compound characterization. Y.M. thanks the Minerva-Stiftung of the Max Planck Society for a postdoctoral fellowship. A.V. and D.S. thank Prof. Dr. Gerhard Wolber (Freie Universität Berlin) for providing a license for LigandScout 4.4.

## ■ ABBREVIATIONS

SHP2, Src homology-2 domain containing protein tyrosine phosphatase-2; PTP, protein tyrosine phosphatase; MAPK, mitogen-activated protein kinase; JAK-STAT, Janus kinase/signal transducer and activator of transcription; PI3K-akt, phosphatidylinositol-3-kinase-Akt; MEK, MAPK/ERK kinase; BRAF, v-raf murine sarcoma viral oncogene homolog B1; STAT3, signal transducer and activator of transcription 3; PAINS, pan-assay interference compounds; SAR, structure−activity relationship; Boc, *tert*-butyloxycarbonyl; NIS, *N*-iodosuccinimide; DIPEA, *N*,*N*-diisopropylethylamine; DiFMUP, difluoromethylumbelliferyl phosphate; THP, tetrahydropyran; EGFR, epidermal growth factor receptor; ERK, extracellular signal-regulated protein kinase; DMSO, dimethylsulfoxide; DCM, dichloromethane; ACN, acetonitrile; BSA, bovine serum albumin; SDS, sodium dodecyl sulfate

## ■ REFERENCES

(1) Chan, G.; Kalaitzidis, D.; Neel, B. G. The Tyrosine Phosphatase Shp2 (PTPN11) in Cancer. *Cancer Metastasis Rev.* **2008**, *27*, 179−192.
(2) Grossmann, K. S.; Rosário, M.; Birchmeier, C.; Birchmeier, W. The Tyrosine Phosphatase Shp2 In Development And Cancer. *Adv. Cancer Res.* **2010**, *106*, 53−89.
(3) Yuan, X.; Bu, H.; Zhou, J.; Yang, C.-Y.; Zhang, H. Recent Advances of SHP2 Inhibitors in Cancer Therapy: Current Development and Clinical Application. *J. Med. Chem.* **2020**, *63*, 11368.
(4) Schaeper, U.; Gehring, N. H.; Fuchs, K. P.; Sachs, M.; Kempkes, B.; Birchmeier, W. Coupling of Gab1 to c-Met, Grb2, and Shp2 Mediates Biological Responses. *J. Cell Biol.* **2000**, *149*, 1419−1432.
(5) Mohi, M. G.; Neel, B. G. The Role of Shp2 (PTPN11) in Cancer. *Curr. Opin. Genet. Dev.* **2007**, *17*, 23−30.
(6) Jopling, C.; van Geemen, D.; den Hertog, J. Shp2 Knockdown and Noonan/LEOPARD Mutant Shp2-Induced Gastrulation Defects. *PLoS Genet.* **2007**, *3*, No. e225.
(7) Prahallad, A.; Heynen, G. J. J. E.; Germano, G.; Willems, S. M.; Evers, B.; Vecchione, L.; Gambino, V.; Lieftink, C.; Beijersbergen, R. L.; Di Nicolantonio, F.; Bardelli, A.; Bernards, R. PTPN11 Is a Central Node in Intrinsic and Acquired Resistance to Targeted Cancer Drugs. *Cell Rep.* **2015**, *12*, 1978−1985.
(8) Mainardi, S.; Mulero-Sánchez, A.; Prahallad, A.; Germano, G.; Bosma, A.; Krimpenfort, P.; Lieftink, C.; Steinberg, J. D.; de Wit, N.; Gonçalves-Ribeiro, S.; Nadal, E.; Bardelli, A.; Villanueva, A.; Bernards, R. SHP2 is Required for Growth of KRAS-Mutant Non-Small-Cell Lung Cancer In Vivo. *Nat. Med.* **2018**, *24*, 961−967.
(9) Ruess, D. A.; Heynen, G. J.; Ciecielski, K. J.; Ai, J.; Berninger, A.; Kabacaoglu, D.; Görgülü, K.; Dantes, Z.; Wörmann, S. M.; Diakopoulos, K. N.; Karpathaki, A. F.; Kowalska, M.; Kaya-Aksoy, E.; Song, L.; van der Laan, E. A. Z.; López-Alberca, M. P.; Nazaré, M.; Reichert, M.; Saur, D.; Erkan, M. M.; Hopt, U. T.; Sainz, B., Jr.; Birchmeier, W.; Schmid, R. M.; Lesina, M.; Algül, H. Mutant KRAS-driven Cancers Depend on PTPN11/SHP2 Phosphatase. *Nat. Med.* **2018**, *24*, 954−960.

(10) Chitranshi, N.; Dheer, Y.; Mirzaei, M.; Wu, Y.; Salekdeh, G. H.; Abbasi, M.; Gupta, V.; Vander Wall, R.; You, Y.; Graham, S. L.; Gupta, V. Loss of Shp2 Rescues BDNF/TrkB Signaling and Contributes to Improved Retinal Ganglion Cell Neuroprotection. *Mol. Ther.* **2019**, *27*, 424−441.
(11) Wang, L.; Huang, J.; Moore, D. C.; Song, Y.; Ehrlich, M. G.; Yang, W. SHP2 Regulates Intramembranous Ossification by Modifying the TGFbeta and BMP2 Signaling Pathway. *Bone* **2019**, *120*, 327−335.
(12) Kim, Y.; Liu, G.; Leugers, C. J.; Mueller, J. D.; Francis, M. B.; Hefti, M. M.; Schneider, J. A.; Lee, G. Tau Interacts With SHP2 in Neuronal Systems And in Alzheimer's Disease Brains. *J. Cell Sci.* **2019**, *132*, jcs229054.
(13) Shen, D.; Chen, W.; Zhu, J.; Wu, G.; Shen, R.; Xi, M.; Sun, H. Therapeutic Potential of Targeting SHP2 in Human Developmental Disorders and Cancers. *Eur. J. Med. Chem.* **2020**, *190*, 112117.
(14) Liu, Q.; Qu, J.; Zhao, M.; Xu, Q.; Sun, Y. Targeting SHP2 as a Promising Strategy for Cancer Immunotherapy. *Pharmacol. Res.* **2020**, *152*, 104595.
(15) Sarver, P.; Acker, M.; Bagdanoff, J. T.; Chen, Z.; Chen, Y.-N.; Chan, H.; Firestone, B.; Fodor, M.; Fortanet, J.; Hao, H.; Hentemann, M.; Kato, M.; Koenig, R.; LaBonte, L. R.; Liu, G.; Liu, S.; Liu, C.; McNeill, E.; Mohseni, M.; Sendzik, M.; Stams, T.; Spence, S.; Tamez, V.; Tichkule, R.; Towler, C.; Wang, H.; Wang, P.; Williams, S. L.; Yu, B.; LaMarche, M. J. 6-Amino-3-methylpyrimidinones as Potent, Selective, and Orally Efficacious SHP2 Inhibitors. *J. Med. Chem.* **2019**, *62*, 1793−1802.
(16) Wu, X.; Xu, G.; Li, X.; Xu, W.; Li, Q.; Liu, W.; Kirby, K. A.; Loh, M. L.; Li, J.; Sarafianos, S. G.; Qu, C.-K. Small Molecule Inhibitor that Stabilizes the Autoinhibited Conformation of the Oncogenic Tyrosine Phosphatase SHP2. *J. Med. Chem.* **2019**, *62*, 1125−1137.
(17) Chen, Y.-N. P.; LaMarche, M. J.; Chan, H. M.; Fekkes, P.; Garcia-Fortanet, J.; Acker, M. G.; Antonakos, B.; Chen, C. H.-T.; Chen, Z.; Cooke, V. G.; Dobson, J. R.; Deng, Z.; Fei, F.; Firestone, B.; Fodor, M.; Fridrich, C.; Gao, H.; Grunenfelder, D.; Hao, H.-X.; Jacob, J.; Ho, S.; Hsiao, K.; Kang, Z. B.; Karki, R.; Kato, M.; Larrow, J.; La Bonte, L. R.; Lenoir, F.; Liu, G.; Liu, S.; Majumdar, D.; Meyer, M. J.; Palermo, M.; Perez, L.; Pu, M.; Price, E.; Quinn, C.; Shakya, S.; Shultz, M. D.; Slisz, J.; Venkatesan, K.; Wang, P.; Warmuth, M.; Williams, S.; Yang, G.; Yuan, J.; Zhang, J.-H.; Zhu, P.; Ramsey, T.; Keen, N. J.; Sellers, W. R.; Stams, T.; Fortin, P. D. Allosteric Inhibition of SHP2 Phosphatase Inhibits Cancers Driven by Receptor Tyrosine Kinases. *Nature* **2016**, *535*, 148−152.
(18) Garcia Fortanet, J.; Chen, C. H.-T.; Chen, Y.-N. P.; Chen, Z.; Deng, Z.; Firestone, B.; Fekkes, P.; Fodor, M.; Fortin, P. D.; Fridrich, C.; Grunenfelder, D.; Ho, S.; Kang, Z. B.; Karki, R.; Kato, M.; Keen, N.; LaBonte, L. R.; Larrow, J.; Lenoir, F.; Liu, G.; Liu, S.; Lombardo, F.; Majumdar, D.; Meyer, M. J.; Palermo, M.; Perez, L.; Pu, M.; Ramsey, T.; Sellers, W. R.; Shultz, M. D.; Stams, T.; Towler, C.; Wang, P.; Williams, S. L.; Zhang, J.-H.; LaMarche, M. J. Allosteric Inhibition of SHP2: Identification of a Potent, Selective, and Orally Efficacious Phosphatase Inhibitor. *J. Med. Chem.* **2016**, *59*, 7773−7782.
(19) Chen, C.; Cao, M.; Zhu, S.; Wang, C.; Liang, F.; Yan, L.; Luo, D. Discovery of a Novel Inhibitor of the Protein Tyrosine Phosphatase Shp2. *Sci. Rep.* **2015**, *5*, 17626.
(20) Zhen, X.-l.; Yin, W.-h.; Tian, X.; Ma, Z.-j.; Fan, S.-m.; Han, J.-r.; Liu, S. Synthesis and Biological Evaluation of Open-Chain Analogs of Cyclic Peptides as Inhibitors of Cellular Shp2 Activity. *Bioorg. Med. Chem.* **2015**, *23*, 2562−2567.
(21) Zeng, L.-F.; Zhang, R.-Y.; Yu, Z.-H.; Li, S.; Wu, L.; Gunawan, A. M.; Lane, B. S.; Mali, R. S.; Li, X.; Chan, R. J.; Kapur, R.; Wells, C. D.; Zhang, Z.-Y. Therapeutic Potential of Targeting the Oncogenic SHP2 Phosphatase. *J. Med. Chem.* **2014**, *57*, 6594−6609.
(22) Yu, Z.-H.; Chen, L.; Wu, L.; Liu, S.; Wang, L.; Zhang, Z.-Y. Small Molecule Inhibitors of SHP2 Tyrosine Phosphatase Discovered by Virtual Screening. *Bioorg. Med. Chem. Lett.* **2011**, *21*, 4238−4242.
(23) Chen, L.; Sung, S.-S.; Yip, M. L. R.; Lawrence, H. R.; Ren, Y.; Guida, W. C.; Sebti, S. M.; Lawrence, N. J.; Wu, J. Discovery of a Novel Shp2 Protein Tyrosine Phosphatase Inhibitor. *Mol. Pharmacol.* **2006**, *70*, 562−570.
(24) Zhang, X.; He, Y.; Liu, S.; Yu, Z.; Jiang, Z.-X.; Yang, Z.; Dong, Y.; Nabinger, S. C.; Wu, L.; Gunawan, A. M.; Wang, L.; Chan, R. J.; Zhang, Z.-Y. Salicylic Acid Based Small Molecule Inhibitor for the Oncogenic Src homology-2 Domain Containing Protein Tyrosine Phosphatase-2 (SHP2). *J. Med. Chem.* **2010**, *53*, 2482−2493.
(25) Lawrence, H. R.; Pireddu, R.; Chen, L.; Luo, Y.; Sung, S.-S.; Szymanski, A. M.; Yip, M. L. R.; Guida, W. C.; Sebti, S. M.; Wu, J.; Lawrence, N. J. Inhibitors of Src homology-2 Domain Containing Protein Tyrosine Phosphatase-2 (Shp2) Based on Oxindole Scaffolds. *J. Med. Chem.* **2008**, *51*, 4948−4956.
(26) Marasco, M.; Berteotti, A.; Weyershaeuser, J.; Thorausch, N.; Sikorska, J.; Krausze, J.; Brandt, H. J.; Kirkpatrick, J.; Rios, P.; Schamel, W. W.; Kohn, M.; Carlomagno, T. Molecular Mechanism of SHP2 Activation by PD-1 Stimulation. *Sci. Adv.* **2020**, *6*, No. eaay4458.
(27) Zhang, Z.-Y. Protein Tyrosine Phosphatases: Prospects for Therapeutics. *Curr. Opin. Chem. Biol.* **2001**, *5*, 416−423.
(28) Sun, J.-P.; Fedorov, A. A.; Lee, S.-Y.; Guo, X.-L.; Shen, K.; Lawrence, D. S.; Almo, S. C.; Zhang, Z.-Y. Crystal Structure of PTP1B Complexed With a Potent and Selective Bidentate Inhibitor. *J. Biol. Chem.* **2003**, *278*, 12406−12414.
(29) Bagdanoff, J. T.; Chen, Z.; Acker, M.; Chen, Y.-N.; Chan, H.; Dore, M.; Firestone, B.; Fodor, M.; Fortanet, J.; Hentemann, M.; Kato, M.; Koenig, R.; LaBonte, L. R.; Liu, S.; Mohseni, M.; Ntaganda, R.; Sarver, P.; Smith, T.; Sendzik, M.; Stams, T.; Spence, S.; Towler, C.; Wang, H.; Wang, P.; Williams, S. L.; LaMarche, M. J. Optimization of Fused Bicyclic Allosteric SHP2 Inhibitors. *J. Med. Chem.* **2019**, *62*, 1781−1792.
(30) Jin, W.-Y.; Ma, Y.; Li, W.-Y.; Li, H.-L.; Wang, R.-L. Scaffold-based Novel SHP2 Allosteric Inhibitors Design Using Receptor-Ligand Pharmacophore Model, Virtual Screening and Molecular Dynamics. *Comput. Biol. Chem.* **2018**, *73*, 179−188.
(31) LaRochelle, J. R.; Fodor, M.; Ellegast, J. M.; Liu, X.; Vemulapalli, V.; Mohseni, M.; Stams, T.; Buhrlage, S. J.; Stegmaier, K.; LaMarche, M. J.; Acker, M. G.; Blacklow, S. C. Identification of an Allosteric Benzothiazolopyrimidone Inhibitor of the Oncogenic Protein Tyrosine Phosphatase SHP2. *Bioorg. Med. Chem.* **2017**, *25*, 6479−6485.
(32) LaRochelle, J. R.; Fodor, M.; Vemulapalli, V.; Mohseni, M.; Wang, P.; Stams, T.; LaMarche, M. J.; Chopra, R.; Acker, M. G.; Blacklow, S. C. Structural Reorganization of SHP2 by Oncogenic Mutations and Implications for Oncoprotein Resistance to Allosteric Inhibition. *Nat. Commun.* **2018**, *9*, 4508.
(33) Lu, H.; Liu, C.; Huynh, H.; Le, T. B. U.; LaMarche, M. J.; Mohseni, M.; Engelman, J. A.; Hammerman, P. S.; Caponigro, G.; Hao, H.-X. Resistance to Allosteric SHP2 Inhibition in FGFR-Driven Cancers Through Rapid Feedback Activation of FGFR. *Oncotarget* **2020**, *11*, 265−281.
(34) Lu, S.; Qiu, Y.; Ni, D.; He, X.; Pu, J.; Zhang, J. Emergence of Allosteric Drug-Resistance Mutations: New Challenges for Allosteric Drug Discovery. *Drug Discovery Today* **2020**, *25*, 177−184.
(35) Sun, X.; Ren, Y.; Gunawan, S.; Teng, P.; Chen, Z.; Lawrence, H.; Cai, J.; Lawrence, N.; Wu, J. Selective Inhibition of Leukemia-Associated SHP2(E69K) Mutant by the Allosteric SHP2 Inhibitor SHP099. *Leukemia* **2018**, *32*, 1246−1249.
(36) Romero, C.; Lambert, L. J.; Sheffler, D. J.; De Backer, L. J. S.; Raveendra-Panickar, D.; Celeridad, M.; Grotegut, S.; Rodiles, S.; Holleran, J.; Sergienko, E.; Pasquale, E. B.; Cosford, N. D. P.; Tautz, L. A Cellular Target Engagement Assay for the Characterization of SHP2 (PTPN11) Phosphatase Inhibitors. *J. Bio. Chem.* **2020**, *295*, 2601−2613.
(37) Hellmuth, K.; Grosskopf, S.; Lum, C. T.; Wurtele, M.; Roder, N.; von Kries, J. P.; Rosario, M.; Rademann, J.; Birchmeier, W. Specific Inhibitors of the Protein Tyrosine Phosphatase Shp2


https://dx.doi.org/10.1021/acs.jmedchem.0c01265
J. Med. Chem. XXXX, XXX, XXX−XXX

Identified by High-Throughput Docking. *Proc. Natl. Acad. Sci. U.S.A.* **2008**, *105*, 7275−7280.
(38) Grosskopf, S.; Eckert, C.; Arkona, C.; Radetzki, S.; Böhm, K.; Heinemann, U.; Wolber, G.; von Kries, J.-P.; Birchmeier, W.; Rademann, J. Selective Inhibitors of the Protein Tyrosine Phosphatase SHP2 Block Cellular Motility and Growth of Cancer Cells In Vitro and In Vivo. *ChemMedChem* **2015**, *10*, 815−826.
(39) Gannett, P. M.; Shi, X.; Lawson, T.; Kolar, C.; Toth, B. Aryl Radical Formation During the Metabolism of Arylhydrazines by Microsomes. *Chem. Res. Toxicol.* **1997**, *10*, 1372−1377.
(40) Baell, J. B.; Nissink, J. W. M. Seven Year Itch: Pan-Assay Interference Compounds (PAINS) in 2017-Utility and Limitations. *ACS Chem. Biol.* **2018**, *13*, 36−44.
(41) Chung, K.-T.; Murdock, C. A.; Zhou, Y.; Stevens, S. E., Jr.; Li, Y.-S.; Wei, C.-I.; Fernando, S. Y.; Chou, M.-W. Effects of the Nitro-Group on the Mutagenicity and Toxicity of Some Benzamines. *Environ. Mol. Mutagen.* **1996**, *27*, 67−74.
(42) Macherey, A. C.; Dansette, P. M. Biotransformations Leading to Toxic Metabolites. In *The Practice of Medicinal Chemistry*; Wermuth, C., Aldous, D., Raboisson, P., Rognan, D., Eds.; Academic Press: New York, 2015; pp 675−696.
(43) Shultz, M. D. Two Decades under the Influence of the Rule of Five and the Changing Properties of Approved Oral Drugs. *J. Med. Chem.* **2019**, *62*, 1701−1714.
(44) Ursu, O.; Rayan, A.; Goldblum, A.; Oprea, T. I. Understanding Drug-Likeness. *Wiley Interdiscip. Rev.: Comput. Mol. Sci.* **2011**, *1*, 760−781.
(45) Benet, L. Z.; Hosey, C. M.; Ursu, O.; Oprea, T. I. BDDCS, the Rule of 5 and Drugability. *Adv. Drug Delivery Rev.* **2016**, *101*, 89−98.
(46) Brown, N. Bioisosteres and Scaffold Hopping in Medicinal Chemistry. *Mol. Inf.* **2014**, *33*, 458−462.
(47) Langdon, S. R.; Ertl, P.; Brown, N. Bioisosteric Replacement and Scaffold Hopping in Lead Generation and Optimization. *Mol. Inf.* **2010**, *29*, 366−385.
(48) Kuhn, B.; Mohr, P.; Stahl, M. Intramolecular Hydrogen Bonding in Medicinal Chemistry. *J. Med. Chem.* **2010**, *53*, 2601−2611.
(49) Chang, C.-F.; Lin, W.-H.; Ke, Y.-Y.; Lin, Y.-S.; Wang, W.-C.; Chen, C.-H.; Kuo, P.-C.; Hsu, J. T. A.; Uang, B.-J.; Hsieh, H.-P. Discovery of Novel Inhibitors of Aurora Kinases with Indazole Scaffold: In Silico Fragment-Based and Knowledge-Based Drug Design. *Eur. J. Med. Chem.* **2016**, *124*, 186−199.
(50) Ye, M.; Edmunds, A. J. F.; Morris, J. A.; Sale, D.; Zhang, Y.; Yu, J.-Q. A Robust Protocol for Pd(II)-catalyzed C-3 Arylation of (1H) Indazoles and Pyrazoles: Total Synthesis of Nigellidine Hydrobromide. *Chem. Sci.* **2013**, *4*, 2374−2379.
(51) Ali, N. A. S.; Dar, B. A.; Pradhan, V.; Farooqui, M. Chemistry and Biology of Indoles and Indazoles: a Mini-Review. *Mini-Rev. Med. Chem.* **2013**, *13*, 1792−1800.
(52) Irie, T.; Sawa, M. 7-Azaindole: A Versatile Scaffold for Developing Kinase Inhibitors. *Chem. Pharm. Bull.* **2018**, *66*, 29−36.
(53) Mérour, J.-Y.; Buron, F.; Plé, K.; Bonnet, P.; Routier, S. The Azaindole Framework in the Design of Kinase Inhibitors. *Molecules* **2014**, *19*, 19935−19979.
(54) Goodfellow, V. S.; Loweth, C. J.; Ravula, S. B.; Wiemann, T.; Nguyen, T.; Xu, Y.; Todd, D. E.; Sheppard, D.; Pollack, S.; Polesskaya, O.; Marker, D. F.; Dewhurst, S.; Gelbard, H. A. Discovery, Synthesis, and Characterization of an Orally Bioavailable, Brain Penetrant Inhibitor of Mixed Lineage Kinase 3. *J. Med. Chem.* **2013**, *56*, 8032−8048.
(55) Billedeau, R. J.; Kondru, R. K.; Lopez-Tapia, F. J.; Lou, Y.; Owens, T. D.; Qian, Y.; So, S.-S.; Thakkar, K. C.; Wanner, J. Inhibitors of Bruton's Tyrosine Kinase. U.S. Patent 20,120,295,885A1, Nov 22, 2012, CA157:734758.
(56) Patnaik, A.; Axford, L.; Deng, L.; Cohick, E.; Ren, X.; Loi, S.; Kecman, S.; Hollis-Symynkywicz, M.; Harrison, T. J.; Papillon, J. P. N.; Dales, N.; Hamann, L. G.; Lee, L.; Regard, J. B.; Marcinkeviciene, J.; Marro, M. L.; Patterson, A. W. Discovery of a Novel Indole Pharmacophore for the Irreversible Inhibition of Myeloperoxidase (MPO). *Bioorg. Med. Chem.* **2020**, *28*, 115548.
(57) Macchiarulo, A.; Pellicciari, R. Exploring the Other Side of Biologically Relevant Chemical Space: Insights into Carboxylic, Sulfonic and Phosphonic Acid Bioisosteric Relationships. *J. Mol. Graphics Modell.* **2007**, *26*, 728−739.
(58) Grosskopf, S. Entwicklung und Synthese von Protein-Tyrosin-Phosphatase Inhibitoren sowie Synthese und Validierung von SHP-2-Inhibitoren in vitro und in vivo. Ph.D. Thesis, Freien Universität, Berlin, 2010.
(59) Ballatore, C.; Huryn, D. M.; Smith, A. B., 3rd Carboxylic Acid (Bio)Isosteres in Drug Design. *ChemMedChem* **2013**, *8*, 385−395.
(60) Nepali, K.; Lee, H.-Y.; Liou, J.-P. Nitro-Group-Containing Drugs. *J. Med. Chem.* **2019**, *62*, 2851−2893.
(61) Tseng, C.-C.; Baillie, G.; Donvito, G.; Mustafa, M. A.; Juola, S. E.; Zanato, C.; Massarenti, C.; Dall'Angelo, S.; Harrison, W. T. A.; Lichtman, A. H.; Ross, R. A.; Zanda, M.; Greig, I. R. The Trifluoromethyl Group as a Bioisosteric Replacement of the Aliphatic Nitro Group in CB1 Receptor Positive Allosteric Modulators. *J. Med. Chem.* **2019**, *62*, 5049−5062.
(62) Beck, D. E.; Abdelmalak, M.; Lv, W.; Reddy, P. V. N.; Tender, G. S.; O'Neill, E.; Agama, K.; Marchand, C.; Pommier, Y.; Cushman, M. Discovery of Potent Indenoisoquinoline Topoisomerase I Poisons Lacking the 3-Nitro Toxicophore. *J. Med. Chem.* **2015**, *58*, 3997−4015.
(63) Nagarathnam, D.; Miao, S. W.; Lagu, B.; Chiu, G.; Fang, J.; Murali Dhar, T. G.; Zhang, J.; Tyagarajan, S.; Marzabadi, M. R.; Zhang, F.; Wong, W. C.; Sun, W.; Tian, D.; Wetzel, J. M.; Forray, C.; Chang, R. S. L.; Broten, T. P.; Ransom, R. W.; Schorn, T. W.; Chen, T. B.; O'Malley, S.; Kling, P.; Schneck, K.; Bendesky, R.; Harrell, C. M.; Vyas, K. P.; Gluchowski, C. Design and Synthesis of Novel Alpha(1)(A) Adrenoceptor-Selective Antagonists. 1. Structure-Activity Relationship in Dihydropyrimidinones. *J. Med. Chem.* **1999**, *42*, 4764−4777.
(64) Troxler, T.; Hurth, K.; Schuh, K.-H.; Schoeffter, P.; Langenegger, D.; Enz, A.; Hoyer, D. Decahydroisoquinoline Derivatives as Novel Non-Peptidic, Potent and Subtype-Selective Somatostatin SST(3) Receptor Antagonists. *Bioorg. Med. Chem. Lett.* **2010**, *20*, 1728−1734.
(65) Troxler, T.; Enz, A.; Hoyer, D.; Langenegger, D.; Neumann, P.; Pfäffli, P.; Schoeffter, P.; Hurth, K. Ergoline Derivatives as Highly Potent and Selective Antagonists at the Somatostatin SST 1 Receptor. *Bioorg. Med. Chem. Lett.* **2008**, *18*, 979−982.
(66) Anana, R. D.; Knaus, E. E. Synthesis and Smooth Muscle Calcium Channel Antagonist Effects of Alkyl 1,4-dihydro-2,6-dimethyl-4-(pyridinyl)-5-[2-(4,5-dihydro- 4,4-dimethyloxazolin-2-yl)]-3-pyridinecarboxylates. *Arch. Pharm.* **1996**, *329*, 408−412.
(67) Mittapalli, G. K.; Zhao, F.; Jackson, A.; Gao, H.; Lee, H.; Chow, S.; Kaur, M. P.; Nguyen, N.; Zamboni, R.; McKelvy, J.; Wong-Staal, F.; Macdonald, J. E. Discovery of ITX 4520: a Highly Potent Orally Bioavailable Hepatitis C Virus Entry Inhibitor. *Bioorg. Med. Chem. Lett.* **2012**, *22*, 4955−4961.
(68) Sakanyan, V.; Angelini, M.; Le Bechec, M.; Lecocq, M. F.; Benaiteau, F.; Rousseau, B.; Gyulkhandanyan, A.; Gyulkhandanyan, L.; Loge, C.; Reiter, E.; Roussakis, C.; Fleury, F. Screening and Discovery of Nitro-Benzoxadiazole Compounds Activating Epidermal Growth Factor Receptor (EGFR) in Cancer Cells. *Sci. Rep.* **2014**, *4*, 3977.
(69) Patani, G. A.; LaVoie, E. J. Bioisosterism: A Rational Approach in Drug Design. *Chem. Rev.* **1996**, *96*, 3147−3176.
(70) *OpenEye Toolkits 2019.Oct.2*; OpenEye Scientific Software: Santa Fe, NM, 2019.
(71) McGann, M. FRED and HYBRID Docking Performance on Standardized Datasets. *J. Comput.-Aided Mol. Des.* **2012**, *26*, 897−906.
(72) Wolber, G.; Langer, T. LigandScout: 3-D Pharmacophores Derived From Protein-Bound Ligands and their use as Virtual Screening Filters. *J. Chem. Inf. Model.* **2005**, *45*, 160−169.
(73) *Desmond 6.1, Schrödinger Release 2020-1*; Schrödinger, LLC: New York, NY, 2020.


https://dx.doi.org/10.1021/acs.jmedchem.0c01265
J. Med. Chem. XXXX, XXX, XXX−XXX

(74) Humphrey, W.; Dalke, A.; Schulten, K. VMD: Visual Molecular Dynamics. *J. Mol. Graphics* **1996**, *14*, 33−38.
(75) *PyMol 2.5*; Schrödinger, LLC: New York, NY, 2020.
(76) Wu, Y.-J. Heterocycles and medicine: a survey of the heterocyclic drugs approved by the U.S. FDA from 2000 to Present. In *Progress in Heterocyclic Chemistry*; Gribble, G. W., Joule, J. A., Ed.; Elsevier, 2012; Chapter 1, Vol. *24*, pp 1−53.
(77) Porter, J.; Lumb, S.; Franklin, R. J.; Gascon-Simorte, J. M.; Calmiano, M.; Riche, K. L.; Lallemand, B.; Keyaerts, J.; Edwards, H.; Maloney, A.; Delgado, J.; King, L.; Foley, A.; Lecomte, F.; Reuberson, J.; Meier, C.; Batchelor, M. Discovery of 4-Azaindoles as Novel Inhibitors of c-Met Kinase. *Bioorg. Med. Chem. Lett.* **2009**, *19*, 2780−2784.
(78) Vogler, M.; Dinsdale, D.; Dyer, M. J. S.; Cohen, G. M. Bcl-2 inhibitors: Small Molecules with a Big Impact on Cancer Therapy. *Cell Death Differ.* **2009**, *16*, 360−367.
(79) Wormald, M. M.; Ernst, G.; Wei, H.; Barrow, J. C. Synthesis and Characterization of Novel Isoform-Selective IP6K1 Inhibitors. *Bioorg. Med. Chem. Lett.* **2019**, *29*, 126628.
(80) Kodama, A.; Matozaki, T.; Fukuhara, A.; Kikyo, M.; Ichihashi, M.; Takai, Y. Involvement of an SHP-2-Rho Small G protein Pathway in Hepatocyte Growth Factor/Scatter Factor-Induced Cell Scattering. *Mol. Biol. Cell* **2000**, *11*, 2565−2575.
(81) Chan, G. K. Y.; Lutterbach, B. A.; Pan, B.-S.; Kariv, I.; Szewczak, A. A. High-Throughput Analysis of HGF-Stimulated Cell Scattering. *J. Biomol. Screening* **2008**, *13*, 847−854.
(82) Wasserman, H. H.; Baldino, C. M.; Coats, S. J. Selective Oxidation of Phosphorus Ylides by Dimethyldioxirane. Application to the Formation of Vicinal Tricarbonyls. *J. Org. Chem.* **1995**, *60*, 8231−8235.


https://dx.doi.org/10.1021/acs.jmedchem.0c01265
*J. Med. Chem.* XXXX, XXX, XXX−XXX